Establishment of a novel *in vitro* implant infection model - Effects of electrical stimulation on staphylococci using alternating current

Dissertation

zur

Erlangung des akademischen Grades
doctor rerum naturalium (Dr. rer. nat.)

am Institut für Biowissenschaften
der Mathematisch-Naturwissenschaftlichen Fakultät
der Universität Rostock

vorgelegt von:
Thomas Josef Dauben
aus Rostock

Rostock, 2017

urn:nbn:de:gbv:28-diss2018-0031-8

Gutachter:

1. Gutachter:

   Prof. Dr. rer. nat. Bernd Kreikemeyer,

   Institut für Medizinische Mikrobiologie, Virologie und Hygiene, Universitätsmedizin Rostock

2. Gutachter:

   Prof. Dr. rer. nat. Hubert Bahl,

   Institut für Biowissenschaften, Universität Rostock

3. Gutachter:

   Prof. Dr. med. Rainer Bader

   Forschungslabor für Biomechanik und Implantattechnologie, Universitätsmedizin Rostock

Datum der Einreichung: 27. Juni 2017

Datum der Verteidigung: 12. Januar 2018

List of Abbreviations ..... **IV**

List of Figures ..... **V**

List of Tables ..... **VIII**

1 Introduction **1**

1.1 Electrical stimulation in clinical practice 1

1.1.1 Effects of electrical stimulation on bone cells 1

1.1.2 Complications and revision causes 2

1.2 Electrical stimulation of bacteria 3

1.2.1 *Staphylococcus aureus* 4

1.2.2 *Staphylococcus epidermidis* 5

1.2.3 Biofilm formation 6

1.2.4 Interactions with bone 8

1.3 Aim of the work 9

1.4 Interdisciplinary aspect and integration in WELISA 9

2 Materials and Methods **11**

2.1 Chemicals, Enzymes & Kits 11

2.2 Laboratory Equipment 13

2.3 Construction of the stimulation system 14

2.3.1 Basic idea and purpose of construction 14

2.3.2 Construction of the stimulation chamber 15

2.3.3 Simulation and validation of electric field distribution 17

2.4 Bacteria 19

2.4.1 Bacterial Strains 19

2.4.2 Cultivation and preservation 19

2.4.3 Growth experiments 20

2.4.4 Biofilm formation on solid materials 22

2.4.5 Scanning electron microscopy 23

2.4.6 Electrical stimulation protocol 24

2.4.6.1 Determination of CFU/ml from the supernatant 24
2.4.6.2 Antibiotic resistance 25
2.4.6.3 Determination of CFU/ml from the electrode surface 25
2.4.6.4 Quantification of biofilm mass 26
2.4.6.5 pH measurement 26
2.4.6.6 Quantification of biofilm mass following electrical stimulation 26
2.4.6.7 Determination of biofilm composition 27
2.4.6.8 Determination of ATP concentration 28
2.4.6.9 Fluorescence activated cell-sorting / FACS analyses 28
2.5 Cells and cell lines 29
2.5.1 Cell culture and preservation 29
2.5.2 Adherence and internalization assay 30
2.5.3 Cytokine ELISA 31
2.6 Co-culture under electrical stimulation 32
2.7 Statistical analysis 33
3 Results 34
3.1 Numeric simulation of electric potential and field distribution in the stimulation system 34
3.2 Growth of *S. epidermidis* and *S. aureus* in complex and cell culture media 35
3.3 Biofilm mass production of *S. epidermidis* on solid materials 38
3.3.1 Determination of CFU/ml from supernatants 38
3.3.2 Determination of CFU/ml recovered from biofilms 39
3.3.3 Quantification of biofilm mass 40
3.4 Scanning electron microscopy imaging of biofilms of *S. epidermidis* 41
3.5 Electrical stimulation of *S. epidermidis* and *S. aureus* 43
3.5.1 Determination of CFU/ml from the supernatant 43
3.5.2 Determination of CFU/ml recovered from electrode surfaces 45
3.5.3 Biofilm mass quantification 46

3.5.4 pH measurements 48
3.5.5 Antibiotic resistance 49
3.5.6 Biofilm mass production following electrical stimulation 50
3.5.7 Biofilm Composition 51
3.5.8 Determination of ATP concentration in supernatants and lysates 53
3.5.9 Determination of live and dead bacteria by FACS analyses 54
3.6 Co-culture of staphylococci and bone cells 55
3.6.1 Adherence and internalization of staphylococci to and into bone cells 55
3.6.2 Cytokine production following infection of bone cells with staphylococci 57
3.6.3 SEM imaging of MG63 cells and hOB infected with *S. epidermidis* 60
3.6.4 Co-culture of *S. epidermidis* and MG63 cells under electrical stimulation 60
4 Discussion 63
4.1 Numerical simulation and choice of material 63
4.2 Effects of electrical stimulation on bacteria 65
4.3 Influences of AC stimulation on biofilm composition 66
4.4 Interactions of *S. epidermidis* with cells 67
4.5 Limitations and Outlook 69
5 Summary 71
6 References IX
7 Appendix XVIII
Acknowledgements XXIII
Selbstständigkeitserklärung .....

List of Abbreviations

AC	alternating current
Aqua dest.	destilled / deionized water
Adh.	adherence
ATP	adenosine triphosphate
CFU	colony forming units
DC	direct current
DMEM	Dulbecco's Modified Eagle Medium
DMSO	dimethyl sulfoxide
DNA	deoxyribonucleic acid
E. coli	*Escherichia coli*
EDTA	ethylenediaminetetraacetic acid
ELISA	enzyme-linked immunosorbent assay
EthD-III	ethidium homodimer III
FACS	fluorescence activated cell sorting
FCS	fetal calf serum
HEPES	2-[4-(2-hydroxyethyl)piperazin-1-yl]ethanesulfonic acid
hOB	human osteoblasts
Int.	internalization
IL-6	interleukin-6
IL-12	interleukin-12
magn.	magnification
MCP-1	monocyte chemoattractant protein 1
MEM	Minimal Essential Medium
MG63	osteosarcoma cell line
MIC	minimal inhibitory concentration [µg/ml]
MOI	multiplicity of infection
μ	specific growth rate [h^{-1}]
OD	optical density
P. aeruginosa	*Pseudomonas aeruginosa*
PBS	phosphate buffered saline
PI	propidium iodide

Prot. K	proteinase K
RLU	relative luminescence units
ROI	region of interest
rpm	rotations per minute
SDS	sodiumdodecylsulfate
SEM	scanning electron microscopy
S. aureus	*Staphylococcus aureus*
S. epidermidis	*Staphylococcus epidermidis*
Ti6Al4V	titanium-6 aluminium-4 vanadium alloy
TNF-α	tumor necrosis factor α
TO	thiazolorange
TSB	tryptic soy broth
t_d	doubling time [h]
V_{RMS}	voltage root mean squared / effective voltage
v/v	volume per volume
w/v	weight per volume

List of Figures

Figure 1: Distribution of organisms causing surgical site infection in patients undergoing knee and hip arthroplasty 3

Figure 2: Representative SEM image of *S. epidermidis*. 6

Figure 3: General steps of biofilm formation. 7

Figure 4: Confocal images of Ti6Al4V electrode surfaces including roughness measurements. 16

Figure 5: Technical drawing and realization of the stimulation system. 17

Figure 6: Representative validation setup of the stimulation chamber. 19

Figure 7: Simulations of potential and field distributions inside the stimulation system. 34

Figure 8: Representative growth curves of *S. epiderimidis* in different media.. 36

Figure 9: Representative growth curves of *S. aureus* in different media. 37

Figure 10: Determination of planktonic CFU/ml of *S. epidermidis*. 38

Figure 11: Determination of biofilm-bound CFU/ml of *S. epidermidis*. 39

Figure 12: Quantification of *S. epidermidis* formed biofilms. 40

Figure 13: Representative SEM images of *S. epidermidis* cultivated in TSB..... 41

Figure 14: Representative SEM images of *S. epidermidis* cultivated in DMEM..... 42

Figure 15: Representative SEM images of *S. epidermidis* cultivated in MEM. 42

Figure 16: Determination of planktonic *S. epidermidis* and *S. aureus* following electrical stimulation. 44

Figure 17: Determination of electrode-bound *S. epidermidis* and *S. aureus* following electrical stimulation. 45

Figure 18: Quantification of biofilms formed by *S. epidermidis* and *S. aureus* following electrical stimulation. 47

Figure 19: pH of supernatants of *S. epidermidis* and *S. aureus* samples following electrical stimulation. 48

Figure 20: Quantification of general biofilm formation of *S. epidermidis* and *S. aureus* following electrical stimulation. 50

Figure 21: Determination of composition of *S. epidermidis* and *S. aureus* formed biofilms. 51

Figure 22: Determination of extracellular DNA in *S. epidermidis* and *S. aureus* formed biofilms.. 51

Figure 23: Determination of ATP amounts following electrical stimulation of *S. aureus* in TSB. 53

Figure 24: Population distributions of viable and damaged *S. aureus* following electrical stimulation. 54

Figure 25: Adherence and internalization of *S. epidermidis* on and into hOB and MG63 cells. 56

Figure 26: Adherence and internalization of *S. aureus* on and into MG63 cells. 56

Figure 27: Interleukin-6 secretion of hOB and MG63 cells infected with *S. epidermidis*. 57

Figure 28: MCP-1 secretion of hOB and MG63 cells infected with *S. epidermidis*. 58

Figure 29: Interleukin-6 and MCP-1 secretion of MG63 cells infected with *S. aureus*. 59

Figure 30: Representative SEM images of MG63 cells infected with *S. epidermidis*.... 60

Figure 31: Representative SEM images of hOB infected with *S. epidermidis*. 60

Figure 32: Determination of CFU/ml of *S. epidermidis* during co-culture and electrical stimulation. 61

Figure 33: Cell count of viable MG63 cells following coculture with *S. epidermidis* under electrical stimulation and pH measurements. 62

Figure 34: Determination of planktonic *S. epidermidis* and *S. aureus* following electrical stimulation in TSB with 10^4 CFU/ml inoculum. XVIII

Figure 35: Determination of electrode-bound *S. epidermidis* and *S. aureus* following electrical stimulation in TSB with 10^4 CFU/ml inoculum. XVIII

Figure 36: Quantification of biofilms formed by *S. epidermidis* and *S. aureus* following electrical stimulation in TSB with 10^4 CFU/ml inoculum. XIX

Figure 37: pH of supernatants of *S. epidermidis* and *S. aureus* samples following electrical stimulation in TSB with 10^4 CFU/ml inoculum.. XIX

Figure 38: Minimal inhibitory concentrations of gentamicin following electrical stimulation of *S. epidermidis* and *S. aureus* in TSB with 10^6 CFU/ml inoculum.. XX

Figure 39: Minimal inhibitory concentrations of levofloxacin following electrical stimulation of *S. epidermidis* and *S. aureus* in TSB with 10^6 CFU/ml inoculum.. XX

Figure 40: Minimal inhibitory concentrations of gentamicin following electrical stimulation of *S. epidermidis* and *S. aureus* in TSB with 10^4 CFU/ml inoculum. XXI

Figure 41: Minimal inhibitory concentrations of levofloxacin following electrical stimulation of *S. epidermidis* and *S. aureus* in TSB with 10^4 CFU/ml inoculum. XXI

Figure 42: Minimal inhibitory concentrations of gentamicin following electrical stimulation of *S. epidermidis* and *S. aureus* in DMEM with 10^4 CFU/ml inoculum..XXII

Figure 43: Minimal inhibitory concentrations of levofloxacin following electrical stimulation of *S. epidermidis* and *S. aureus* in DMEM with 10^4 CFU/ml inoculum..XXII

List of Tables

Table 1: Chemicals and enzymes 11

Table 2: Utilized kits 12

Table 3: Laboratory equipment and consumables 13

Table 4: Electric properties of materials and medium used for numerical simulation ... 18

Table 5: Bacterial strains 19

Table 6: Cells and cell lines 29

Table 7: Measured and simulated electric potential of the measurement pattern of the stimulation system in the ROI 34

Table 8 Calculated growth rates and doubling times for *S. epidermidis* 36

Table 9: Calculated growth rates and doubling times for *S. aureus*. 37

Table 10: Parameter settings for electrical stimulation of *S. epidermidis* and *S. aureus* 43

1 Introduction

1.1 Electrical stimulation in clinical practice

Electrical stimulation (ES) is widely applied in different clinical contexts and gained importance in treatment of various diseases and disabilities. Today, various types of electrical stimulation for different tissues are common in clinical use. Deep brain stimulation for treatment of Parkinson's Disease as well as cochlear implants or cardiac pacemaker represent prominent examples (Perlmutter and Mink 2006, Zeng and Fay 2013, Bradshaw *et al.* 2014). Furthermore, therapies combine conventional treatment strategies with ES to approach cutaneous wound-healing complications, paralyzed muscle or muscle atrophy in immobilized patients. Furthermore, ES is applied in pain relief therapy and in treatment of optic neuropathy as well as retina degeneration. (Rushton 2002, Zanotti *et al.* 2003, Kern *et al.* 2005, Kloth 2005, Schatz *et al.* 2011). Another field of application lies within the orthopedic field. Here, electrical stimulating implants or devices are used as supportive therapy in treatment of bone fractures or to improve bone and tissue regeneration (Latham and Lau 2011, Griffin and Bayat 2011, Dolbow *et al.* 2014).

1.1.1 Effects of electrical stimulation on bone cells

Improved fracture healing and, in this case especially, an accelerated bone remodeling after insertion of an implant can be achieved by application of electric or electromagnetic fields (Kraus 1992, Meng *et al.* 2013). Electrical stimulation has shown to be effective in treatment of infected non-unions, as well as failed arthrodesis and osteoporosis. Furthermore, positive effects in treatment of osteonecrosis could be shown (Griffin and Bayat 2011). According to Onibere and Khanna, applications of ES can be grouped into three basic categories. First, invasive bone stimulators or devices, which function by providing direct current via implantable devices. These devices are connected to a generator, which is implanted into the fascia of the lower leg. Second, semi-invasive bone stimulators or devices, involving application of direct current through a Teflon coated stainless cathode, which is inserted percutaneously into the site of the defect. A self-adherent anode is placed on the surface of the skin and is attached to a power pack.

Third, non-invasive bone stimulators or devices, which function by either capacitive and inductive coupling. Capacitive stimulators consist of a power source unit and two electrode disks, which are attached directly to the skin on each non-union. They produce internal electrical fields at a frequency of 60 kilohertz (KHz) with an ideal operating current level between 5 and 10 milliamperes (mA). Inductive coupling, however, uses pulsed electromagnetic fields (PEMF) producing an inductive coupled electromagnetic field at the site of the non-union. This system consists of two external coils placed parallel to each other over the non-union site. The generated fields expand outwards at right angle from the coil bases and thereby penetrate the bone (Onibere and Khanna 2008). Electrical stimulation is a minimally invasive possibility for delayed fracture healing compared with revisions of joints, bones or implant devices (Onibere and Khanna 2008, Kuzyk and Schemitsch 2009). In previous studies, upregulation of different growth factors, e.g. BMPs (bone morphogenetic-proteinases) and TGF-β (tissue growth factor β) in osteoblasts under electrical stimulation were shown. Furthermore, influence on different receptors such as PTH (parathyroid hormone) could be shown (Onibere and Khanna 2008). Electrical stimulation could also be associated with increased cutaneous perfusion supporting wound healing (Thakral *et al.* 2013).

1.1.2 Complications and revision causes

Steady progress in the enhancement of stability and compatibility of orthopedic implants has been made over the last decades. Nevertheless, malfunction, aseptic loosening, but also implant-associated infections impede the clinical success in this field. The number of patients with implant-associated infections or so-called prosthetic joint infections (PJI) is increasing (Tande and Patel 2014).

A successful treatment of PJI is difficult due to the lifelong risk of bacterial infections on the implant surface (Zimmerli *et al.* 2004). PJI can lead to implant loosening and destruction of peri-implant bone tissue followed by complicated treatment and high revision rates of the implants. PJI after total joint arthroplasty occur less frequently than aseptic loosening but cause dramatic complications often combined with substantial bone loss (Steckelberg and Osmon 2000).

Successful treatment of PJI is a significant problem resulting in high recurrent infection rates and failure of antibiotics. This is due to biofilm formation of bacteria on the implant surface and persistence in the host cells.

Both processes decrease the susceptibility of the bacteria towards antimicrobial substances (Costerton *et al.* 1994, Shi and Zhang 2012). In most cases, revision surgery is the only option to eradicate the infection (Klouche *et al.* 2010, Kurtz *et al.* 2012).
A list of microorganisms leading to PJI is shown in Figure 1. *Staphylococcus aureus* and coagulase-negative staphylococci are the most frequently occurring pathogens associated with PJI following joint replacement or bone fracture treatment (Saadatian-Elahi *et al.* 2008, Harrasser *et al.* 2012, Lamagni 2014). Another fact worth mentioning is the increasing number of bacteria which are resistant to commonly used antibiotics. The number of available antibiotics against e.g. methicillin-resistant *S. aureus* or other multiresistant bacterial species is limited. Additionally, treatment with reserve antibiotics often includes various side effects, higher treatment costs and the possibility for resistance development in treated bacterial strains.

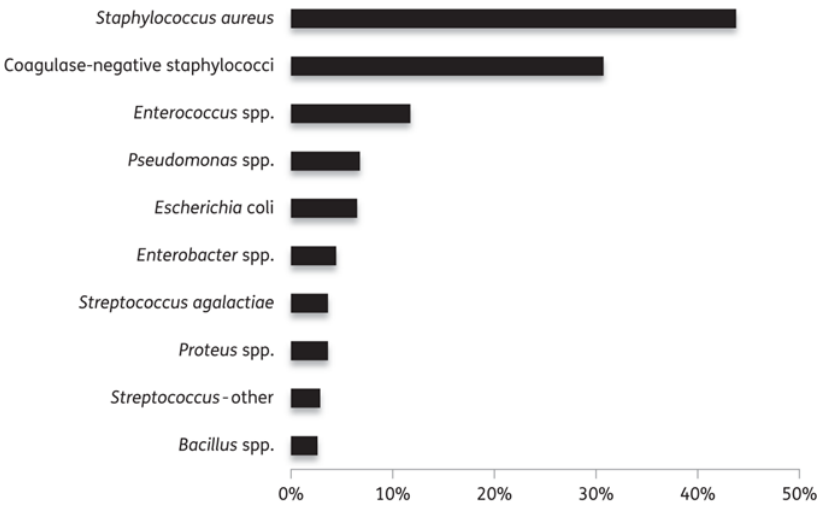

Figure 1: Distribution of organisms (the top 10 ranking organisms are identified to genus/species level) causing surgical site infection in patients undergoing knee and hip arthroplasty (Lamagni 2014)

1.2 Electrical stimulation of bacteria

Electrical stimulation is not only applied on different cell types, it was also used in the last decades to investigate effects on different bacterial species. Different electrical stimulation methods are applied in research, e.g. high-voltage pulsed current (HVPC), direct current (DC) but also alternating current (AC) (Giladi *et al.* 2008, Asadi and Torkaman 2014).

Several studies showed that electric and electromagnetic stimulation have influence and reduction potential of bacterial growth and biofilm formation, e.g. for *Staphylococcus aureus*, *Pseudomonas aeruginosa*, or *Escherichia coli* (Merriman *et al.* 2004, del Pozo *et al.* 2009a, del Pozo *et al.* 2009b, Obermeier *et al.* 2009, Matl *et al.* 2011, Zituni *et al.* 2014). Nevertheless, there are varying application protocols and parameters as well as the choice of the electrode material. Mostly, platinum, gold, or titanium electrodes are used, in varying appearances, e.g. titanium nanotubules, thin gold wires, plates, or rod-shaped electrodes (Ercan *et al.* 2011, Ehrensberger *et al.* 2015). Furthermore, augmentation of inhibitive effects of electrical stimulation in combination with antibiotic treatment could be shown in different studies (Caubet *et al.* 2004, Matl *et al.* 2011, Nodzo *et al.* 2015).

Additionally, different experimental setups concerning the used media exist. Experiments were performed in liquid media, using e.g. two metal plates directly immersed in the culture medium. Other approaches use bacterial cultures transferred in reaction chambers where a surrounding coil induces electromagnetic stimulation. Solid media are also used for experiments, where bacteria are grown and cultivated under different conditions (Obermeier *et al.* 2009, Zituni *et al.* 2014). In general, highest effects on bacteria concerning electrical stimulation are achieved by application of DC, while principle underlying mechanisms are not yet understood (Asadi and Torkaman 2014).

Currently two mechanisms are proposed to be responsible for bactericidal effects of ES, the direct and indirect effect. Direct effects include disruption of bacterial membranes or electrolytic reactions on membrane surfaces. Furthermore, indirect effects include e.g. the development of toxic substances such as H_2O_2 or chlorine molecules through electrolytic reactions in the surrounding medium (Asadi and Torkaman 2014, Sandvik *et al.* 2013). However, most experiments were done *in vitro,* leaving the question of effects of ES on bacteria in a PJI situation open. Despite huge numbers of experimental setups and literature about electrical stimulation, optimal stimulation parameters have not yet been identified and further knowledge about the effects of applied electric fields is needed.

1.2.1 *Staphylococcus aureus*

S. aureus is a Gram-positive, coccoid, coagulase-positive, and non-motile bacterium, which cannot form spores. It appears almost everywhere in nature and can also be found on food. Additionally, it can colonize the skin and mucous membranes of warm-blooded

organism and appears in 20 – 30 % of all humans on the skin and mucous membranes of the upper respiratory tract (Liu 2009).

When cultivated on blood agar, where *S. aureus* appears as white-golden colonies, clear areas around the bacteria appear. Within these areas, erythrocytes and hemoglobins are completely degraded by *S. aureus*, namely called β-hemolysis. Normally, *S. aureus* is a commensal bacterium (according to new definitions called pathobiont) which does not cause infections in healthy individuals. However, if the opportunity arises, *S. aureus* can lead to different types of infections, ranging from superficial lesions to toxin-mediated infections and life-threatening conditions such as endocarditis, osteomyelitis, bacteremia and TSST with sepsis (Aires De Sousa and De Lencastre 2004, Bien *et al.* 2011). It possesses a large variety of different virulence factors, such as adhesins termed Microbial Surface Component Recognizing Adhesive Matrix Molecules (MSCRAMMSs), recognizing extracellular matrix components or plasma components (Lowy 1998, Foster and Höök 1998, Joh *et al.* 1999, Speziale *et al.* 2009). Since antibiotics are widely and often used, antibiotic resistances occur more frequently leading to difficult, expensive, and prolonged treatment of infections, e.g. infections with methicillin-resistant *S. aureus* (MRSA). These resistances challenge successful treatment and diminish the number of potent antibiotics available to prevent life-threatening courses of infections.

1.2.2 *Staphylococcus epidermidis*

S. epidermidis, usually belonging to the commensal skin flora of humans (Grice *et al.* 2009), can occur as facultative pathogenic bacterium in nosocomial infections, especially implant-related infections. It is a Gram-positive, coccoid bacterium appearing mostly in aggregations. *S. epidermidis* is non-motile, forms no spores and belongs to the coagulase-negative staphylococci (CoNS). A representative SEM image of *S. epidermidis* with beginning production of extracellular matrix components is shown in Figure 2. Next to indwelling medical device infections with *S. aureus* as causative agent, the major part of CoNS infections can be assumed to be caused by *S. epidermidis* (Otto 2009). This bacterial species has a variety of virulence factors, and most strains form biofilms. When biofilm formation occurs on an implant surface, this mostly leads to dramatic and challenging treatment issues since bacteria within the biofilm are strongly protected from therapy through different properties of the biofilm. *S. epidermidis* possesses specific

proteins, which impact surface adhesion to abiotic surfaces, e.g. AtlE, which is a bifunctional adhesion/autolysin (Heilmann *et al.* 1997).

Furthermore, *S. epidermidis* can produce the protective expolymers PGA (poly-γ-glutamic acid) and PNAG/PIA (poly-N-acetylglucosamine homopolymer), protecting it from innate host defense mechanisms, such as neutrophil phagocytosis and antimicrobial peptides (Otto 2009). However, underlying mechanisms of *S. epidermidis* infections are poorly understood. In case a *S. epidermidis* infection occurs, treatment is very difficult and often leads to revision of the implant and broad debridement of the surrounding tissue.

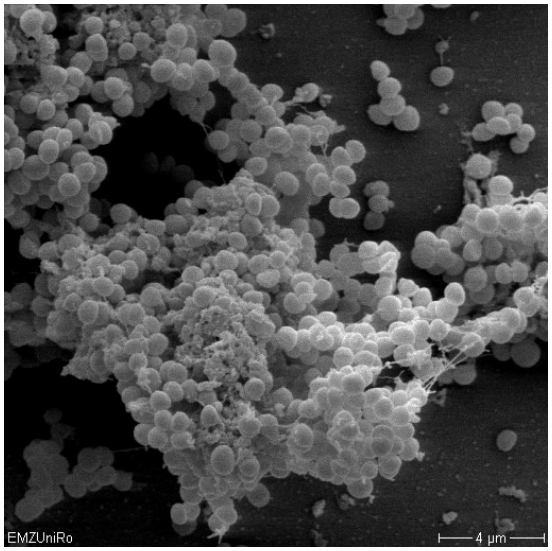

Figure 2: *Representative SEM image of S. epidermidis*. *S. epidermidis* was cultivated on polystyrene coverslips in complex medium TSB over 72 h. Image taken at the Electron Microscopy Center University Medical Center, 5000 x magnification.

1.2.3 Biofilm formation

One major problem in treating implant-associated infections is the ability of nearly all bacteria to form biofilm (Jamal *et al.* 2015). Biofilm formation is a well-regulated complex mechanism and includes five basic steps, schematically shown in Figure 3.

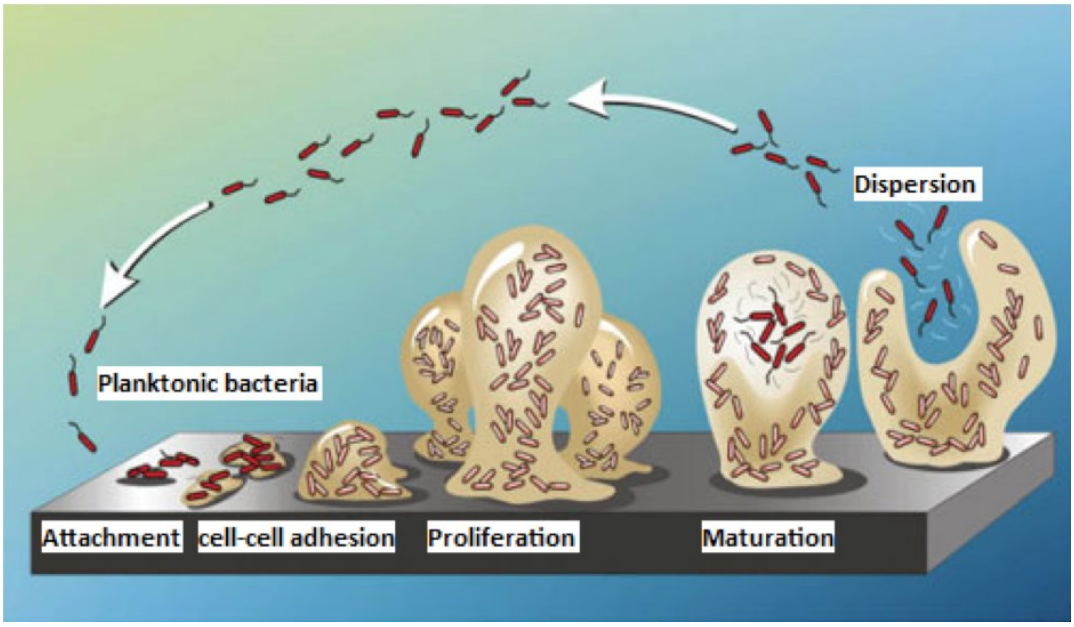

Figure 3: *General steps of biofilm formation.* (Source: https://microbewiki.kenyon.edu/images/8/84/Biofilm.png, 11:55, 18.06.2017)

First, single planktonic bacteria adhere to a specific point, e.g. the implant surface and switch from planktonic phase to a sessile form. The second step is the proliferation of bacteria as well as cell-cell adhesion resulting in the formation of micro-colonies with additional aggregation of more bacteria. Next, the bacteria start to produce extracellular matrix proteins and structures connecting and tightening them, leading to three-dimensional biofilm structures. These structures consist mainly of bacterial cells itself, DNA / RNA, proteins and polysaccharides, though the major component of an intact biofilm is water, responsible for nutrient flow within the biofilm structure. The fourth step is the maturation of the biofilm. Bacteria are proliferating and more extracellular proteins and matrix structures are formed. This complex network is tightly connected and serves different purposes to facilitate and support bacterial survival. The last step is the detachment or dispersal of parts of the biofilm which are transported by e.g. blood or wound liquid to other places, where new biofilms can be formed (Jamal *et al.* 2015, Costerton *et al.* 1999).

Within biofilms, bacteria show reduced metabolic activity, slow growth rates, and are efficiently protected against host immune responses or antimicrobial substances (Sekhar *et al.* 2009, Mah and O'Toole 2001). Diffusion rates inside biofilms are limited. Therefore, antibiotics need a long time to reach deep in the biofilm and are for example degraded through enzymes within the biofilm or matrix-bound substances modifying antimicrobial agents.

Furthermore, the existence of persistent (non-dividing) cells, as well as adaptive mechanisms confer antibiotic resistance and lower the susceptibility to environmental stress factors (Poole 2002). Besides, immune cells of the host cannot penetrate the biofilm and the host immune response is thereby impaired. In case of *S. epidermidis*, bacteria are suppressing the aerobic metabolism, expression of virulence factors and phenol-soluble modulins while activating protective factors and fermentation pathways when bound inside a biofilm (Yao *et al.* 2005).

1.2.4 Interactions with bone

S. epidermidis is more likely to cause dramatic infections due to biofilm formation and less immune response of the host, because it is permanently colonizing the human skin (Otto 2009, Valour *et al.* 2013), *S. aureus* possesses a large variety of factors and substances to interact with different cell types. *S. aureus* can e.g. bind bone extracellular matrix components via multiple adhesins (MSCRAMMs) (Heilmann 2011, Josse *et al.* 2015) or adhere to bone cells through fibronectin-mediated mechanisms (Rasigade *et al.* 2011). Though lacking several virulence factors compared to *S. aureus, S. epidermidis* is also capable of invading bone cells (Shi and Zang 2012, Valour *et al.* 2013). When invading bone cells, *S. aureus* induces the production and secretion of large amounts of interleukin-6 and interleukin-12, as well as monocyte chemoattractant protein-1 (Bost *et al.* 1999, Ning *et al.* 2011), a phenotype is not yet shown for *S. epidermidis*. Additionally, *S. aureus* can induce apoptosis of bone cells, leading to massive bone destruction, due to inflammation and osteoclast activation (Shi and Zang 2012, Josse *et al.* 2015). Besides, *S. aureus* can also persist in osteoblasts and macrophages, while possessing several types of membrane-damaging factors to facilitate its escape from intracellular vesicles (Josse *et al.* 2015, Vandenesch *et al.* 2012). Together, bone infections with *S. aureus* lead to difficult treatment and often recurrent infections due to the protection against antimicrobial substances and the host's immune system by its own cells.

Additionally, *S. aureus* biofilms can impair osteoblast viability, osteogenic differentiation while increasing bone resorption (Sanchez *et al.* 2013). Regarding the interaction of bone cells and *S. epidermidis*, the mechanisms are poorly understood.

Khalil *et al.* 2007 described internalization capability of *S. epidermidis* into osteoblasts, however suggested that internalization does not take place via interaction between bacterial adhesins and α5β1 integrin, as it is possible for *S. aureus* (Khalil *et al.* 2007).

1.3 Aim of the work

The aim of this work is the establishment of a novel *in vitro* implant infection system suitable for bone cells as well as for bacteria. The system design should allow electrical stimulation using sine waves enable studies of electrical stimulation and effects on *S. epidermidis* and *S. aureus*. Currently no *in vitro* system is available which allows combined experiments with cells and with bacteria. However, such a system could serve as base for future studies in the implant infection context. Besides, this work aims to investigate if there are possible electrical stimulation conditions, which benefit osteoblast proliferation, differentiation, and bone healing in general, but at the same time impair bacterial growth and biofilm formation on the implant and in the surrounding area.
The focus in this work lies on electrical stimulation of bacteria, while another associated PhD thesis focusses on electrical stimulation of osteoblast cells using the identical system.

1.4 Interdisciplinary aspect and integration in WELISA

This work is integrated as part M4 in the DFG funded research training group WELISA (GRK 1505/2 welisa). WELISA stands for “Analysis and Simulation of Electrical Interactions between Implants and Biological Systems”. It is an inter- and multidisciplinary research project combining different expertise’s and fields of research. This work focusses on interactions of implants and biological systems, specifically orthopedic implants. Other working groups in WELISA are studying cochlea implants or deep brain stimulation. Within this work, not only microbiological background is needed. To design the stimulation system, engineering knowledge is needed to generate the 3D technical drawings. Another important point are the simulations, which are done in COMSOL with background facts about engineering and mathematics. Besides, specific material properties have to be taken into account for the choice of the chamber material and the electrodes. Since the electrodes are further treated to reach a certain surface roughness occurring in clinically used implants, changes in surface properties of the electrode have to be considered.
In case of the experiments performed with the new stimulation system, the possibility should be considered, that specific electrode reactions could occur, requiring some sort of electrochemical understanding.

Overall, engineering, mathematical, biological as well as chemical, physical, and biological and medical aspects are all combined in this work for the establishment of this stimulation system and the interpretation of the results.

2 Materials and Methods

2.1 Chemicals, Enzymes & Kits

The following chemicals and enzymes were used.

Table 1: Chemicals and enzymes

Chemical/Enzyme	**Manufacturer**
Agar Technical	Oxoid Ltd., Basingstoke, Hampshire, UK
L-Ascorbic acid sodium salt	Sigma-Aldrich Chemie GmbH, Steinheim, Germany
Crystal violet	Fluka Chemie AG, Buchs, Switzerland
Dexamethasone	Sigma-Aldrich Chemie GmbH, Steinheim, Germany
DMEM (1X) /w GlutaMAX, high glucose, pyruvate	Life Technologies, Eugene, OR, USA
Dimethyl Sulfoxide (DMSO)	Merck KGaA, Darmstadt, Germany
EDTA (Ethylendiamine-tetraacetic acid)	Sigma-Aldrich Chemie GmbH, Steinheim, Germany
Ethanol (absolute)	Central Pharmacy of the Hospital of the University of Rostock, Rostock, Germany
Fetal calf serum	Life technologies, Eugene, OR, USA
Gentamicin solution 50 mg/ml	Sigma-Aldrich Chemie GmbH, Steinheim, Germany
Glutardialdehyde solution 25 %	Merck KGaA, Darmstadt, Germany
Glycerin (99 %)	Merck KGaA, Darmstadt, Germany
β- Glycerophosphate disodium salt hydrate	Sigma-Aldrich Chemie GmbH, Steinheim, Germany
Proteinase K	AppliChem GmbH, Darmstadt, Germany
Levofloxacin	Sigma-Aldrich Chemie GmbH, Steinheim, Germany
MEM w/o Ca^{2+}	Biochrom, Berlin, Germany
Potassium Dihydrogenphosphate	Merck KGaA, Darmstadt, Germany

Sodium Chloride	Carl Roth GmbH + Co.KG, Karlsruhe, Germany
Sodium Dihydrogenphosphate monohydrate	Merck KGaA, Darmstadt, Germany
$NaIO_4$ (Sodium metaperiodate)	Merck KGaA, Darmstadt, Germany
SDS (Sodiumdodecylsulfate)	Carl Roth GmbH + Co.KG, Karlsruhe, Germany
di-Sodium Hydrogenphosphate dihydrate	Merck KGaA, Darmstadt, Germany
Sodium Hydroxide	Merck KGaA, Darmstadt, Germany
Trypsin/EDTA solution (1X)	Life Technologies, Eugene, OR, USA
Tryptic Soy Broth	Applichem GmbH, Darmstadt, Germany
Tween 20 pure	Serva Electrophoresis GmbH, Heidelberg, Germany

Utilized Kits are listed in Table 2.

Table 2: Utilized kits

Kit	**Manufacturer**
ATP Determination Kit	Life Technologies, Eugene, OR, USA
BD Cell Viability Kit TO/PI	BD Biosciences, Erebodegum, Belgium
Multiplex ELISA	Biorad Laboratories, Hercules, CA, USA
PromoKine #PK-CA707-30027 Kit	PromoCell GmbH, Heidelberg, Germany

2.2 Laboratory Equipment

Laboratory equipment and materials used for this work are listed in Table 3.

Table 3: Laboratory equipment and consumables

Laboratory Instrument / Consumables	**Manufacturer**
Accuri C6 FACS	BD Biosciences
CellStar Cell Culture Plate (6, 24, 96 well)	Greiner Bio-One GmbH, Frickenhausen, Germany
Cotton Sticks	NerbePlus GmbH, Winsen/Luhe, Germany
Dielectric Broadband Spectrometer	Novocontrol Technologies GmbH & Co. KG, Montabaur, Germany
Eddy Jet spiral plater	IUL instruments, Barcelona, Espana
E-Test Gentamicin 0.016-256 µg/ml	bioMérieux SA, Marcy-l'Etoile, France
E-Test Levofloxacin 0.002-32 µg/ml	bioMérieux SA, Marcy-l'Etoile, France
Function Generator Metrix GX305	Chauvin Arnoux GmbH, Kehl/Rhein, Germany
Biozero-BZ8000 fluorescence microscope	Keyence, Osaka, Japan
Luminometer Lumat LB9501	Berthold Technologies GmbH & Co. KG, Bad Wildbad, Germany
Nunc Thermanox Coverslips (13, 25 mm diameter)	Thermo Fisher Scientific, Waltham, MA, USA
pH meter WTW series Typ pH720	WTW GmbH, Weilheim, Germany
Ribolyser precellys 24	VWR International GmbH, Erlangen, Germany
Secusept	Ecolab Deutschland GmbH, Monheim am Rhein, Germany

Sonorex Digital 10P Ultrasonic Bath	Bandelin electronic, Berlin, Germany
Spectrophotometer SmartSpec™ 3000	Biorad-Laboratories, Hercules, CA, USA
Spectrophotometer SpectraMax M2	Molecular Devices, Sunnyvale, CA, USA
Sterifix® injection filters (0.2 µm)	B. Braun Melsungen AG, Melsungen, Germany

The following software was used:

- BD Accuri C6 Software (BD Biosciences, Erebodegum, Belgium)
- GraphPad Prism 6.01 (GraphPad Software, Inc., CA, USA)
- Microsoft Office 2010 / 2013 (Microsoft Corporation, Redmond, WA, USA)
- WinDeta Software (Novocontrol Technologies GmbH & Co. KG, Montabaur, Germany)
- Windows 7 (Microsoft Corporation, Redmond, WA, USA)
- Softmax Pro V. 5.4 (Molecular Devices, Sunnyvale, CA, USA)

2.3 Construction of the stimulation system

2.3.1 Basic idea and purpose of construction

Over the past decades, electrical stimulation *in vitro* was carried out investigating different microorganisms and eukaryotic cell lines. However, methodical and experimental setups display a huge variety depending on the focus of the investigation. So far, no stimulation system appropriate for basic research was established combining the possibilities of stimulating both microorganisms and cells under similar yet defined conditions. Therefore, our goal was the construction of a stimulation system enabling experiments with bone cells as well as bacteria under similar conditions.

The generated system should be suitable for basic research and should offer a broad range of applicable methods for investigation of effects of electrical stimulation. Although direct current is discussed as a more potent stimulation method than alternating current in literature, we chose alternating current as the stimulation method for this system. This is due to the fact, that our starting parameter setting should somehow get near to the clinically used ASNIS screw system, which is working with alternating current and defined frequency and stimulation periods in patients. It is important to state that the generated system should not serve as opportunity to evaluate clinically observed effects of electrical stimulation or to mimic an implant-infection situation. It should solely serve as an experimental tool suitable for widespread basic research of effects of electrical stimulation on different bacteria and cells under similar conditions and the underlying mechanisms. The system enables three basic aspects to be investigated, which are:
1) bacterial growth and behavior in the supernatants, 2) changes of bacterial attachment and survival on the electrode surfaces and 3) biofilm formation on the chamber bottom, which was realized by a coverslip on the chamber bottom and further staining of formed biofilm mass.

2.3.2 Construction of the stimulation chamber

Foto Med® LED.A (Innovation MediTech GmbH, Unna, Germany) was chosen as material for the construction of the stimulation chamber. The material can be sterilized, which is an essential part in handling and experimental design, when working with bacteria. Furthermore, it provides biocompatible properties fulfilling the DIN ISO 10993. An additional advantage is the fact, that this material is non-conductive, serving as an isolator of the generated electric field inside the chamber to the surrounding area. Electrodes were generated in a triangular shape to allow seeding of cells as well as bacteria directly on the electrode surface. Length of the electrodes measures 23 mm with an equilateral base of 5 x 5 x 5 mm. Electrode and contact rods, enabling connection of voltage supply to electrodes, were produced of Ti6Al4V. Contact rods were produced by cutting and purchased from Primec GmbH (Bentwisch, Germany). These rods were screwed together with electrodes via threads. Electrodes were modified by corundum blasting reaching a surface roughness of 21.38 ± 4.67 µm, analyzed with the laser scanning microscope Keyence VK-X260 (Keyence Deutschland GmbH, Neu-Isenburg, Germany).

Images of roughness measurement and electrode surface are presented in Figure 4. A polyether ether ketone (PEEK) part of 5 mm width between the electrodes serves as insulator to allow application of alternating current to the system. Triangular electrodes with insulator and contact rods are shown in Figure 5D. Three-dimensional technical drawings generated with CAD software as well as top view of the technical drawing, including a coordinate grid used for validation, are shown in Figure 5A and 5B. Geometric scales of the generated chamber measure 54 x 54 x 26 mm. Additional components of the stimulation system are a lid containing holes for contact rods and an electrode holder shown in Figure 5C. A distance of 5 mm between chamber bottom and electrodes was chosen to allow investigations of electric field effects on e.g. biofilms in short distance to the electrodes.

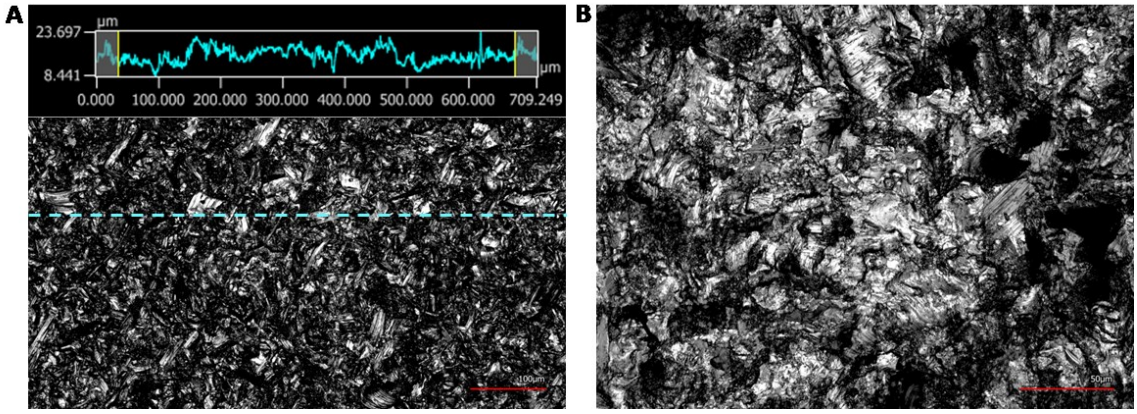

Figure 4: Confocal images of Ti6Al4V electrode surfaces including roughness measurements. **A:** Confocal 3D laser scanning image of the surface roughness measurement of corundum-blasted Ti6Al4V electrodes with 20x magnification. Dashed horizontal line shows the measured path with respective roughness values above. Red bar represents 100 µm. **B:** 40x magnified image of the surface of a corundum-blasted Ti6Al4V electrode. Red bar represents 50 µm. (Dauben *et al.* 2016)

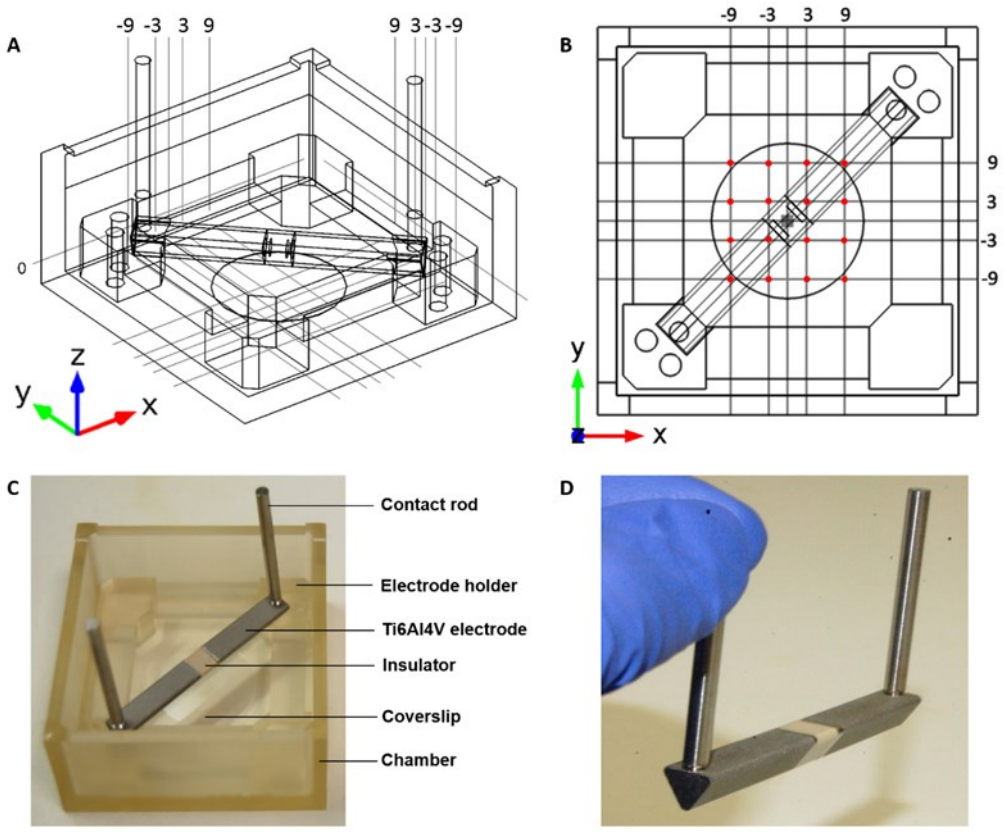

Figure 5: Technical drawing and realization of the stimulation system. **A:** Three-dimensional technical drawing of the stimulation system including coordinate grid and round coverslip on bottom. **B:** Top view technical drawing of the stimulation system with coordinates. Red dots show coordinates where measurements for validation were done. **C:** Composition of the electrical stimulation chamber. **D:** Triangular electrodes with contact rods separated by insulator. (Dauben *et al.* 2016)

2.3.3 Simulation and validation of electric field distribution

To compute electric field distributions within the CAD model of the stimulation system, the finite element method (FEM) software of Comsol Multiphysics (Comsol Multiphysics 5.2, COMSOL, Stockholm, Sweden) was used. Frequency-dependent medium and electrode electric properties were previously determined under defined conditions using a Broadband Dielectric Spectrometer located at the Department of Physics, University of Rostock (Novocontrol, Montabaur, Germany). Relevant values were subsequently embedded in numerical simulations. Numerical simulations were done assuming full assembly of the stimulation chamber including electrode holder, electrodes as well as medium done in Solidworks software. Numerical simulation and validation are described as follows: In Comsol a Frequency Domain Study with a harmonic excitation of 20 Hz and an Electric Currents Physics was created. The mesh was arranged as a free tetrahedral mesh, consisting of approximately 1.63 million mesh cells.

To compare and validate the simulation of the electric field distribution with the *in vitro* situation, a simulation was performed using a RMS voltage of 1.35 V. Used electrical properties of materials for numerical simulation are presented in Table 4. Potentials inside the chamber were measured as V_{RMS} using 20 Hz frequency, 1.35 V_{RMS} and DC-free sine wave. The measuring needle was a completely isolated stainless-steel needle (20 mm in length) with a conical tip of 0.4 mm diameter as contact surface. The measuring needle was grounded to one contact rod of the stimulation system and connected to an oscilloscope (TDS 2012B, Tektronix, Bracknell, Berkshire, UK). V_{RMS} measurements were done at defined coordinates in a 3 mm distance pattern plotted on the center of the chamber bottom according to the measurement grid (Figure5B). V_{RMS} at the defined grid points were manually measured directly at the chamber bottom and measurements were repeated three times.

To prevent external influence of the generated electric field, all technical devices except function generator and oscilloscope were switched off during the measurements. Measured V_{RMS} were then compared to RMS voltages given by numerical simulation. (Dauben *et al.* 2016). The validation set-up is shown in Figure 6.

Table 4: Electric properties of materials and medium used for numerical simulation (Dauben *et al.* 2016)

Material	Relative permittivity ε_r [1]	Electrical conductivity σ [S/m]	Reference
air	1	0	Comsol (ideal)
insulator	4	1.00E-11	Comsol (ideal)
Ti6Al4V	1	5,62E+05	[31]
medium	1.08E+08	1.14E-01	measured

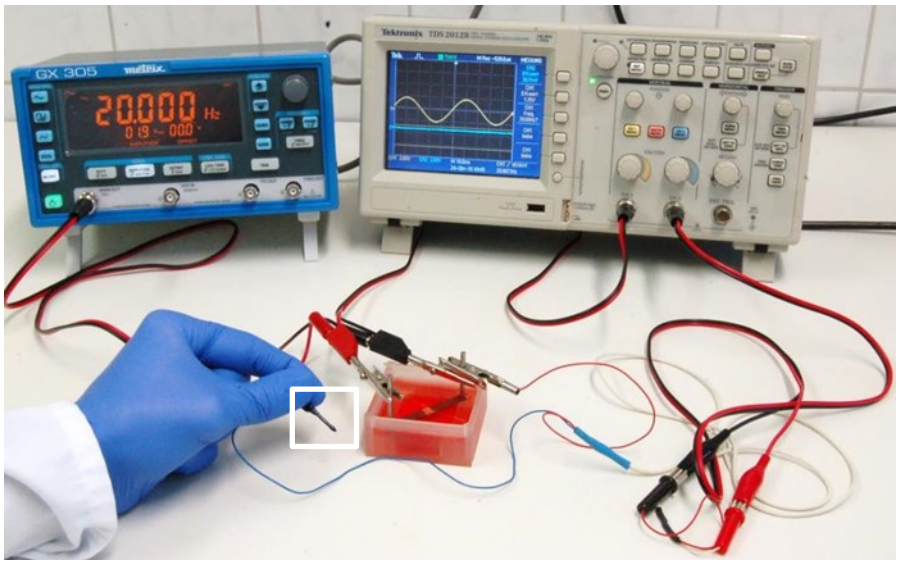

Figure 6: Representative validation setup of the stimulation chamber. Representative image of the setup for validation of electric potential distribution obtained from numerical simulations within the stimulation system. Electric potentials were measured with a pick-up electrode (white frame) connected to an oscilloscope (Dauben *et al.* 2016).

2.4 Bacteria

2.4.1 Bacterial Strains

Bacterial strains used during this work are listed in Table 5.

Table 5: Bacterial strains

Bacterial strains	**Origin**	**Laboratory Collection No.**
Staphylococcus aureus subsp. *aureus* Rosenbach (ATCC® 25923™)	Clinical isolate 1945, ATCC	4735
Staphylococcus epidermidis (Winslow & Winslow) Evans (ATCC® 35984™)	Catheter Sepsis, Tennessee, ATCC	4734

2.4.2 Cultivation and preservation

Bacteria were cultivated from glycerin stocks on blood agar plates overnight and were then stored at 4 °C up to 3 – 4 weeks before passaging onto fresh blood agar plates.

Both *S. aureus* and *S. epidermidis* were cultivated in tryptic soy broth (TSB) complex medium, where 20 ml TSB were inoculated with colony material from glycerin stocks by using a sterile inoculation loop.
The ingredients for 1 l medium were as follows:

TSB medium

TSB	24.0 g
pH	7.5
A. dest.	*ad* 800 ml

TSB medium was sterilized by autoclaving for 20 min at 121 °C and 2 bar,
To produce solid media 1.5 % (w/v) agar was added to the medium before sterilization.

Overnight cultures of *S. aureus* were additionally shaken at 180 rpm at 37 °C while overnight cultures of *S. epidermidis* were incubated without shaking at 37 °C under 5 % CO_2 atmosphere.
For long-term storage of bacterial strains, 200 µl glycerin (99 % [v/v]) were added to 800 µl of an overnight culture and stored at -20 °C and -80 °C, respectively.

2.4.3 Growth experiments

Since staphylococcal infections can occur after joint transplantation, the growth behavior of *S. aureus* and *S. epidermidis* was investigated in standard cell culture medium DMEM as well as in medium suitable for human primary osteoblasts (MEM). Complex medium TSB served as reference for optimal growth. Growth experiments were performed in 96 well plates over 24 h using the spectrophotometer SpectraMax M2. Optical densities (OD) at 600 nm were measured every 30 min until 24 h after inoculation. For washing steps, if not otherwise noted, 1 x Phosphate Buffered Saline (PBS), was used. 10 x PBS consisted of the following components:

NaCl	1.37	M
KCl	0.027	M
Na_2HPO_4 *2 H_2O	0.1	M
KH_2PO_4	0.02	M

pH adjusted to 7.4 with NaOH

A. dest. *ad* 1000 ml

PBS was sterilized at 121 °C and 2 bar for 20 min before use.

Bacterial cultures were prepared according to the following protocol:

1. Inoculation of the respective bacterium into 20 ml TSB
2. Incubation at 37 °C under 5 % CO_2 atmosphere (*S. epidermidis*) or without CO_2 but additional shaking at 180 rpm (*S. aureus*) overnight
3. Centrifugation of overnight cultures for 10 min at 3.345 g
4. Washing of the pellet with sterile 1 x PBS
5. Centrifugation for 5 min at 3.345 g
6. Repetition of step 4 and 5
7. Suspension of the pellet in 1 ml of TSB, DMEM / or MEM
8. Adjustment of optical density at 600 nm to 0.35 (*S. epidermidis*) or 1.5 (*S. aureus*); 0.35 or 1.5 represent approximately 10^8 Colony forming units per ml (CFU/ml) bacteria, respectively
9. Dilution of the bacterial suspension 1:10 in the respective medium
10. Adding of 200 µl of the dilution to wells in a 96 well plate
11. Incubation over 24 h at 37 °C using the SpectraMax M2

Data points of measured optical densities were transferred to Microsoft Excel at the end of the experiment and specific growth rates as well as doubling times were further calculated using the following formulas:

Specific growth rate μ: $$\mu = \frac{log(x(t_2)) - log(x(t_1))}{log(e) * (t_2 - t_1)}$$

Doubling time t_d: $$t_d = \frac{ln(2)}{\mu}$$

2.4.4 Biofilm formation on solid materials

Growth and biofilm formation on titanium aluminum vanadium samples (Ti6Al4V) with an average RZ value of 20 were tested in TSB as well as DMEM and MEM. Both DMEM and MEM were supplemented with 10 % FCS. Further supplemental substances are noted in 2.5.1. Since biofilm formation could not be detected for *S. aureus* in preliminary experiments, only *S. epidermidis* was used for these experiments. The preparation of the experiment was according to the following protocol:

1. Inoculation of an overnight culture in 20 ml TSB and incubation overnight under appropriate conditions (see 2.4.3)
2. Centrifugation of the overnight culture for 10 min at 3.345 g
3. Washing of the bacterial pellet with 1 x PBS (once when TSB was used, twice when cell culture media were used)
4. Suspension of pellet in 1 ml of the respective medium
5. Adjustment of the optical density at 600 nm to 0.35, matching ~ 10^8 CFU/ml
6. 100-fold dilution in respective medium to reach final starting concentration of 10^6 CFU/ml
7. Adding of 1 ml/well bacterial suspension to 24 well plates consisting of 6 wells with polystyrene coverslips (Nunc Thermanox Coverslips, 13 mm) and 6 wells with Ti6Al4V samples
8. Adding of fresh medium without bacteria to 2 wells with coverslips and 2 wells with titanium samples serving as controls
9. Incubation over 24, 48 and 72 h

Every 24 h up to 72 h incubation, three wells containing coverslips and Ti6Al4V samples were used to determine planktonic CFU/ml and CFU/ml of biofilm-bound bacteria on test samples. Remaining wells were used to determine biofilm mass using crystal violet staining. Crystal violet, in this case, stains mainly biofilm proteins and extracellular matrix (ECM) structures and absorbance was measured at 590 nm allowing a relative quantification of formed biofilms.

To determine planktonic CFU/ml, supernatants from each well were collected in separate tubes and wells were washed twice with 1 x PBS. Washing fractions were pooled with respective supernatant to collect all planktonic bacteria. Next, all samples were centrifuged for 10 min at 3.345 g and supernatants were discarded.

Bacteria were suspended in 1 ml 1 x PBS and different dilution steps were plated out using the EddyJet spiral plater. Plates were incubated at 37 °C under 5 % CO_2 atmosphere overnight. CFU/ml were enumerated the following day.

To determine living biofilm-bound bacteria on test surfaces, coverslips and Ti6Al4V samples were washed twice with 1 x PBS to remove all planktonic bacteria. Subsequently, samples were then transferred into glass tubes containing 1 ml 1 x PBS and were ultrasonically agitated using a Sonorex Digital 10P ultrasonic bath for 4 min at 100 % to remove the formed biofilm including bound bacteria. Samples were then vigorously vortexed and serial dilutions were plated. Plating and determination of CFU/ml followed the same principle used for the supernatants. One well with medium and test samples was treated the same way serving as control.

Regarding quantification of biofilm mass, coverslips and Ti6Al4V samples were washed twice with 1 x PBS and transferred to a new well. 1 ml 0.1 % crystal violet was added to each well and samples were incubated for 20 min at room temperature. Stained samples were washed three times with *Aqua dest.* to remove excess crystal violet. Subsequently, bound crystal violet was dissolved by adding 1 ml 1 % SDS and shaking for 20 min at 37 °C with 350 rpm. 500 µl supernatant were transferred to plastic cuvettes and absorbance was measured at 590 nm using a spectrophotometer against 1 % SDS blank. Absorbance values of control wells were subtracted from the sample values afterwards. Experiments were performed with three biological replicates and each with at least two technical replicates.

2.4.5 Scanning Electron Microscopy

To image formed biofilm on both plastic coverslips and titanium surfaces, scanning electron microscopy was used. Samples were washed once with 1 x PBS and subsequently immersed in fixation buffer (0.1 M $Na_2HPO_4*2H_20$ / 0.1 M $NaH_2PO_4*H_20$, pH 7.3) supplemented with 2.5 % glutaraldehyde for at least 24 h. Samples were then dehydrated using an increasing ethanol gradient and were subsequently dried following the critical point drying protocol of the Electron Microscopy Center, University of Rostock. Dried samples were sputtered with gold and imaged using a Merlin VP Compact scanning electron microscope (Zeiss, Jena, Germany).

2.4.6 Electrical stimulation protocol

All pieces of the stimulation system were assembled under sterile conditions prior to the experiments. Polystyrene coverslips with 25 mm diameter were attached to the center of stimulation chambers using silica gel.

Subsequently electrode holder were put into the chambers and two electrodes with respective contact rods were attached to the holders. While drying the silica gel, overnight cultures of bacteria were centrifuged for 10 min at 3.345 g and the pellet was suspended in TSB. OD was adjusted to 0.35 (*S. epidermidis*) or 1.5 (*S. aureus*) and 300 µl of the suspension were added to 29.7 ml fresh TSB. 30 ml of bacterial suspension with a final concentration of ~ 10^6 CFU/ml were added to the chamber and the chamber was closed with a lid. Gaps between contact rods and lid were sealed with parafilm and the stimulation chambers were transferred into the incubator and connected to a time-switch and a Metrix GX305 function generator.

Desired stimulation periods as well as stimulation parameters (frequency, V_{RMS}) were adjusted and the stimulation was started. During the experiments, stimulated and non-stimulated chambers were incubated at 37 °C under 5 % CO_2 atmosphere.

The basic parameter constellation comprised of 20 Hz frequency, 0.2 and 1.4 V_{RMS} (effective voltage), 3 x 45 min with 225 min interval per day starting directly after adding of the bacteria.

Experiments were performed, if not otherwise noted, with at least four biological replicates.

2.4.6.1 Determination of CFU/ml from the supernatant

Supernatants from control and stimulated samples were collected and stimulation chambers were washed twice with PBS to remove all non-adherent bacteria. Washing fractions and supernatants of corresponding samples were pooled and centrifuged for 10 min at 3.345 g. Supernatants were discarded and pellets were suspended in 1 x PBS. Serial dilutions were plated out on TSB agar plates and incubated overnight at 37 °C under 5 % CO_2 atmosphere. Respective CFU/ml were determined on the following day.

2.4.6.2 Antibiotic resistance

Since it was shown, that electrical stimulation in addition to antibiotic treatment further enhances bactericidal effects, possible changes in antibiotic sensitivity of the treated bacteria were investigated. Therefore, the so-called E-Test was performed with gentamicin and levofloxacin (purchased from Biomérieux, France) after electrical stimulation or without electrical stimulation in case of unstimulated samples. Gentamicin was chosen because *S. epidermidis* was resistant against this antibiotic (previously tested by the Resistance Laboratory, Institute of Medical Microbiology, Virology and Hygiene, University Medical Center Rostock) while being sensitive towards levofloxacin. *S. aureus* was tested sensitive towards both antibiotics. Both antibiotics are incapable of penetrating the cell membrane of eukaryotic cells, which is relevant for adherence and internalization assays described later.

Samples of supernatants were diluted in 1 x PBS adjusting optical density to match approximately 10^7 CFU/ml. Cotton swab sticks were immersed for 10 s in the bacterial suspension and bacteria were subsequently spread out evenly on TSB agar plates. In the following, E-Test stripes with gentamicin and levofloxacin were opposite aligned on the respective agar plates and plates were incubated overnight at 37 °C under 5 % CO_2 atmosphere. On the following day, minimal inhibitory concentrations (MIC [µg/ml]) of both antibiotics were determined resembling the highest concentration where bacteria at least reached the antibiotic stripe before inhibition zones appeared.

2.4.6.3 Determination of CFU/ml from the electrode surface

Electrodes were removed from the stimulation system and rinsed two times with 1 x PBS to remove non-adherent bacteria and subsequently transferred into glass tubes containing 1 x PBS. Electrodes were ultrasonically agitated to remove all adherent bacteria. Suspensions containing former surface-bound bacteria were centrifuged for 10 min at 3.345 g, supernatants were discarded and pellets were suspended in 1 x PBS. Serial dilutions were plated out on TSB agar plates and incubated overnight at 37 °C under 5 % CO_2 atmosphere. Respective CFU/ml were determined on the following day.

2.4.6.4 Quantification of biofilm mass

To assess the influence of electrical stimulation on biofilm formation in the surrounding area of the electrode, coverslips at the bottom of the chamber were used for biofilm mass quantification. Polystyrene coverslips were removed from the chamber bottom and rinsed twice with 1 x PBS. Biofilm mass was stained using 0.1 % w/v crystal violet dissolved in *Aqua dest.* for 20 min at room temperature. Subsequently, coverslips were washed three times with *Aqua dest.* to remove excess crystal violet. Bound crystal violet was dissolved in 1 % SDS for 20 min at 37 °C with 350 rpm. Subsequently, absorption was measured at 590 nm against 1 % SDS as blank. Measured values were further calculated regarding the surface area to determine formed biofilm mass / cm^2.

2.4.6.5 pH measurement

To measure potential pH shifts caused by electrical stimulation, samples from supernatants of controls and stimulated samples were taken at each time point and pH was measured using a calibrated pH-meter. pH measurements were only done for stimulation experiments using DMEM.

2.4.6.6 Quantification of biofilm mass following electrical stimulation

Samples from the supernatant used for antibiotic resistance analyses and from the electrode surface following 72 h of incubation and stimulation were diluted 10-fold in fresh TSB. Three wells of a 24 well plate containing polystyrene coverslips were filled with each 1 ml per sample and incubated subsequently for 72 h at 37 °C under 5 CO_2 atmosphere. Following incubation, supernatants were removed and wells were washed with PBS. Supernatants and respective washing fractions were pooled and stored for biofilm composition assay. Coverslips were stained with 0.1 % crystal violet, wells were washed with *Aqua dest.*, bound crystal violet was dissolved using 1 % SDS and absorption was measured at 590 nm. This assay was done only for experiments using DMEM.

2.4.6.7 Determination of biofilm composition

Pooled samples from biofilm formation following electrical stimulation were centrifuged and pellets were suspended in PBS. Samples were diluted 10-fold in fresh TSB and 200 µl were added to each 2 wells using four 96 well plates. On one plate, 200 µl of fresh TSB were added to 4 wells as controls. All four plates were incubated 24 h at 37 °C under 5 % CO_2 atmosphere. Following incubation, the 96 well plate with the medium samples was used as control plate. Supernatants were removed and wells were washed with PBS. Formed biofilm was stained for 2 – 3 minutes with 1.6 % crystal violet and consecutively wells were washed three times with *Aqua dest.* The control plate was dried for 1 h at 67 °C using a static heating block and absorption was measured with a SpectraMax plate reader at 492 nm according to the protocol **(**modified following personal communication with PD Dr. Wilma Ziebuhr, IMIB Würzburg, Germany). The obtained values served as reference / untreated samples during this assay.

For the second plate, supernatants were removed, wells were washed with PBS and 200 µl of 40 mM $NaIO_4$ was added to each well to dissolve carbohydrate components of the formed biofilm. The plate was wrapped in aluminum foil and incubated 24 h at 4 °C. Subsequently, $NaIO_4$ was removed, wells were washed twice with PBS, stained and measured with the same protocol as the control plate.

In case of the third plate, supernatants were removed, wells were washed with PBS and 200 µl of 1 mg/ml Proteinase K was added to each well to dissolve all protein components of the biofilm. The plate was then incubated for 4 h at 37 °C under 5 % CO_2 atmosphere and static conditions. Following incubation, wells were treated as described above following $NaIO_4$ treatment.

The fourth plate was used to stain and measure the amount of extracellular DNA in the formed biofilm. For this purpose, supernatants were removed and cells were washed with PBS. Extracellular DNA was consecutively stained using 1x “dead stain” (ethidium homodimer III, EthD-III) of the PromoKine #PK-CA707-30027 Kit for 30 min in the dark at room temperature. After incubation, wells were washed twice with PBS and fluorescence was measured at 535 / 595 nm using a SpectraMax M2 plate reader (Molecular Devices, Sunnyvale, CA, USA). This assay was done only for experiments using DMEM.

2.4.6.8 Determination of ATP concentration

ATP is normally intracellularly used and not released into the medium. ATP is released, if the cell wall of bacteria is compromised, so the bacteria are either damaged or dead. To investigate possible damage during electrical stimulation, samples of supernatants were removed after 24, 48 and 72 h of electrical stimulation and non-stimulated samples. Samples were centrifuged and supernatants were transferred to new tubes. Bacteria were lysed using a ribolyser for determination of intracellular ATP amount. Extracellular ATP concentrations were determined using the supernatant after centrifugation. The ATP determination kit (ATP Determination Kit, Life Technologies, Eugene, OR, USA) was used for these experiments and samples were treated according to manufacturer's instructions. The utilized kit is based on luminescence intensity measurement. Luciferase converts a substrate under consumption of ATP. The substrate is luminescent and the intensity, which is equal to the amount of converted substrate, was measured using a Lumat LB 9501 luminometer.

In principle, since ATP consumption is linear to the conversion of substrate into the luminescent product, ATP concentrations can be calculated. This method is also suitable to get a relative impression of changes in intra- and extracellular ATP ratios.

Measurements of ATP concentrations were done only once when stimulating *S. aureus* with 1.4 V_{RMS} using an inoculum of 10^6 CFU/ml in complex medium TSB.

2.4.6.9 Fluorescence activated cell-sorting / FACS analyses

Since determination of CFU/ml only includes viable and culturable bacteria, the TO/PI Bacterial Viability Kit was used in connection with an Accuri C6 Flowcytometer. Bacteria or cells are detected with so called forward / sideward detectors, giving an overview about the size and possible aggregation of the tested organisms. Furthermore, bacteria and eukaryotic cells can be stained with fluorescent dyes and, in this case, four fluorescence detectors with different wavelengths can detect the signals. With the help of the Accuri C6 Software the forward and sideward scatter signals as well as the fluorescence signals can be used to distinguish different populations of bacteria or cells, e.g. living and dead bacteria.

The principle of TO/PI staining is, that thiazolorange (TO) stains all cells/bacteria, regardless if living or dead, to different intensities. On the contrary, propidium iodide (PI) stains DNA and cannot pass the cell membrane of intact cells/bacteria.

If the cell membrane is damaged, PI can enter the cells/bacteria, stains the DNA and these cells/bacteria will be detected from the respective fluorescence detector. To test, whether electrical stimulation influences or even kills the bacteria, samples from the stimulated and non-stimulated supernatants were taken and treated according to the manufacturer's instructions.

FACS analyses were done only once when stimulating *S. aureus* with 1.4 V_{RMS} using an inoculum of 10^6 CFU/ml in complex medium TSB.

2.5 Cells and cell lines

Used cells and cell lines are shown in Table 6.

Table 6: Cells and cell lines

Cell /Cell Line	Origin
MG63 osteosarcoma cell line ATCC® CRL-1427™	Homo sapiens bone osteosarcoma cell line, LGC Standards GmbH, Wesel, D
Human osteoblasts (hOB)	Isolated from patient hips

2.5.1 Cell culture and preservation

MG63 cells were cultured in DMEM high glucose supplemented with 1 % GlutaMAX, 1 % pyruvate as well as 10 % FCS.

Human primary osteoblasts were cultured in MEM supplemented with HEPES and 10 % FCS, 10 mM β-glycerolphosphate, 50 µg/ml ascorbic acid and 0.1 µM dexamethasone.

MG63 cells were cultivated in DMEM. hOB were cultivated in MEM. Cells were splitted when 80 – 95 % confluence was reached.

During splitting, the medium was removed and the cells were washed once with 1x PBS. Afterwards, 2 ml 0.5 % Trypsin-EDTA solution was added to the cells and the cells were incubated for 3 minutes at 37 °C to detach the cells from the surface. The detachment process was stopped by adding 8 ml of the respective culture medium and the cell suspension was transferred into a sterile tube and centrifuged at 300 g for 10 min. The supernatant was removed and the cells were suspended in 5 ml fresh culture medium. Depending on the cell number, a part of the suspension was added to a new cell culture flask and fresh culture medium was added to reach 20 ml final volume.

Cells were further incubated at 37 °C under 5 % CO_2 atmosphere. Regarding experiments, MG63 cells were used until reaching passage 50, while hOB were solely used in passage 3.

Respective cell culture media were changed every 2 – 3 days until cells were used.

For long term storage, cells were cultivated until 90 - 95 % confluence, removed from the cell culture flask, and were stored in cell culture medium and dimethyl sulfoxide (DMSO) in liquid nitrogen.

2.5.2 Adherence and internalization assay

MG63 cells or human primary osteoblasts were removed from the cell culture flasks, were seeded into two 24 well plates with a density of 40.000 cells / ml and were incubated overnight at 37 °C under 5 % CO_2 atmosphere to allow adherence to the well plate. Cells were seeded into 3 x 3 wells for adherence and 3 x 3 wells for internalization to allow the investigation of three infection doses at the same time point. Multiplicities of infection (MOI) were chosen to be 1:1, 10:1 and 100:1 bacteria per osteoblast.

Meanwhile, overnight cultures of *S. epidermidis* or *S. aureus* in TSB were prepared and incubated under the conditions described in 2.5.1. On the following day, overnight cultures were centrifuged for 10 min at 3.345 g and washed twice with 1 x PBS. Bacteria were then suspended in DMEM, when MG63 cells were used, and in MEM, when primary osteoblasts were used. Optical density was adjusted to 0.35 or 1.5 respectively and MOIs were prepared with 10^4, 10^5 and 10^6 CFU/ml in the respective medium to reach desired MOI values.

Supernatants from osteoblast cells were removed and cells were washed once with 1 x PBS to remove FCS residues. FCS can coat the surface of osteoblasts and interferes with adherence and internalization ability. Therefore, the medium used for the adherence step contained no FCS.

1 ml bacterial suspension with the respective MOI was added to three wells of the adherence and three wells of the internalization plate. Additionally, 1 ml of each suspension were added to empty wells on the adherence plate and served as growth control of the bacteria. Both 24 well plates were incubated for 2 h at 37 °C under 5 % CO_2 atmosphere to allow adherence of bacteria onto the tested cells.

After two hours, supernatants of both plates were removed, sterile filtered using a 22 µm filter and stored at -20 °C until further use. 1 ml of DMEM or MEM containing 200 µg/ml levofloxacin were added to each well of the internalization plate to kill adherent bacteria. Levofloxacin cannot penetrate the membrane of cells and therefore kills only adherent bacteria, while internalized bacteria remain vital. This plate was incubated for an additional hour at 37 °C under 5 % CO_2 atmosphere. Following incubation, supernatants were removed and cells were washed once with 1 x PBS.

Wells containing cells and bacteria on both adherence and internalization plates were treated similar after incubation. 200 µl trypsin-EDTA solution were added and plates were incubated for 5 min at 37 °C. Cells from wells of the same MOI were pooled and respective wells were washed with 1 x PBS. Washing fractions were additionally added to respective pooled samples. Next, cells with adherent and internalized bacteria were centrifuged for 2 min at 11.000 g rpm, supernatants were removed and cells were lysed for 10 min in *Aqua dest.* with periodic shaking. Subsequently, different dilutions were plated out on TSB agar. 100 µl of control wells with only bacteria were taken, serially diluted and plated on TSB agar to determine bacterial growth within the two hours of adherence. All plates were incubated overnight at 37 °C under 5 % CO_2 atmosphere. CFU/ml were determined the following day. Additionally, 100 µl of supernatants following antibiotic treatment were plated out to check for proper eradication of bacteria during incubation with levofloxacin.

Experiments were performed at least four times and in case of hOB with different osteoblast donors.

2.5.3 Cytokine ELISA

Supernatants from adherence and internalization assays were collected, sterile filtered and stored at -20 °C until use. Samples were taken either following 2 h of adherence or after a prolonged internalization time combined with antibiotic treatment over 24 h. Cells cultured in the respective medium for 2 h or with antibiotic treatment over 24 h served as controls. Adherence and internalization experiments were conducted with hOB and MG63 when investigating *S. epidermidis* and solely with MG63 cells for *S. aureus*. Cytokines measured included interleukin 6, interleukin 12, tumor necrosis factor α and monocyte chemoattractant protein 1 (IL-6, IL-12, TNF-α and MCP-1) using a multiplex

ELISA purchased from BioRad laboratories (Multiplex ELISA, Bio-Rad Laboratories GmbH, München, Germany).
The experimental preparation was according to manufacturer's instructions. Cytokine concentrations were then measured using a Luminex plate reader with assistance of Dr. Müller (Department of Cell Biology, University Medical Center Rostock, Germany). Subsequently, control values (cells incubated under identical conditions but without bacteria) were deducted from the respective sample values.

2.6 Co-culture under electrical stimulation

To test the suitability of the constructed stimulation system regarding a co-culture setup, MG63 osteosarcoma cells as well as *S: epidermidis* were used. 500 µl with 10^5 cells were added on the coverslip in the system and 3 x 10^4 cells in 50 µl were added on top of each electrode. Cells were incubated for 30 min to allow adherence to the surfaces and subsequently 30 ml DMEM without phenol red supplemented with 10 % FCS were added to the system. Cells were then incubated for 12 h without any stimulation. On the following day, overnight cultures of *S. epidermidis* were centrifuged and optical densities were adjusted to 0.35 in DMEM. Subsequently, appropriate volumes of bacterial suspensions were added to the system and carefully mixed, resulting in a MOI of 100, meaning final infection doses of 100 bacteria per cell. Samples were then incubated for 24 h at 37 °C under 5 % CO_2 atmosphere. Stimulated samples were treated with 2.8 V_{RMS} and 20 Hz frequency under continuous stimulation.
Determination of bacterial numbers was done as described previously with the addition that MG63 cells from electrode surfaces and coverslips were lysed using *Aqua dest.* prior to plating. Coverslips were taken from the system and rinsed with 1 x PBS. Subsequently, 0.25 % trypsin-EDTA solution were added to the coverslips and incubated for 5 min. Detached cells were collected and coverslips were washed with 1 x PBS and pooled with respective samples. Samples were centrifuged and cells were lysed using 1 ml *Aqua dest.* Subsequently, serial dilutions were plated and CFU/ml were enumerated after 24 h of incubation at 37 °C under 5 % CO_2 atmosphere.
Additionally, cell numbers from electrode surfaces and coverslips were enumerated using a TC 10™ automated cell counter (Bio-Rad Laboratories GmbH, München, Germany). Detached cells were centrifuged and suspended in 10 µl 1 x PBS while 10 µl trypan blue was added. 10 µl of the solution was placed inside a counting chamber and cell numbers were determined.

2.7 Statistical analysis

All experiments were, if not otherwise noted, performed with at least four independent biological replicates. Statistical analyses were performed using implemented significance tests of GraphPad Prism 6.0. Since normal distributions of data were not expected and not tested, Mann Whitney U Test was utilized comparing two groups of four or more independent samples. If more than two groups were compared, Multiple Comparison Kruskal Wallis Test followed by Dunn's Correction was used to determine significance levels. P values less than 0.05 were considered statistically significant.

3 Results

3.1 Numeric simulation of electric potential and field distribution in the stimulation system

Numerical simulations of electric potential and electric displacement field norms are shown in Figure 7 while measured V_{RMS} compared to simulated values are shown in Table 7.

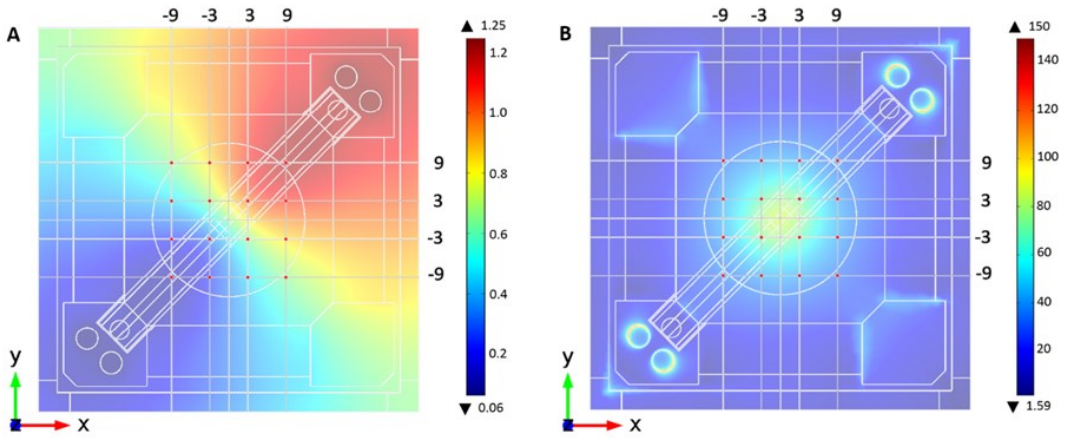

Figure 7: Simulations of potential and field distributions inside the stimulation system. **A:** Numerical simulation of electric potential in V. **B:** Numerical simulation of electric displacement field norm in V/m at the bottom of stimulation system. Red dots show coordinates where measurements for validation were done (Dauben *et al.* 2016).

Table 7: Measured and simulated electric potential of the measurement pattern of the stimulation system in the ROI (Dauben *et al.*, 2016)

x / y / z [mm]	measured V_{RMS} mean ± SD [mV]	simulated V_{RMS} [mV]	$\lvert \Delta V_{simulated} - V_{measured} \rvert$ [mV]
-9 / 9 / 0	662 ± 1	655	7
-3 / 9 / 0	716 ± 7	840	124
3 / 9 / 0	773 ± 10	1072	299
9 / 9 / 0	812 ± 5	1195	383
-9 / 3 / 0	626 ± 4	470	156
-3 / 3 / 0	668 ± 9	655	13
3 / 3 / 0	728 ± 10	975	247
9 / 3 / 0	763 ± 6	1072	309
-9 / -3 / 0	583 ± 2	238	345
-3 / -3 / 0	617 ± 4	335	282
3 / -3 / 0	671 ± 6	655	16
9 / -3 / 0	713 ± 7	840	127
-9 / -9 / 0	540 ± 1	115	425
-3 / -9 / 0	573 ± 4	238	335
3 / -9 / 0	623 ± 3	470	153
9 / -9 / 0	665 ± 4	655	10

First, the simulated potential gradient was higher than measured in the stimulation system. When comparing measured values of the four grid points (coordinates -9/9; -3/3; 3/-3; and 9/-9) to simulated data, they showed good approximation to real data with maximum deviations of 16 mV (Table 7). Additionally, with increasing distance in direction of both electrodes, differences rose to maximum deviations of around 400 mV. It is clear at this point, that the simulation assumes a broader and more extensive potential gradient than it appears in the real stimulation system. However, measured and simulation data showed good approximations in the middle of the chamber bottom, the region of interest (ROI). In the ROI, measured and real values were nearly identical. Concerning the electric displacement field norm shown in Figure 7B, maximum values of field strengths reaching around 80 – 90 V/m were obtained. Field strengths decreased steadily with increasing distance to the center of the ROI.

3.2 Growth of *S. epidermidis* and *S. aureus* in complex and cell culture media

Growth behavior of *S. epidermidis* and *S. aureus* was tested in TSB, MEM, DMEM with phenol red and DMEM without phenol red. The last three media were supplemented with 10 % FCS. Growth was determined in 96 well plates incubated at 37 °C and 24 h. Measurements were done electronically every 30 minutes. Representative growth curves of at least three independent experiments are shown in Figure 8 and Figure 9. Based on these values, specific growth rates and doubling times were calculated and are presented in Table 8 for *S. epidermidis* and Table 9 for *S. aureus*, respectively.

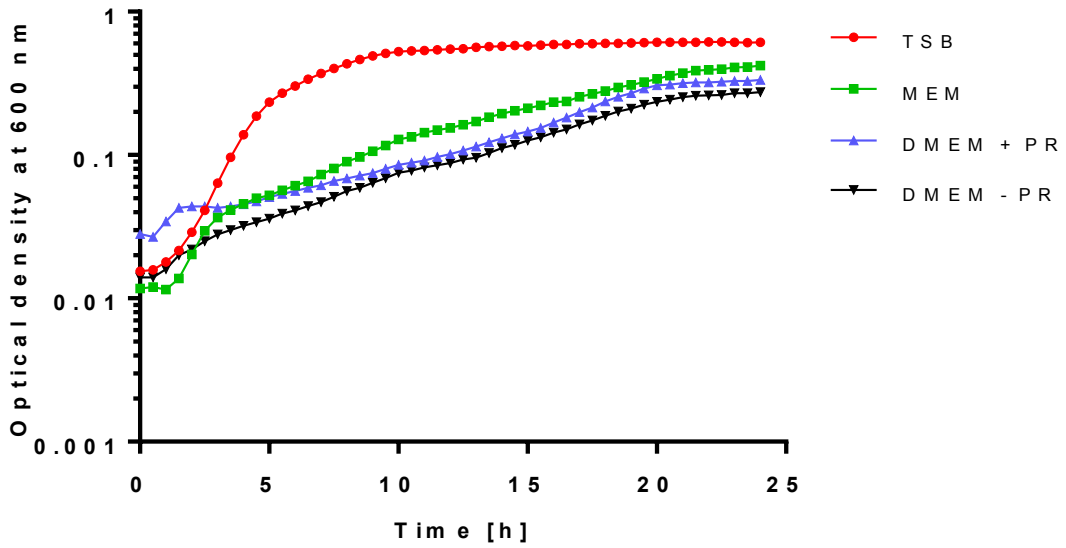

Figure 8: Representative growth curves of S. epidermidis in different media. Optical densities measured at 600 nm representing growth of *S. epidermidis* in TSB, MEM, DMEM with phenol red and DMEM without phenol red over 24 h. Bacteria were cultured in 96 well plates and optical densities were measured every 30 min.

Table 8: Calculated growth rates and doubling times for S. epidermidis. Values presented are means ± SD determined for growth in TSB, MEM, DMEM with phenol red and DMEM without phenol red (PR).

Medium	specific growth rate μ [h^{-1}]	doubling time t_d [h]
TSB	0.790 ± 0.053	0.880 ± 0.060
MEM	0.219 ± 0.031	3.219 ± 0.489
DMEM+PR	0.135 ± 0.071	5.934 ± 3.096
DMEM-PR	0.106 ± 0.016	6.663 ± 1.147

S. epidermidis shows normal growth behavior in the complex medium TSB. A slight lag-phase was followed by an exponential phase between 2 and 6 hours of growth and flattened into the late exponential and subsequent stationary phase. In cell culture media, *S. epidermidis* showed a short lag phase followed by a short exponential phase which flattened slowly during the experiment reaching stationary phase like behavior after 20 to 22 hours of growth (Figure 8). Growth rates were highest in TSB, while a maximum growth rate of around 25 % of TSB could be determined for MEM. Using DMEM with and without phenol red, only 17 % and around 13 %, respectively, of growth rates were reached compared to TSB. This results in doubling times of around 0.88 h in TSB, while doubling times increased in cell culture media up to 3 to nearly 7 hours (Table 8). As done with *S. epidermidis*, growth behavior of *S. aureus* was also tested in the before-mentioned media.

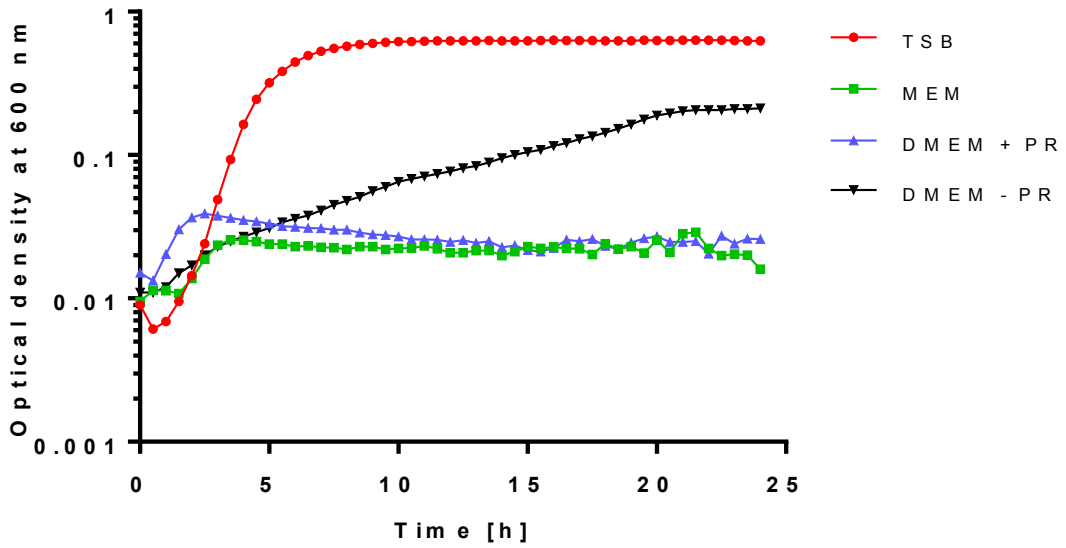

Figure 9: Representative growth curves of S. aureus in different media. Optical densities measured at 600 nm representing growth of *S. epidermidis* in TSB, MEM, DMEM with phenol red and DMEM without phenol red over 24 h. Bacteria were cultured in 96 well plates and optical densities were measured every 30 min.

Table 9: Calculated growth rates and doubling times for S. aureus. Values presented are means ± SD determined for growth in TSB, MEM, DMEM with phenol red and DMEM without phenol red (PR).

Medium	specific growth rate μ [h^{-1}]	doubling time t_d [h]
TSB	1.351 ± 0.090	0.515 ± 0.034
MEM	0.691 ± 0.262	1.285 ± 0.602
DMEM+PR	0.592 ± 0.095	1.193 ± 0.212
DMEM-PR	0.229 ± 0.012	3.035 ± 0.161

In general, *S. aureus* showed similar growth behavior as *S. epidermidis* in complex medium TSB (Figure 9) despite the higher growth rate of 1.35 per h (Table 9) compared to 0.79 per h (Table 8). A short lag phase was followed by an exponential growth phase, reaching the stationary phase between 6 and 8 hours of growth. In MEM and DMEM with phenol red, *S. aureus* shows a short and, compared to TSB, weak exponential phase between 1 and 3 hours of growth. Following this short phase, no further growth could be detected until 24 h. Doubling times in those cell culture media were around twice as high as determined for TSB (Table 9). Using DMEM without phenol red, weak but steady exponential growth was detected, while *S. aureus* was reaching the stationary phase after around 20 h of growth. Growth rates reached around 17 % of determined growth rates when using TSB, resulting in doubling times of around 3 h.

Based on these results, DMEM with phenol red was chosen as medium for adherence and internalization assays using MG63 cells, while DMEM without phenol red was used for all electrical stimulation experiments of bacteria done in cell culture medium.

3.3 Biofilm mass production of *S. epidermidis* on solid materials

Prior to stimulation experiments, biofilm mass production of *S. epidermidis* was tested in three different media and on two different surfaces. In 24 well plates, CFU/ml of planktonic and biofilm-bound bacteria were determined over an incubation period of 72 h in TSB, DMEM and MEM. Coverslips or Ti6Al4V samples were inserted in wells to allow biofilm mass production on these artificial surfaces. Formed biofilm mass of *S. epidermidis* was stained with crystal violet to quantify the biofilm mass and changes of biofilm formation dependent on the used medium and sample surface.

3.3.1 Determination of CFU/ml from supernatants

Figure 10 shows recovered CFU/ml of *S. epidermidis* from supernatants following 72 h of incubation in different media as well as with coverslips or Ti6Al4V samples on the well bottom.

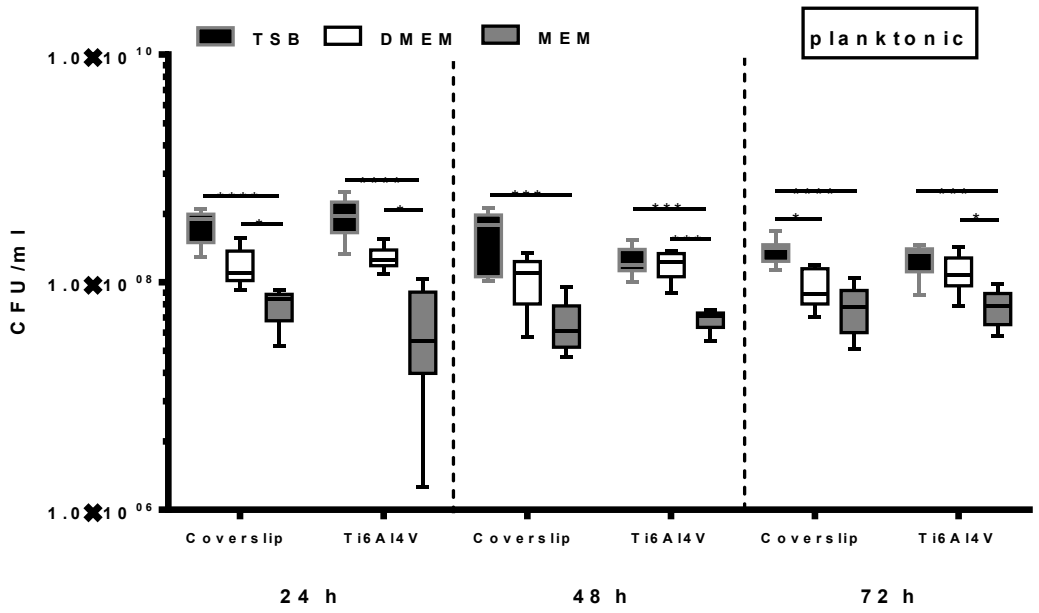

Figure 10: Determination of planktonic CFU/ml of S. epidermidis. CFU/ml of planktonic *S. epidermidis* after cultivation on coverslips or Ti6Al4V samples in different media over 72 h. Values are presented as boxplots of 10th – 90th percentile while whiskers denote minimum and maximum values. n = 9. * $p < 0.05$; *** $p < 0.001$; **** $p < 0.0001$ (Kruskal Wallis Test with multiple comparison followed by Dunn's correction)

In general, similar tendencies could be observed on coverslips as well as on titanium samples at all time points. Highest CFU/ml were always obtained in complex medium TSB, while bacteria cultivated in MEM showed significantly lower CFU/ml regardless the tested material and the time point. Using DMEM as culture medium, CFU/ml were lower compared to experiments in TSB, though no significance levels were reached except following 72 h of incubation.

3.3.2 Determination of CFU/ml recovered from biofilms

Figure 11 shows recovered CFU/ml from biofilm-bound *S. epidermidis* following 72 h of incubation in different media as well as with coverslips or Ti6Al4V samples on the well bottom.

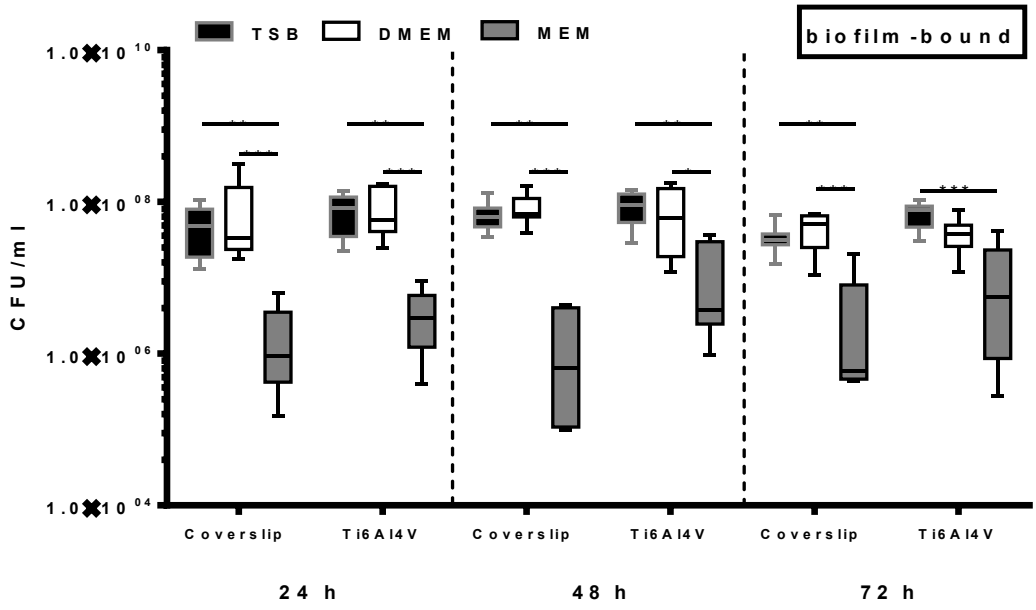

Figure 11: Determination of biofilm-bound CFU/ml of S. epidermidis. CFU/ml of biofilm-bound *S. epidermidis* after cultivation on coverslips or Ti6Al4V samples in different media over 72 h. Values are presented as boxplots of 10^{th} – 90^{th} percentile while whiskers denote minimum and maximum values. n = 9. * $p < 0.05$; ** $p < 0.01$; *** $p < 0.001$ (Kruskal Wallis Test with multiple comparison followed by Dunn's correction)

Similar trends as observed for CFU/ml recovered from supernatants could be detected for biofilm-bound bacteria. CFU/ml of *S. epidermidis* in TSB and DMEM were in a similar range at all sampling points, while CFU/ml were significantly lower in MEM compared to the other two media at every sampling point except 72 h of incubation.

Comparing coverslips and Ti6Al4V samples, no dramatic differences in CFU/ml could be observed, suggesting both materials to be suitable surfaces for *S. epidermidis* biofilm formation.

3.3.3 Quantification of biofilm mass

Respective biofilm mass quantifications are presented in Figure 12.

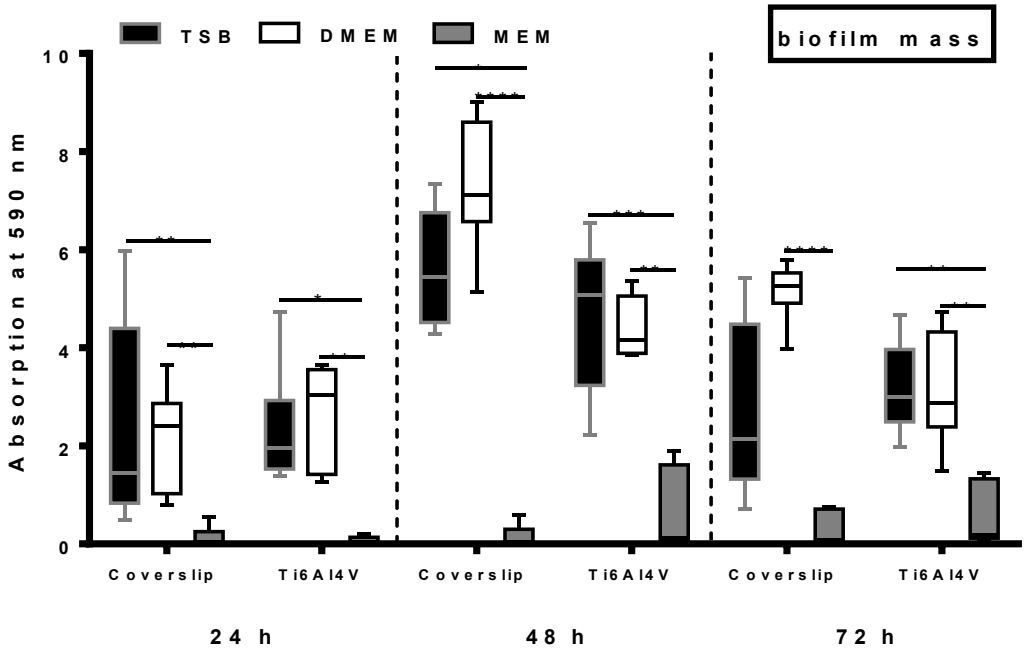

Figure 12: Quantification of S. epidermidis formed biofilms. Quantification of biofilm mass formed by *S. epidermidis* after cultivation on coverslips or Ti6Al4V samples in different media over 72 h. Values are presented as boxplots of 10^{th} – 90^{th} percentile while whiskers denote minimum and maximum values. $n \geq 5$. * $p < 0.05$; ** $p < 0.01$; *** $p < 0.001$; **** $p < 0.0001$ (Kruskal Wallis Test with multiple comparison followed by Dunn's correction)

In general, biofilm mass in MEM was significantly lower compared to TSB and DMEM at any point regardless if coverslips or Ti6Al4V samples were used. Highest biofilm mass in TSB and DMEM was detected following 48 h of incubation while values decreased again during further incubation (72 h). No significant differences in biofilm mass comparing TSB and DMEM could be detected, although biofilm mass on coverslips following 48 and 72 h incubation in DMEM was higher compared to TSB.

Biofilm mass quantification was also tested with *S. aureus*. No biofilm mass production could be detected with this assay in any of the three tested media.

3.4 Scanning electron microscopy imaging of biofilms of *S. epidermidis*

Following determination of biofilm mass production of *S. epidermidis* on both polystyrene coverslips and Ti6Al4V surfaces in different culture media, morphology and distribution of bacteria and produced biofilm mass were evaluated via SEM imaging. Figure 13 shows representative images of *S. epidermidis* after 72 h of incubation on coverslips and Ti6Al4V samples in TSB. SEM images after 72 h incubation in DMEM on coverslips and Ti6Al4V are shown in Figure 14 and SEM imaged after incubation in MEM are shown in Figure 15.

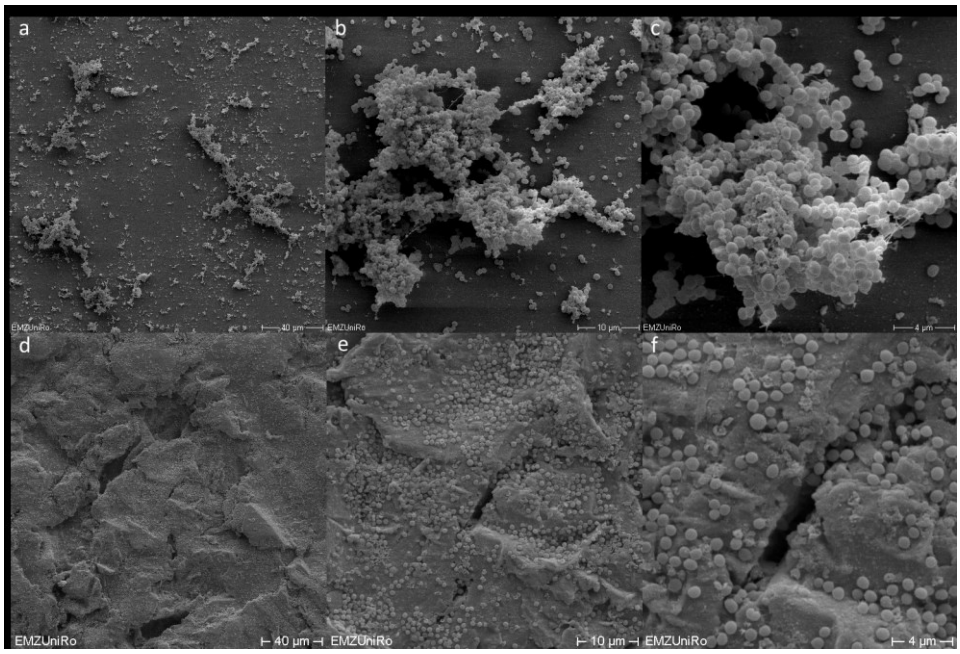

Figure 13: Representative SEM images of S. epidermidis cultivated in TSB. Representative SEM images of *S. epidermidis* incubated on coverslips (a, b, c) and Ti6Al4V (d, e, f) over 72 h in TSB. a, d – 500x magnification; b, e – 2000x magn.; c, f – 5000x magn.

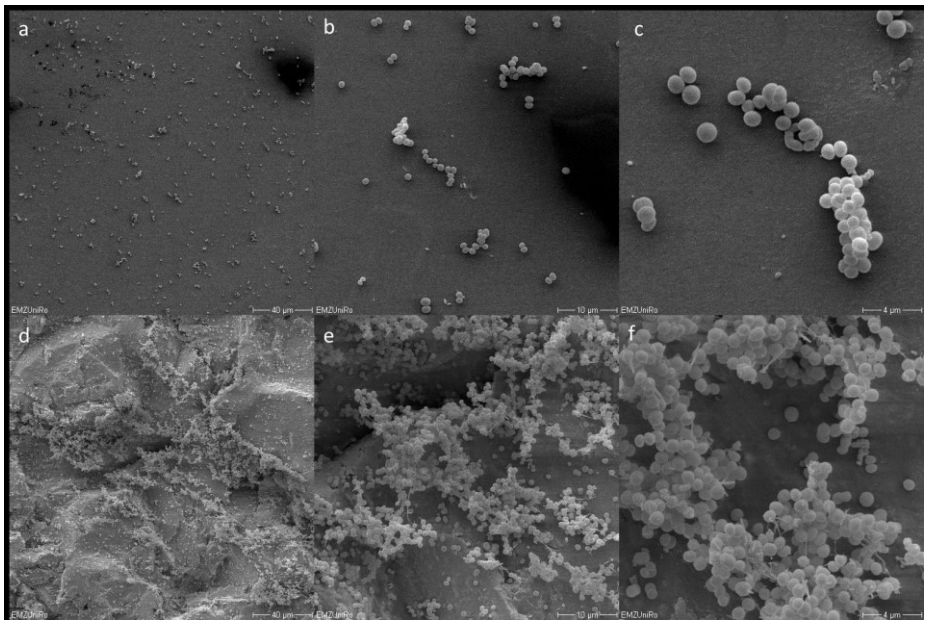

Figure 14: Representative SEM images of S. epidermidis cultivated in DMEM. Representative SEM images of *S. epidermidis* incubated on coverslips (a, b, c) and Ti6Al4V (d, e, f) over 72 h in DMEM /. a, d – 500x magnification; b, e – 2000x magn.; c, f – 5000x magn.

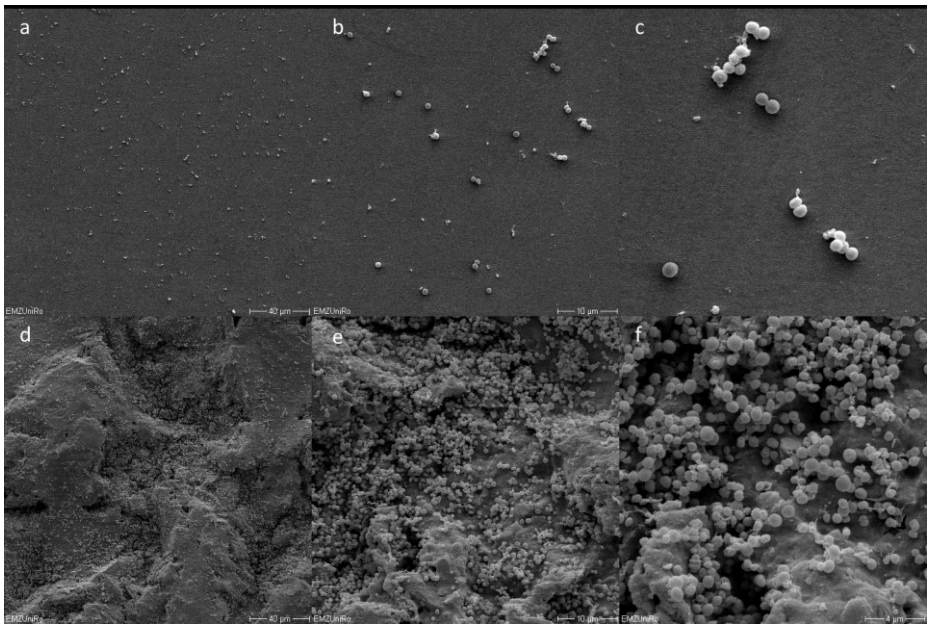

Figure 15: Representative SEM images of S. epidermidis cultivated in MEM. Representative SEM images of *S. epidermidis* incubated on coverslips (a, b, c) and Ti6Al4V (d, e, f) over 72 h in MEM. a, d – 500x magnification; b, e – 2000x magn.; c, f – 5000x magn.

Initiation of biofilm formation with production of extracellular matrix structures can be seen in Figure 13 a-c and Figure 14 d-f. In general, *S. epidermidis* appears more evenly distributed when incubated on Ti6Al4V than on coverslips. When *S. epidermidis* was incubated on coverslips in both cell culture media, no big clusters of aggregated bacteria could be found (see Figure 14 a-c, Figure 15 a-c).

3.5 Electrical stimulation of *S. epidermidis* and *S. aureus*

After evaluation of the basic biofilm characteristics for both species on coverslips and Ti6Al4V surfaces, bacterial species were subjected to electrical stimulation. Using the newly designed stimulation system, effects of alternating electric fields on both bacterial species were investigated. Different parameter settings were used for experiments under electrical stimulation. Table 10 summarizes all performed stimulation experiments with respective parameter settings.

Table 10: Parameter settings for electrical stimulation of S. epidermidis and S. aureus

S. epidermidis* / *S. aureus	**Medium**	**V_{RMS} [V]**	**frequency [Hz]**	**stimulation period [d^{-1}]**	**duration [d]**	**inoculum**	**Note**
both	TSB	0.2	20	3 x 45 min	3	10^6 CFU/ml	shown
both	TSB	1.4	20	3 x 45 min	3	10^6 CFU/ml	shown
both	TSB	1.4	20	3 x 45 min	3	10^4 CFU/ml	Appen-dix
both	DMEM	1.4	20	3 x 45 min	3	10^4 CFU/ml	shown
both	DMEM	2.8	20	continuous	3	10^4 CFU/ml	shown
S. epidermidis	TSB	0.7	50	3 x 120 min	3	10^6 CFU/ml	not shown
S. epidermidis	TSB	0.2	20	6 x 45 min	1	10^6 CFU/ml	not shown

Four of seven tested parameter settings are described in the following sections. However, figures of electrical stimulation of both species in TSB with 10^4 CFU/ml as inoculum can be seen in the Appendix to not further complicate the illustrations. The two last-mentioned parameter settings are not shown and described further, since they contain no significant information regarding these parameter settings. Both last settings were tested but no differences were observed between stimulated and control samples.

3.5.1 Determination of CFU/ml from the supernatant

Figure 16 shows CFU/ml determined from supernatants following electrical stimulation of *S. epidermidis* and *S. aureus*.

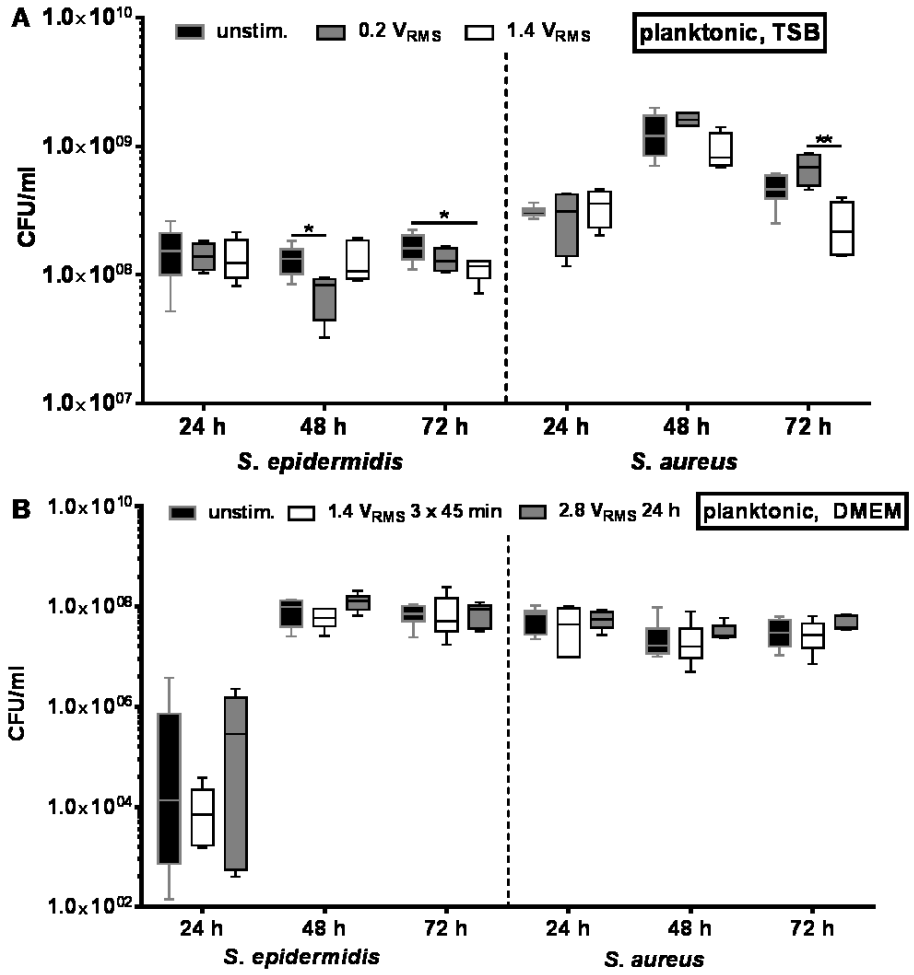

Figure 16: Determination of planktonic S. epidermidis and S. aureus following electrical stimulation. CFU/ml of planktonic *S. epidermidis* and *S. aureus* recovered from supernatants of stimulated and control samples. **A**: Unstimulated controls and bacteria stimulated with either 0.2 or 1.4 V_{RMS}, stimulation period 3 x 45 min / day, inoculum of 10^6 CFU/ml in TSB. **B**: Unstimulated controls and bacteria stimulated with either 1.4 V_{RMS} and stimulation period 3 x 45 min / day or 2.8 V_{RMS} and continuous stimulation, inoculum of 10^4 CFU/ml in DMEM without phenol red supplemented with 10 % FCS. $n \geq 4$. * $p < 0.05$; ** $p < 0.01$ (Multiple Comparison Kruskal Wallis Test followed by Dunn's Correction).

In general, CFU/ml recovered from supernatants of stimulated and control samples remained relatively stable throughout the experiments. In complex medium TSB, *S. epidermidis* reached maximum CFU/ml after 24 h of incubation with around 10^8 CFU/ml, while *S. aureus* reached peak bacterial numbers of around 10^9 CFU/ml following 48 h of incubation, independent of any stimulation. Significantly lower CFU/ml were obtained in case of *S. epidermidis* following 48 h treatment with 0.2 V_{RMS} compared to controls as well as after 72 h treatment with 1.4 V_{RMS} compared to controls. Regarding *S. aureus*, significant differences following 72 h of incubation were observed between 1.4 and 2.8 V_{RMS} treated samples. However, these differences did not reach significance levels in comparison with unstimulated controls.

Experiments with 1.4 V_{RMS} and a lower inoculum of 10^4 CFU/ml in complex medium TSB showed no significant differences between controls and stimulated samples (see Appendix Figure 34). When using DMEM as culture medium as well as a lower inoculum of 10^4 CFU/ml, no significant differences could be observed between controls and 1.4 as well as 2.8 V_{RMS} treated samples of both species tested. However, *S. aureus* showed stable CFU/ml at all time points with around 10^8 CFU/ml while *S. epidermidis* reached similar bacterial numbers only after 48 h of incubation.

3.5.2 Determination of CFU/ml recovered from electrode surfaces

CFU/ml of *S. epidermidis* and *S. aureus* recovered from electrode surfaces following electrical stimulation are depicted in Figure 17.

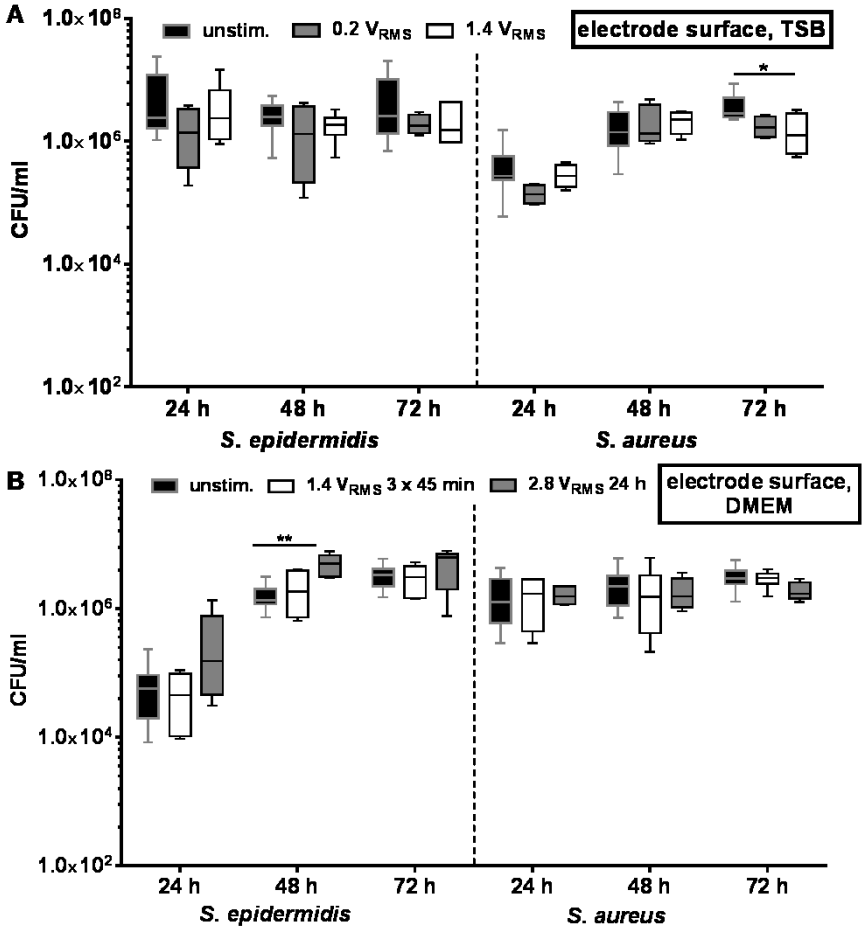

Figure 17: Determination of electrode-bound S. epidermidis and S. aureus following electrical stimulation. CFU/ml of adherent *S. epidermidis* and *S. aureus* recovered from electrode surfaces of stimulated and control samples. **A**: Unstimulated controls and bacteria stimulated with either 0.2 or 1.4 V_{RMS}, stimulation period 3 x 45 min / day, inoculum of 10^6 CFU/ml in TSB. **B**: Unstimulated controls and bacteria stimulated with either 1.4 V_{RMS} and stimulation period 3 x 45 min / day or 2.8 V_{RMS} and continuous stimulation, inoculum of 10^4 CFU/ml in DMEM without phenol red supplemented with 10 % FCS. $n \geq 4$. * $p < 0.05$; ** $p < 0.01$ (Multiple Comparison Kruskal Wallis Test followed by Dunn's Correction).

When stimulating *S. epidermidis* in TSB, no significant differences could be detected between controls and stimulated samples. However, bacterial numbers of control samples were slightly higher at every time point compared to stimulated samples. Stimulating *S. aureus* in TSB, significantly lower CFU/ml were recovered from samples treated with 1.4 V_{RMS} compared to controls following 72 h of incubation. However, no significant differences could be observed when experiments were done with the lower inoculum (see Appendix Figure 35), while CFU/ml were slowly decreasing for *S. aureus*. In DMEM, *S. epidermidis* showed steadily increasing bacterial numbers recovered from electrode surfaces, regardless if stimulated or not. Following 48 h of incubation, 2.8 V_{RMS} treated samples reached significantly higher CFU/ml recovered from electrode surface compared to unstimulated controls. When experiments were performed using *S. aureus*, no differences between both stimulation settings and controls could be observed at any given time.

3.5.3 Biofilm mass quantification

To investigate potential influence of electrical stimulation on biofilm formation in the surrounding area of the electrode, formed biofilm at the coverslip on the chamber bottom was stained with crystal violet and photometrical quantified measuring the absorption at 590 nm as described in 2.4.4. Absorption values were further calculated in relation to the surface of the used coverslip and are depicted in Figure 18.

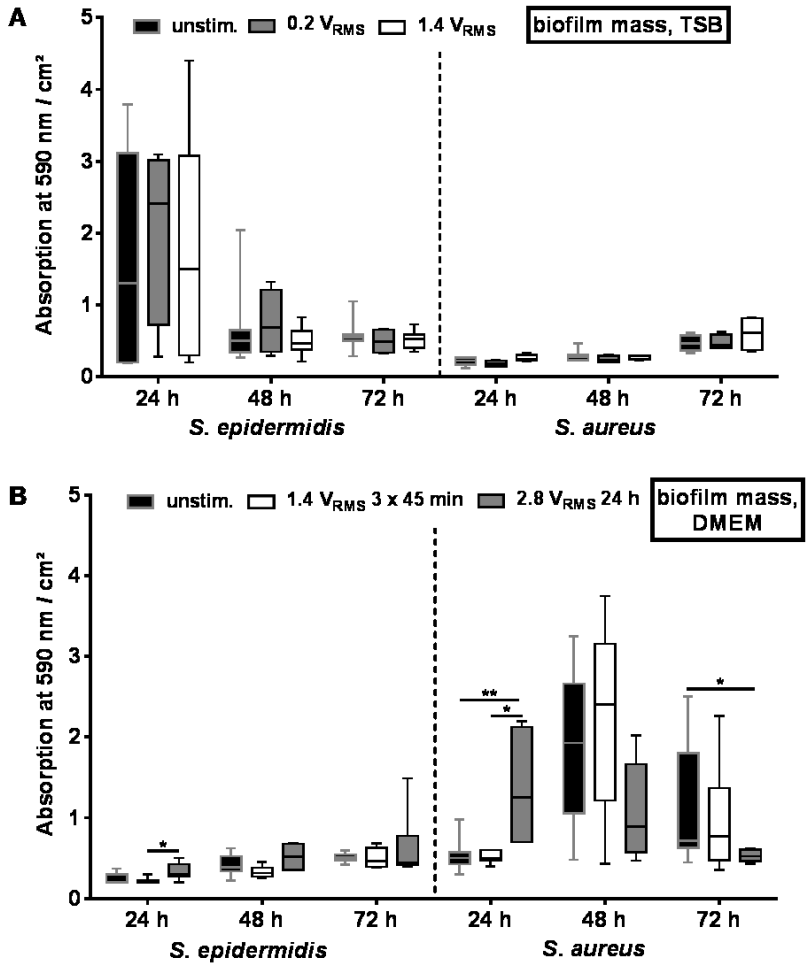

Figure 18: Quantification of biofilms formed by S. epidermidis and S. aureus following electrical stimulation. Biofilm mass quantification via crystal violet staining of *S. epidermidis* and *S. aureus* formed biofilm in relation to the surface area of the coverslip of stimulated and control samples. **A**: Unstimulated controls and bacteria stimulated with either 0.2 or 1.4 V_{RMS}, stimulation period 3 x 45 min / day, inoculum of 10^6 CFU/ml in TSB. **B**: Unstimulated controls and bacteria stimulated with either 1.4 V_{RMS} and stimulation period 3 x 45 min / day or 2.8 V_{RMS} and continuous stimulation, inoculum of 10^4 CFU/ml in DMEM without phenol red supplemented with 10 % FCS. $n \geq 4$. * $p < 0.05$; ** $p < 0.01$ (Multiple Comparison Kruskal Wallis Test followed by Dunn's Correction).

S. epidermidis showed highest biofilm mass after 24 h of incubation in TSB with no differences between controls and stimulated samples and decreased until 72 h of incubation. In contrast, *S. aureus* showed very low biofilm mass which was slowly increasing during the experiments. No differences could be observed between controls and stimulated samples when cultivating *S. aureus* in TSB. When stimulating both species in TSB using the lower inoculum, no significant differences could be observed (see Appendix Figure 36). Interestingly, effects were reversed when using DMEM as culture medium. *S. epidermidis* showed slow biofilm mass formation over the course of the experiment. *S. aureus* showed highest biofilm mass following 48 h of incubation, though variances were very high.

Notably, biofilm formation after 24 h treatment using 2.8 V_{RMS} resulted in significantly increased biofilm formation compared o controls and 1.4 V_{RMS} treated samples. In general, biofilm formed by *S. aureus* was highest after 48 h and decreased to 72 h of incubation.

3.5.4 pH measurements

To observe pH shifts due to possible electrolytic reactions during electrical stimulation, samples were taken from supernatants at every time point and pH was measured. Values obtained from respective experiments are depicted in Figure 19.

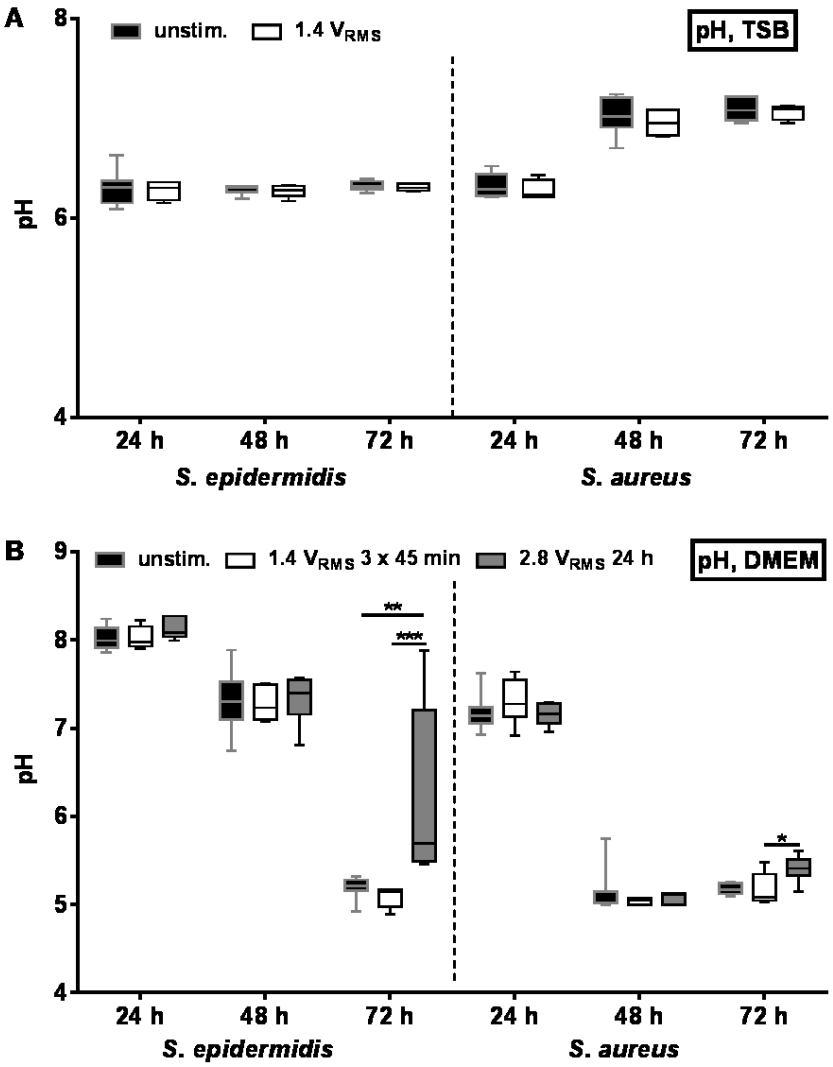

Figure 19: pH of supernatants of S. epidermidis and S. aureus samples following electrical stimulation. pH values of supernatants of *S. epidermidis* and *S. aureus* of stimulated and control samples. **A**: Unstimulated controls and bacteria stimulated with 1.4 V_{RMS}, stimulation period 3 x 45 min / day, inoculum of 10^6 CFU/ml in TSB. **B**: Unstimulated controls and bacteria stimulated with either 1.4 V_{RMS} and stimulation period 3 x 45 min / day or 2.8 V_{RMS} and continuous stimulation, inoculum of 10^4 CFU/ml in DMEM without phenol red supplemented with 10 % FCS. $n \geq 4$. * $p < 0.05$; ** $p < 0.01$; *** $p < 0.001$ (Multiple Comparison Kruskal Wallis Test followed by Dunn's Correction).

In general, no differences in pH values were observed for experiments performed in complex medium TSB between stimulated and control samples. Of note, pH values obtained from experiments using *S. aureus* rose again after 48 h and remained constant until 72 h of incubation. Using lower inoculum, pH of *S. aureus* samples treated with 1.4 V_{RMS} showed slightly higher pH compared to controls, while no differences could be observed for all other time points (see Appendix Figure 37). When using cell culture medium DMEM, pH decreased for both species, regardless if stimulated or not. This decrease is due to lactic acid production during growth of bacteria leading to a decreased pH over time. Interestingly, samples from *S. epidermidis* treated with 2.8 V_{RMS} showed significantly higher pH after 72 h of incubation compared to controls and 1.4 V_{RMS} treated samples. A similar effect could be observed when *S. aureus* was treated with 2.8 V_{RMS} though differences were not as high as for *S. epidermidis* at the same time point.

3.5.5 Antibiotic resistance

Matl *et al.* showed in 2011, that bactericidal effects of electrical stimulation by additional antibiosis could be enhanced, leading to increased reduction of bacteria in broth media, i.e. *S.* aureus (Matl *et al.* 2011). An important fact is, that bacteria more sensitive to clinically used antibiotics could lead to reduced amounts of antibiotics needed in treatment of implant infections and perhaps even to the potential re-use of antibiotics, to which bacteria were previously resistant. In addition, since electrical stimulation of fractures and implants is widely used in medicine, the potential effects of electrical stimulation in case of an infection of the stimulated area had to be investigated. In this work, the effect of electrical stimulations prior to antibiotic treatment was tested. Therefore, samples from the supernatants were taken after electrical stimulation and E-Tests were performed to investigate possible changes in antibiotic susceptibility.

High variances were detected regarding susceptibility for gentamicin in case of *S. epidermidis*. These variances are due to its natural resistance towards gentamicin. In case of *S. aureus*, very low MIC were determined for gentamicin, which was expected, since *S. aureus* was previously tested sensitive towards gentamicin. Both species were sensitive towards levofloxacin. In general, no notable differences between stimulated and unstimulated samples could be observed in both species under all tested conditions (see Appendix Figure 38 - 43).

3.5.6 Biofilm mass production following electrical stimulation

Within these experiments, general biofilm mass production following electrical stimulation was observed. Bacteria were treated using the before-mentioned parameter settings and samples were taken at the last time point. Samples were further incubated for three days using complex medium TSB in 24 well plates with inserted polystyrene coverslips to determine short-term effects of electrical stimulation. Following incubation, biofilm mass was quantified using crystal violet as described previously. Quantified biofilm masses are presented in Figure 20.

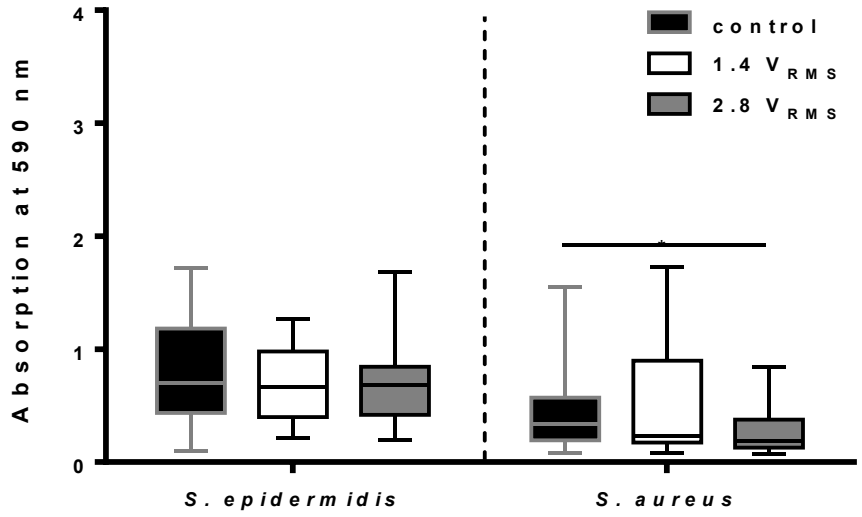

Figure 20: Quantification of general biofilm formation of S. epidermidis and S. aureus following electrical stimulation. Biofilm mass quantification via crystal violet staining of *S. epidermidis* and *S. aureus* formed biofilms after 72 h growth in complex medium of previously stimulated and control samples. $n \geq 32$. * $p < 0.05$(Multiple Comparison Kruskal Wallis Test followed by Dunn's Correction).

In general, no differences in biofilm formation could be observed regarding *S. epidermidis* following incubation of previously stimulated samples with 1.4 and 2.8 V_{RMS} as well as unstimulated samples. Comparing the three treatment settings for *S. aureus*, significantly increased biofilm formation was detected for unstimulated controls in comparison to 2.8 V_{RMS} treated samples following three days without any stimulation in complex medium. However, biofilm formation of both species was rather weak after 72 h of incubation.

3.5.7 Biofilm Composition

Since no notable differences could be observed regarding general biofilm formation, changes in biofilm composition due to previous electrical stimulation were investigated. Samples were differently treated and amounts of biofilm mass as well as extracellular DNA were measured. Results of biofilm composition experiments for both bacterial species are presented in Figure 21 and Figure 22.

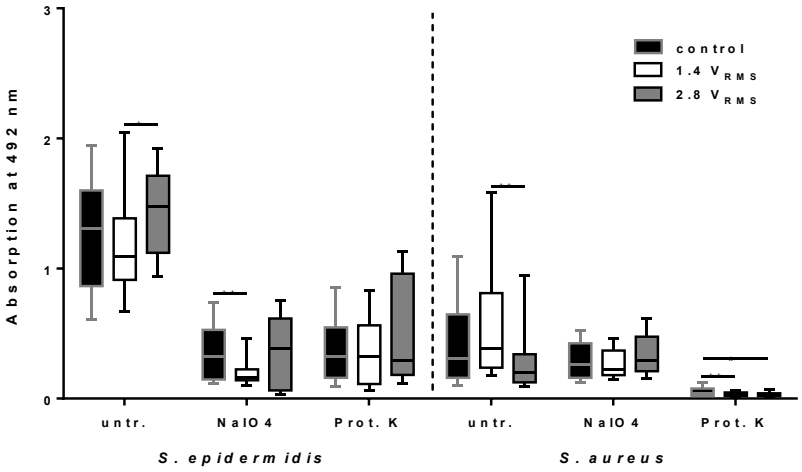

Figure 21: Determination of composition of S. epidermidis and S. aureus formed biofilms. Biofilm mass quantification via crystal violet staining of differently treated *S. epidermidis* and *S. aureus* samples following 24 h of growth in TSB. Samples were taken from outgrowth experiments following electrical stimulation with either 1.4 or 2.8 V_{RMS} or without electrical stimulation. Untr. – untreated samples, only; $NaIO_4$ – samples treated with $NaIO_4$ to dissolve carbohydrates before staining; Prot. K – samples treated with Proteinase K to dissolve all proteins before staining. $n \geq 36$. * - $p < 0.05$; ** - $p < 0.01$ (Multiple Comparison Kruskal Wallis Test followed by Dunn's Correction).

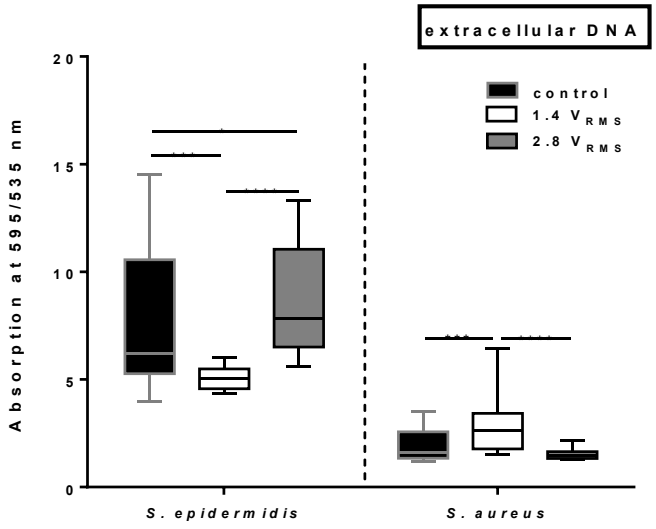

Figure 22: Determination of extracellular DNA in S. epidermidis and S. aureus formed biofilms. Extracellular DNA quantification via EthD-III staining of *S. epidermidis* and *S. aureus* samples following 24 h of growth in TSB. Samples were taken from outgrowth experiments following electrical stimulation with either 1.4 or 2.8 V_{RMS} or without electrical stimulation. $n \geq 24$. * - $p < 0.05$; *** - $p < 0.001$; **** - $p < 0.0001$ (Multiple Comparison Kruskal Wallis Test followed by Dunn's Correction).

Figure 21 shows measured absorptions of differently treated and stained biofilm of *S. epidermidis* and *S. aureus* following 24 h of incubation in 96 well plates. Untreated biofilms of previously stimulated and non-stimulated samples showed highest absorption values, while previously with 1.4 V_{RMS} treated samples of *S. epidermidis* showed significantly decreased biofilm mass formation compared to 2.8 V_{RMS} treated samples. On the contrary, *S. aureus* biofilm mass formation of 1.4 V_{RMS} treated samples was significantly higher compared to 2.8 V_{RMS} treated samples. Comparing both to non-stimulated control samples, no significant differences could be detected. Following treatment with $NaIO_4$, absorption values decreased due to decomposition of carbohydrates. 1.4 V_{RMS} samples of *S. epidermidis* showed significantly decreased absorption values compared to control samples, while no differences in biofilm mass following $NaIO_4$ treatment could be detected between the three tested groups of *S. aureus*. Following Proteinase K treatment, no significant differences in biofilm mass could be detected for *S. epidermidis* formed biofilms. In case of *S. aureus*, previously stimulated samples showed significantly decreased biofilm mass compared to unstimulated samples. However, these changes are probably not that relevant for *S. aureus*, since remaining biofilm mass following Proteinase K treatment was rather very low. Comparing general biofilm composition, *S. epidermidis* showed similar absorption values of remaining biofilm mass following decomposition of carbohydrates as well as proteins. Regarding the different treatment of *S. aureus* formed biofilms, nearly no changes could be detected following treatment with $NaIO_4$ while absorption values of remaining biofilm mass dropped nearly to the detection limit after Proteinase K treatment. This implies, that most of *S. aureus* formed biofilms is composed of proteins while only a small part is represented by carbohydrates. Comparing *S. epidermidis* biofilms, carbohydrates and proteins seem to be represented in a more equal ratio in formed biofilms.

In general, *S. epidermidis* showed higher amounts of extracellular DNA in formed biofilms compared to *S. aureus* samples (Figure 22). This could be due to the fact, that, in general, biofilm formation using *S. epidermidis* was higher compared to *S. aureus* (see Figure 18). Using EthD-III to stain extracellular DNA as a part of formed biofilm, significant differences between the tested parameter settings were observed. When *S. epidermidis* was pre-treated with 1.4 V_{RMS}, obtained values were significantly lower compared to both control and 2.8 V_{RMS} treated samples.

Regarding *S. aureus*, stimulation with 1.4 V_{RMS} previously to outgrowth and biofilm composition experiments led to significantly increased amounts of extracellular DNA compared to controls and 2.8 V_{RMS} treated samples, respectively.

3.5.8 Determination of ATP concentration in supernatants and lysates

ATP concentration was measured only in one parameter setting using *S. aureus* and TSB as medium under the stimulation conditions of 1.4 V_{RMS} and stimulation periods of 3 x 45 min per day over 72 h. Measurement of ATP concentration as well as FACS analysis, described later, were tested as suitable methods for investigation of effects of electrical stimulation using our system but were not further applied to other parameter settings.
Relative luminescence units (RLU) were measured using a sample from the supernatant of control and stimulated samples. Samples were centrifuged and RLUs were measured from the supernatants and lysates of the bacteria. These values were summed up for total ATP concentration. Relative amounts of free and intracellular ATP are shown below.

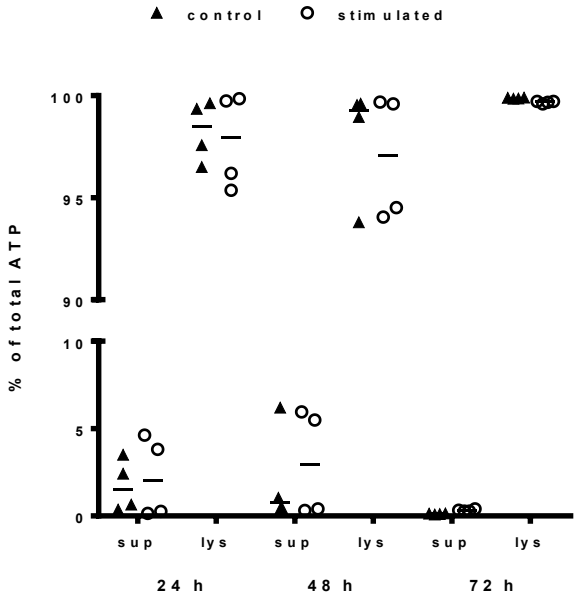

Figure 23: Determination of ATP amounts following electrical stimulation of S. aureus in TSB. Amount of free and intracellular ATP as percentage of total ATP of *S. aureus* with and without electrical stimulation over 72 h. sup – supernatant; lys – lysate. n = 4.

No significant differences were observed when comparing control and stimulated samples in case of intracellular and extracellular ATP. Highest extracellular ATP concentrations were detected after 48 h with a maximum of around 5 -6 % of total ATP.

Lowest free ATP concentrations were detected following 72 h of incubation with a maximum of around 0.5 – 1 % of total ATP. This method confirms the previously described results for this parameter setting, that no differences between stimulated and control samples could be observed.

3.5.9 Determination of live and dead bacteria by FACS analyses

FACS analyses were conducted using thiazolorange and propidium iodide to distinguish living and dead bacteria. Representative pictures of control and stimulated samples after 72 h incubation are shown in Figure 24.

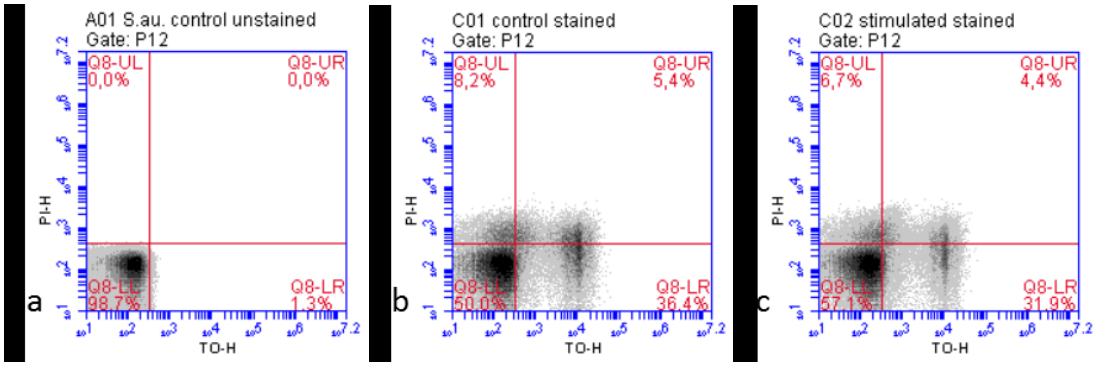

Figure 24: Population distributions of viable and damaged S. aureus following electrical stimulation. Representative FACS analyses of *S. aureus* after 72 h incubation with and without electrical stimulation. Thiazolorange (TO) was used to stain all bacteria while propidium iodide (PI) was used to stain damaged and dead bacteria. **a:** control sample unstained; **b:** control sample stained with TO and PI, **c:** stimulated sample stained with TO and PI.

Using the unstained control sample, the fluorescence border for TO and PI was determined. Unstained bacteria remain in the lower left part, while TO positive bacteria are visible in the lower right part. TO negative/PI positive signals would appear in the upper left part of the diagram, which could be interpreted as cell residues. TO positive/PI positive bacteria would appear in the upper right part. Those bacteria are either damaged or dead bacteria.

Despite the fact, that around 50 – 60 % of the samples were unstained when measured, no significant differences could be detected between stimulated and control samples. In both (Figure 24 b and c) around 32 – 37 % of the stained bacteria appear only TO positive, while 4 – 6 % were TO/PI positive, meaning they were damaged or dead at the point of the measurement.

3.6 Co-culture of staphylococci and bone cells

The generated stimulation system should be used for investigating effects of alternating current electrical stimulation of bacteria, bone cells and both in co-culture to mimic an implant infection situation in a simplified setup. Before combining bacteria and bone cells in the stimulation system, adherence and internalization abilities of *S. epidermidis* and *S. aureus* were determined.

3.6.1 Adherence and internalization of staphylococci to and into bone cells

As previously described, several studies showed that *S. aureus* adheres to and internalizes into MG63 cells as well as human primary osteoblast. Very few studies dealt with the topic of adherence and internalization of *S. epidermidis* to and into MG63 cell and primary osteoblasts (Valour *et al.* 2013). This study showed a very low amount of *S. epidermidis* adhered to and internalized into tested cells. The authors proposed, that the pathogenic mechanism responsible for the dramatic clinical courses of an implant infection by *S. epidermidis* is more likely due to other mechanisms such as biofilm formation than to adherence and internalization, as it was shown for *S. aureus*.

Since the stimulation system generated during this work was designed to be used for co-culture experiments with both staphylococci and osteoblast cells, it is necessary to investigate the adherence and internalization ability of the used bacterial strains in connection with MG63 cells and the human primary osteoblasts.

Adherence and internalization rates of *S. epidermidis* to and into human osteoblasts as well as osteosarcoma cell line MG63 are shown in Figure 25. Regarding *S. aureus,* adherence and internalization was only tested with MG63 cells. Obtained values are presented in Figure 26.

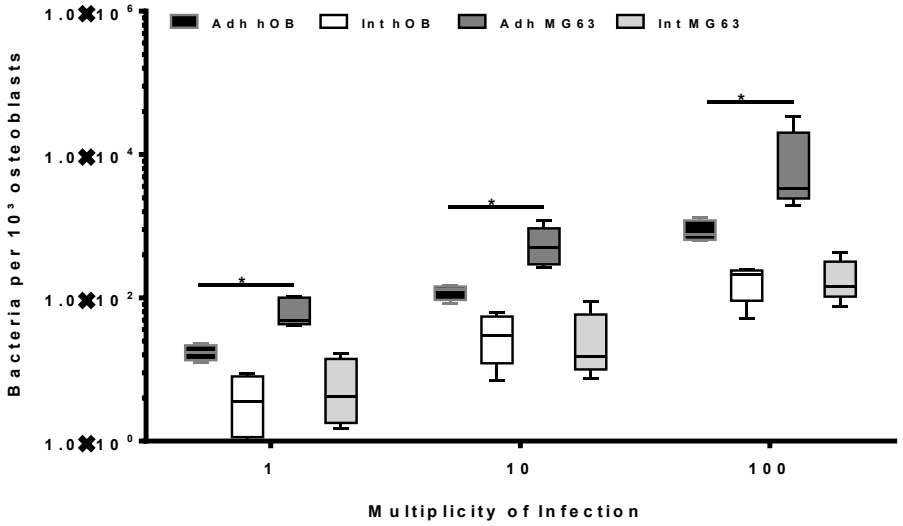

Figure 25: Adherence and internalization of S. epidermidis on and into hOB and MG63 cells. Number of adherent and internalized *S. epidermidis* in relation to 10^3 osteoblast cells. Multiplicity of Infection describes the initially used number of bacteria in relation to the used number of cells. Adh. – adherent/internalized bacteria after 2 h of incubation; Int. – internalized bacteria after additional 1 h of antibiotic treatment. hOB – human osteoblasts; MG63 – MG63 osteosarcoma cells. * - $p < 0.05$ (unpaired Mann Whitney U-Test) $n \geq 4$.

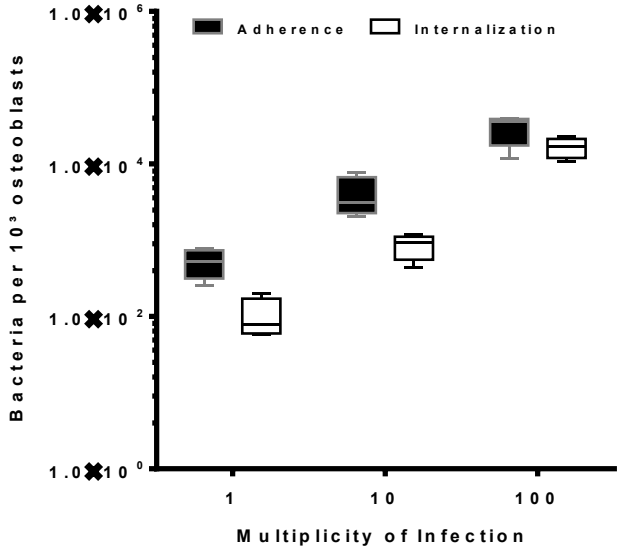

Figure 26: Adherence and internalization of S. aureus on and into MG63 cells. Adherent and internalized *S. aureus* in relation to 10^3 MG63 osteosarcoma cells. Multiplicity of Infection describes the initially used number of bacteria in relation to the used number of cells. Adherence: adherent/internalized bacteria after 2 h of incubation; Internalization: internalized bacteria after additional 1 h of antibiotic treatment. $n = 4$

In general, *S. epidermidis* revealed a low adherence potential to osteoblast cells though adherent and internalized bacteria increase with higher MOIs. While adherence values were significantly higher for all tested MOI when comparing MG63 cells and human osteoblasts, the number of internalized bacteria was similar between the two groups at every MOI tested.

Infection with *S. aureus* shows dose-dependent increasing adherence and internalization rates to MG63 cells, while values obtained were around 10 times higher compared to *S. epidermidis* (Figure 25), suggesting a higher propensity of *S. aureus* for host cell interactions.

3.6.2 Cytokine production following infection of bone cells with staphylococci

Samples of supernatants were taken following 2 h of infection during the adherence and internalization assay and 24 h of antibiotic treatment as prolonged internalization time. Cells incubated only with the respective culture medium served as controls. Samples were sterile filtered and treated according to manufacturer instructions and concentrations of IL-6, IL-12, TNF-α and MCP-1 were determined for samples of *S. epidermidis* and *S. aureus* as described earlier.

Determined concentrations of IL-6 and MCP-1 following infection of hOB and MG63 cells with *S. epidermidis* are shown in Figure 27 and Figure 28, respectively. Concentrations measured for both cytokines following infection of MG63 cells with *S. aureus* are shown in Figure 29.

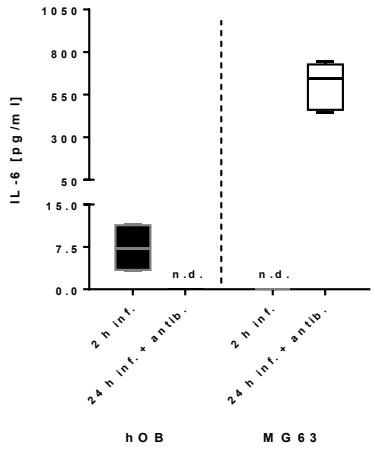

Figure 27: Interleukin-6 secretion of hOB and MG63 cells infected with S. epidermidis. Concentrations of interleukin 6 (IL-6) measured in supernatants of human osteoblasts (hOB) and MG63 cells from adherence and internalization assays with *S. epidermidis*. 2 h inf.: cells infected with *S. epidermidis* for 2 hours in assay medium with a multiplicity of infection of 100; 24 h inf. + antib.: Cells cultivated up to 24 h following 2 h infection with *S. epidermidis* under antibiotic treatment with 200 µg/ml levofloxacin as prolonged internalization time. Values of cells cultured under the same conditions without bacteria were deducted from the respective sample values. $n \geq 4$.

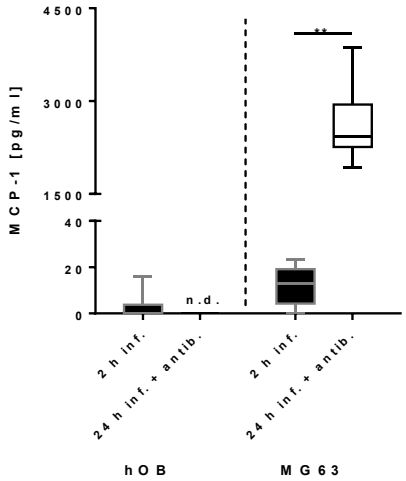

Figure 28: MCP-1 secretion of hOB and MG63 cells infected with S. epidermidis. Concentrations of monocyte chemoattractant protein 1 (MCP-1) measured in supernatants of human osteoblasts (hOB) and MG63 cells from adherence and internalization assays with *S. epidermidis*. 2 h inf.: cells infected with *S. epidermidis* for 2 hours in assay medium with a multiplicity of infection of 100; 24 h inf. + antib.: Cells cultivated up to 24 h following 2 h infection with *S. epidermidis* under antibiotic treatment with 200 µg/ml levofloxacin as prolonged internalization time. Values of cells cultured under the same conditions without bacteria were deducted from the respective sample values. $n \geq 4$. ** $p < 0.01$ (unpaired two-tailed Mann-Whitney U test).

Infection of hOB with *S. epidermidis* led to weak but detectable secretion of IL-6 and MCP-1 after 2 h of incubation. However, no further IL-6 secretion was detected for infected hOB following 24 h of antibiotic treatment. Comparing these results to MG63 cells infected with *S. epidermidis*, similar tendencies for the 2 h infection period were observed. No IL-6 secretion was detected after 2 h of infection while MCP-1 secretion reached values of 5 to 25 pg/ml. Of note, incubation for 24 h with antibiotic treatment of infected MG63 cells lead to notably increasing concentrations of IL-6 and MCP-1 in supernatants. IL-6 concentrations increased up to 800 pg/ml, while MCP-1 concentrations increased to reach values of 2000 to 4000 pg/ml (Figure 27, 28). These results imply, that hOB seem to be more sensitive and responsive to infection with *S. epidermidis* in the first hours of infection, while MG63 cells seem to need longer to respond to an infection with this bacterium. However, MG63 cells secreted much higher amounts of cytokines compared to hOB, which may be due to their origin as tumor cell line compared to primary cell lines.

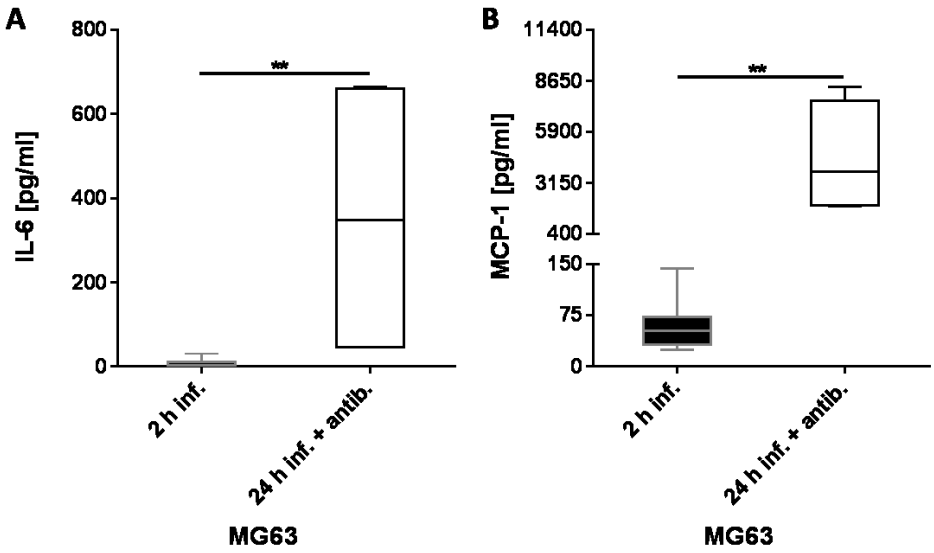

Figure 29: Interleukin-6 and MCP-1 secretion of MG63 cells infected with S. aureus. Concentrations of interleukin 6 (IL-6, **A**) and monocyte chemoattractant protein 1 (MCP-1, **B**) measured in supernatants of MG63 cells from adherence and internalization assays with *S. aureus*. 2 h inf.: cells infected with *S. epidermidis* for 2 hours in assay medium with a multiplicity of infection of 100; 24 h inf. + antib.: Cells cultivated up to 24 h following 2 h infection with *S. epidermidis* under antibiotic treatment with 200 µg/ml levofloxacin as prolonged internalization time. Values of cells cultured under the same conditions without bacteria were deducted from the respective sample values. $n \geq 4$. ** $p < 0.01$ (unpaired two-tailed Mann-Whitney U test).

Determination of cytokine concentrations using *S. aureus* and MG63 cells revealed treatment and time-dependent increase of IL-6 and MCP-1. For both cytokines, 2 h of infection of cells lead to weak secretion of both IL-6 and MCP-1 (Figure 29 A, B), reaching values of around 20 pg/ml IL-6 and 25 to 150 pg/ml MCP-1. However, significantly increased concentrations of IL-6 and MCP-1were detected following 24 h of antibiotic treatment of infected cells, however with high variance in the range of concentration. In general, cytokine secretion of MG63 cells under infection with *S. aureus* resembles those observed when using *S. epidermidis*. Comparing secreted amounts of cytokines of MG63 cells under infection with both bacteria, IL-6 concentrations were nearly similar while MCP-1 concentrations were in tendency higher when cells were infected with *S. aureus* compared to *S. epidermidis*. IL-12 as well as TNF-α secretion were not detected in any sample.

3.6.3 SEM imaging of MG63 cells and hOB infected with *S. epidermidis*

Representative SEM images of MG63 cells and hOB after infection with *S. epidermidis* are shown in Figure 30 and Figure 31, respectively.

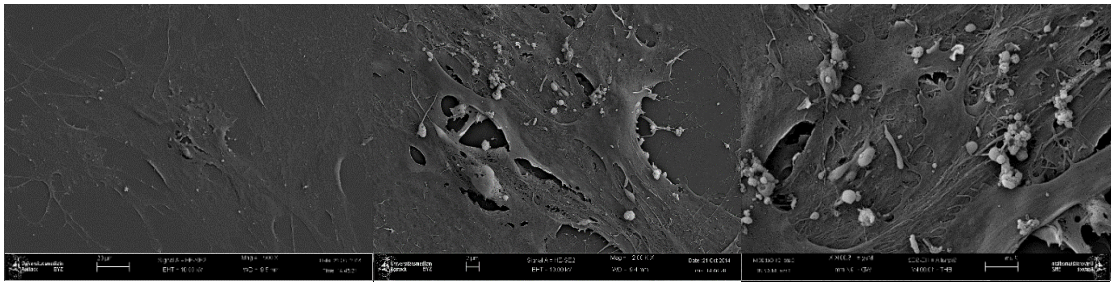

Figure 30: Representative SEM images of MG63 cells infected with S. epidermidis. Representative SEM images of MG63 cells infected with *S. epidermidis* after 2 h adherence. Left: 500x magnification; middle: 2000x magnif.; right: 5000x magnif.

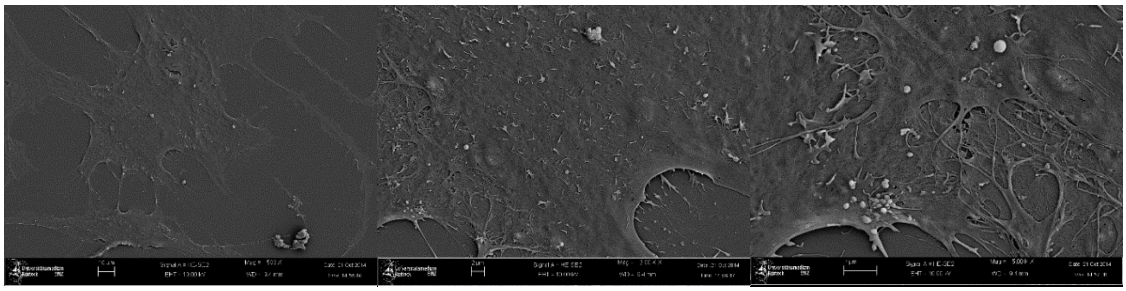

Figure 31: Representative SEM images of hOB infected with S. epidermidis. Representative SEM images of hOB infected with *S. epidermidis* after 2 h adherence. Left: 500x magnification; middle: 2000x magnif.; right: 5000x magnif.

In general, very few *S. epidermidis* were found on the surface of the cells. Large areas of the cells were not covered with *S. epidermidis*, while it also appeared that bacteria aggregated at some spots on the cells.

3.6.4 Co-culture of *S. epidermidis* and MG63 cells under electrical stimulation

To assess general applicability of the generated stimulation system for co-culture experiments, pilot experiments were performed using *S. epidermidis* and MG63 cells under conditions previously described (see Methods 2.6). Stimulation was carried out over 24 h continuously and a MOI of 100 was chosen for the co-culture setup since *S. epidermidis* showed low adherence potential to MG63 cells.

Recovered CFU/ml of *S. epidermidis* from supernatants, electrode surfaces and coverslips following electrical stimulation in the co-culture setup are presented in Figure 32.

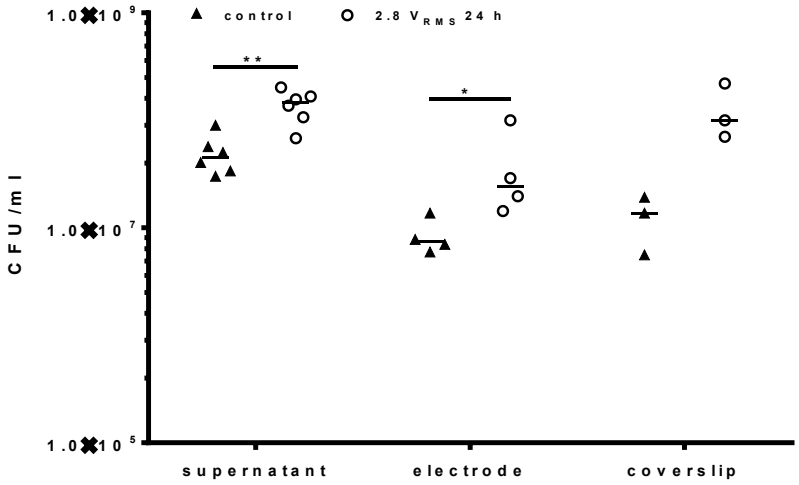

Figure 32: Determination of CFU/ml of S. epidermidis during co-culture and electrical stimulation. Recovered CFU/ml of *S. epidermidis* from supernatants, electrode surfaces and coverslips following 24 h continuous stimulation with 2.8 V_{RMS} and controls in a co-culture setup with MG63 osteosarcoma cells. * - $p < 0.05$; ** - $p < 0.01$ (unpaired Mann Whitney U-Test) $n \geq 3$.

Recovered CFU/ml of 2.8 V_{RMS} treated co-culture samples of *S. epidermidis* were significantly higher compared unstimulated controls for both supernatants and electrode surfaces. CFU/ml recovered from coverslips at the chamber bottom were also higher compared to unstimulated controls. In general, electrical stimulation enhanced bacterial numbers recovered from supernatants, as well as electrodes and coverslips, where MG63 cells were seeded previously.

Figure 33 shows cell count of viable cells on electrode surfaces and coverslips following 24 h of incubation of controls and 2.8 V_{RMS} treated co-culture samples as well as pH values measured at the end of the experiment.

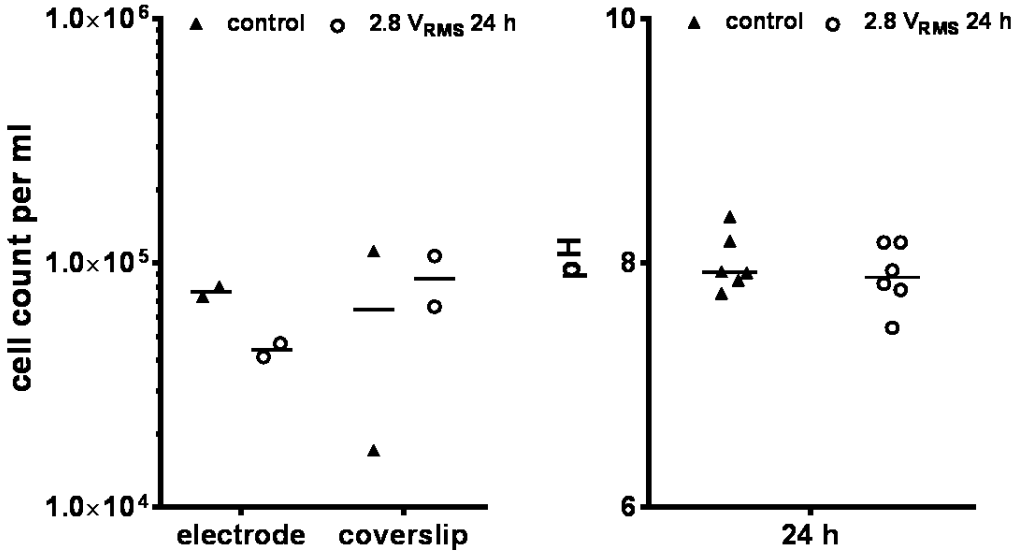

Figure 33: Cell count of viable MG63 cells following coculture with S. epidermidis under electrical stimulation and pH measurements. Left: Viable MG63 cells per ml following incubation for 24 h of controls and stimulated co-culture samples, n = 2. Right: pH measurement following 24 h of incubation of controls and stimulated co-culture samples, n = 6.

Viable osteoblasts recovered from electrode surfaces following stimulation were in tendency lower compared to unstimulated controls. Regarding pH, no differences between stimulated and control samples could be detected.

4 Discussion

This work is integrated in the DFG-funded research training group WELISA and focused on electrical stimulation of bacteria in an implant-associated infection context. For this purpose, an electrical stimulation system was developed to allow electrical stimulation of cells and bacteria using alternating current under similar conditions, which was not yet described in the literature. Additionally, a basic methodical setup was developed to gain maximum data output at minimum costs. The system was functionally validated with numerical simulation, while simulation data approximated measured real data regarding electric potential distribution in the region of interest. Hence, predictions of electric field distributions with varying parameter settings are possible. During this work, *S. epidermidis* and *S. aureus*, both main causatives of implant-associated infections, were subjected to electrical stimulation and effects on growth behavior as well as biofilm formation were investigated.

Furthermore, parameter studies were performed to compare effects of different V_{RMS} and stimulation periods to unravel optimal stimulation parameters to negatively influence the bacteria. However, effects observed were not constant over time and varied in intensity. Of note, using highest stimulation parameter in cell culture medium DMEM, effects on biofilm composition could be observed for both tested species. Subsequently, co-culture experiments with and without electrical stimulation were performed to investigate effects of electrical stimulation in a more infection-related situation. Adherence and internalization assays with following cytokine ELISAs were done for *S. epidermidis* and *S. aureus* in combination with hOB as well as MG63 cells, while pilot co-culture experiments under electrical stimulation were only conducted with *S. epidermidis* and MG63 cells.

4.1 Numerical simulation and choice of material

Numerical simulation proves to be an important tool to predict behavior of different systems *in silico*. In this case, numerical simulation was utilized to predict potential distributions and electric field displacement norms under varying parameter settings as well as to validate the generated system. However, crucial points in numerical simulations are input data as well as the simulation construct itself, which strongly influence the outcoming result.

In this work, impedance spectroscopy was used to determine system- and medium-specific electric properties, which were implemented in the following simulations as well as the CAD-model of the stimulation system. Since electric properties of materials and media can vary depending on temperature, measurements were done in a closed system at 37 °C to ensure experimental relevant data output.

Nevertheless, the obtained field distributions generated by numerical simulation differ compared to measured real data. The simulation assumes a more extensive potential gradient within the stimulation system than it could be observed during validation. Predicted values in the region of interest at the chamber bottom fitted well with measured values, while deviations increased with increasing distance to the electrodes. This results in an electric potential gradient inside the stimulation system, which is considerably smaller compared to the predicted gradient. In turn, this result benefits the fact, that the electric field generated inside the system is more homogenously distributed than predicted by numerical simulation. Hence, cells as well as bacteria are stimulated with similar electric field strengths in the region of interest. Since the system uses alternating current, starting parameters were chosen to reflect field strengths generated by the ASNIS III s-series screw system, resulting in up to 70 V/m field strength, which was used in context with bone fractures, avascular necrosis of femoral heads and foot arthrodesis (Windisch *et al.* 2014, Grunert *et al.* 2014).

Ti6Al4V was chosen as material for the stimulating electrodes because of the following reasons: First, it is widely used as standard material for total joint endoprostheses (Abdel-Hady Gepreel and Niinomi 2013, Wang 1996). Second, it provides good material properties, such as excellent biocompatibility, high fatigue limits as well as low Young's modulus and density (Abdel-Hady Gepreel and Niinomi 2013, Cornet *et al.* 1979, Velasco-Ortega *et al.* 2010). Additionally, this material is highly resistant against corrosion due to formation of a passivation layer on its surface (Fleck and Eifler 2010). Furthermore, electrode surfaces were roughened by corundum blasting, since roughening enlarges the surface of an implant. Rough surfaces were shown to enhance synthesis of growth factor and extracellular matrix in osteoblasts *in vitro* (Marinucci *et al.* 2006, Kieswetter *et al.* 1996, Martin *et al.* 1996). *In vivo*, rough surfaces were shown to enhance osseointegration by promotion of protein adsorption and cell adhesion to the implant surface (Cochran *et al.* 1996, Mavrogenis *et al.* 2009, Alla *et al.* 2011, Suzuki *et al.* 1997).

4.2 Effects of electrical stimulation on bacteria

In the field of electrical stimulation of bacteria, various setups and stimulation methods are applied. Stimulation methods comprise for example direct current (DC), pulsed current or alternating current applications in various forms (Asadi and Torkaman 2014). In this work, alternating current was chosen as stimulation method, because the before-mentioned ASNIS III s-screw series system was used as starting point for parameter choice, also applying alternating current. Furthermore, electrolytic and electrode reactions occurring during DC stimulation should be excluded as factors influencing the stimulated bacteria. However, only a few studies dealt with the topic of AC stimulation on bacteria compared to DC and pulsed current in general (Asadi and Torkaman 2014).
In 1972, Rowley conducted an *in vitro* study with both cathodal direct current and milliampere level alternating current. AC stimulation showed little or no effect on *E. coli* growth rates, while bactericidal effects could be observed under DC stimulation (Rowley 1972). In contrast, Spadaro *et al.* tested silver, platinum, gold, stainless-steel, and copper electrode to evaluate electrochemical effects on growth of four bacterial species using low currents of 0.02 to 20 µA/mm^2. At lower currents, only silver showed antibacterial effects while using the highest currents, all electrodes inhibited growth. The authors noted, that these effects occurred with electrolytic breakdown of the medium as well as severe corrosion of the metal (Spadaro *et al.* 1974). Another study conducted by Petrofsky *et al.* subjected *S. aureus*, *E. coli* and *P. aeruginosa* to AC and DC stimulation. Bacteria were treated for 30 min with either AC or DC and were subsequently incubated 24 h before determination of bacterial counts. The authors reported significantly reduced growth of *P. aeruginosa*, while *S. aureus* and *E. coli* where only marginally affected by AC stimulation (Petrofsky *et al.* 2008). Maadi *et al.* 2010 also observed no inhibitory effect of AC on growth of *P. aeruginosa in vitro*. Here, glass agar plates were connected with stainless-steel electrodes and inhibition zones caused by electrical stimulation were measured (Maadi *et al.* 2010). In contrast, DC stimulation with low amperage (10 µA) showed antimicrobial activity when applied to *S. aureus* and *S. epidermidis* (Liu *et al.* 1997). Furthermore, stimulating bacteria with high voltage pulsed currents (HVPC) was shown to inhibit growth of *S. aureus*, *E. coli*, and *P. aeruginosa* at both the anode and cathode following exposure to HVPC for 2 h at 250 V (Kincaid and Lavoie 1989). Another recent study conducted in 2015 investigated effects of alternating current combined with different disinfectants.

Mirzaii *et al.* applied electric field strengths of 6 to 10 V/cm^2 at 50 KHz, 1 MHz, 10 MHz and 20 MHz during lag phases of *S. aureus* and *P. aeruginosa*. The authors reported effectively reduced growth of *S. aureus* and *P. aeruginosa* when 10 V/cm^2 at 20 MHz was applied (Mirzaii *et al.* 2015). Regarding effects of electrical current combined with antibiotics against bacterial biofilms, del Pozo *et al.* 2009 showed increased eradication of biofilm-bound MRSA (methicillin-resistant *Staphylococcus aureus*) and *S. epidermidis*. In the mentioned study, biofilms were pre-cultured on Teflon disks and were treated in a continuous flow chamber where antimicrobial agents as well as electrical current were applied. The authors concluded, that the activity of antimicrobial substances can be enhanced by additional electrical stimulation. However, this effect is not generalizable across microorganisms and antimicrobial agents (del Pozo *et al.* 2009a). In our work, antibiotic susceptibility was not altered following electrical stimulation. Nevertheless, antibiotic treatment could be combined with electrical stimulation using the novel stimulation system to further evaluate effects and efficacy of antibiotic treatment coupled with electrical stimulation.

Comparing the obtained results of this work to other studies, it can be stated that AC stimulation, under the parameters described earlier, showed little to no effect on growth and general biofilm formation of *S. epidermidis* and *S. aureus*. Since mostly *S. aureus* was used in literature, this work provides evidence, that *S. epidermidis* is also largely unaffected by AC stimulation. However, we can also report no beneficial effects of AC stimulation on bacterial growth. This fact benefits the possibility, that some of the parameter settings tested could have a positive influence on bone cells while resulting in little to no effects on bacteria. Hence, electrical stimulation using AC could be used to enhance wound healing or osteoblast proliferation while not further supporting bacterial growth in an implant infection situation.

4.3 Influences of AC stimulation on biofilm composition

Biofilm formation, regulation and its composition are crucial for facilitating settlement on different surfaces, coping with changing environmental factors or evading the host immune system as well as persisting on artificial surfaces or devices. *S. epidermidis* possesses the so-called autolysin AtlE, which is a protein belonging to a group of bacterial peptidoglycan (PGN) – hydrolases involved in bacterial cell wall degradation processes (Biswas *et al.* 2006). It was also shown to contribute to *S. epidermidis* binding to unmodified polystyrene (Heilmann *et al.* 1997). Furthermore, AtlE is involved in

extracellular DNA (eDNA) mediated biofilm formation of *S. epidermidis* (Qin *et al.* 2007, Christner *et al.* 2012).

eDNA, besides involving primary attachment, contributes to stabilization of biofilms as an intercellular adhesion (Whitchurch *et al.* 2002). It is believed, that these intercellular adhesion processes are critical for biofilm formation, especially during the early accumulative phase (Qin *et al.* 2007). More recently, contribution of eDNA during *S. aureus* surface colonization was shown, where eDNA was observed to be important in the transition of attachment to accumulation under flow conditions (Moormeier *et al.* 2014). Despite being a structural component of biofilm matrix in both *S. epidermidis* and *S. aureus*, different functions, at least to an extent, are assumed for eDNA. However, several studies showed eDNA release through increased cell lysis (Allesen-Holm *et al.* 2006, Rice *et al.* 2007, Christner *et al.* 2012,). A major part of this cell lysis activity depends on AtlE described earlier (Biswas *et al.* 2006). Comparing this to the results obtained from general biofilm formation and the biofilm composition assays, there is a possibility that electrical stimulation somehow influences activity and regulation as well as eDNA amount in biofilm formation of both tested species. It was shown in this work, that previous electrical stimulation lead to significantly decreased amounts of eDNA in *S. epidermidis* biofilms when stimulated with 1.4 V_{RMS}. This in turn, besides the culture conditions, could be responsible for overall weak biofilm formation. Additionally, if electrical stimulation can influence eDNA amount, the general stability of the formed biofilm could be impaired in case of *S. epidermidis*. It is also possible, that electrical stimulation somehow influences AtlE activity, which in turn could lead to decreased cell lysis and therefore to a reduced amount of eDNA present in the formed biofilm. Regarding *S. aureus*, significantly increased eDNA amounts were detected following stimulation with 1.4 V_{RMS}. However, the increase was in a relatively small range questioning biological relevance of this observation. Gene expression and enzyme studies could give an insight on relevant expression levels as well as AtlE activity to investigate possible influence of electrical stimulation on biofilm-relevant molecules and mechanisms.

4.4 Interactions of *S. epidermidis* with cells

During this work, it was shown that *S. epidermidis* adheres and internalizes in hOB as well as in MG63 osteosarcoma cells, however, with a less pronounced phenotype compared to *S. aureus*. Both species express cell surface proteins which can mediate

specific interactions with host extracellular matrix components (ECM) (Patti *et al.* 1994, Büttner *et al.* 2015). Those proteins are believed to play an important role in the development of device infections, since these devices become covered by ECM as soon as they are inserted into the body. Such components are for example fibronectin, fibrinogen, vitronectin or collagen (Arrecubieta *et al.* 2006, Mack *et al.* 2009). One group of such proteins are serine-aspartate repeat (Sdr) proteins (McCrea *et al.* 2000, Büttner *et al.* 2015), which are belonging to MSCRAMMs (Microbial Surface Components Recognizing Adhesive Matrix Molecules) (Josefsson *et al.* 1998, Foster *et al.* 2014). Three different types are described for *S. epidermidis*, SdrF, SdrG, and SdrH (Josefsson *et al.* 1998). The proteins SdrF and SdrG of *S. epidermidis* show an organization which is similar to SdrC, SdrD, and SdrE from *S. aureus*. While SdrG was shown to bind fibronectin, and was therefore called Fbe, SdrF was revealed as a collagen-binding protein (Arrecubieta *et al.*, 2007). However, Arrecubieta *et al* showed 2009, that inhibition of SdrF in *S. epidermidis* resulted only in partial binding inhibition. Hence, other collagen binding factors seem to be involved in this process (Arrecubieta *et al.* 2009).

Concerning electrical stimulation of bacteria and cells in a co-culture setup, increased bacterial numbers were observed when both cells and bacteria were stimulated compared to control samples. Different causes could be discussed, since underlying effects of electrical stimulation are not known yet. It could be possible, that the cells, following pre-incubation for 24 h to adhere to the surfaces in the stimulation system, where influenced by electrical stimulation and expressed increased amounts of collagen or other ECM components. Another contributing factor could be elevated expression of ECM or biofilm related genes in *S. epidermidis* under electrical stimulation. However, changes on transcription level due to electrical stimulation were not investigated so far. Furthermore, Lee *et al.* showed 2010, that *S. epidermidis* did not influence cell adhesion and viability of MC3T3-E1 cells (osteoblasts) in a microfluidic environment (Lee *et al.* 2010). They could show, that cells were initially not influenced in adhesion and viability on a Ti alloy surface. However, at the end of the experiments, cell damaging was reported at the point where bacteria started to proliferate and to aggregate (Lee *et al.* 2010). Similar observations were made for the co-culture experiments described here. During the experiments described in this work, MG63 cells had 24 h time to adhere and to produce ECM components until the onset of electrical stimulation while infecting them with *S. epidermidis*. Since the co-culture experiments were only conducted over 24 h, long

term exposure effects on MG63 cells caused by *S. epidermidis* were not investigated. Still, the underlying mechanisms describing the observations are yet to be elucidated.
Regarding cytokine secretion of osteoblasts following infection, we could show that *S. epidermidis* induces IL-6 and MCP-1 secretion in MG-63 cells. However, to a lower amount compared with *S. aureus.* Additionally, hOB appeared to be quicker in response compared to MG-63, though not reaching maximum secretion levels shown for MG-63. Also of note is the fact, that cytokine secretion in hOB was also observed when using medium control conditions without bacteria. Based on this, the secreted amounts of IL-6 and MCP-1 are most likely caused by influence of the medium and not by presence of the bacteria. Interestingly, when infecting hOB with *S. epidermidis*, secreted amounts of IL-6 and MCP-1 were lower compared to medium controls without bacteria. Bost *et al.* as well as Ning *et al.* showed cytokine secretion by osteoblasts invaded by *S. aureus* (Bost *et al.* 1999, Ning *et al.* 2011), while up until now no information is available on secretion of cytokines under infection with *S. epidermidis*. The observations made in this work therefore give a hint to a better understanding of the outcome of interaction of osteoblasts with *S. epidermidis*, while it remains to be investigated, if *S. epidermidis* is also able to regulate IL-6 and MCP-1 secretion by influencing Nf-κB signaling in osteoblasts (Ning *et al.* 2011).

4.5 Limitations and Outlook

The stimulation system described in this work was developed to provide a novel tool in researching effects of AC on bacteria and cells suitable for basic research. AC circumvents typical electrolytic and electrode reactions occurring when using DC stimulation, providing solely effects of the electric field. However, since formation of radicals and toxic substances, e.g. H_2O_2 or chlorine, are described as a mechanism of effect in electrical stimulation, such effects using AC stimulation could be neglected. Nevertheless, this system is suitable to investigate effects solely based in the generated fields without further influence through electrode reactions. Though it provides a broad methodical setup for data output, there are also limitations of the system, which should be noted. Numerical simulations proved useful for the prediction of electric potentials and field distributions, however, simulations should be optimized for future experiments using this system to approximate real field distributions better than it is currently the case.

Furthermore, only Ti6Al4V was used as electrode material in this work. Since not only titanium implants are used in the orthopedic context, other implant materials should be used as electrode materials to discern the influence of the respective materials on the effects of electrical stimulation. Another point is, that only two *Staphylococcus* species were investigated during this work, namely *S. epidermidis* and *S. aureus*. Despite the fact, that both are the main causatives of prosthetic joint infections, other bacteria commonly found in PJI should also be investigated using this system. Examples would be *Pseudomonas aeruginosa* or *Escherichia coli*, since both are also described as organisms used for DC stimulation experiments in literature. Also, bacterial genome wide transcription analyses should be performed following electrical stimulation of bacteria to obtain information about underlying mechanisms and effects on genome level and not only macroscopically. Additionally, the described system was tested with human osteoblasts isolated from patient hips as well as the MG63 osteosarcoma cell line. Further experimental approaches using different cell types would be beneficial to support better understanding of effects of electrical stimulation in general. Another point is the co-culture setup, which should be extended further to prove the observations made during this work. Co-culture under electrical stimulation was not described until now and should be used to gain further insight in the complex interplay between bacteria and cells subjected to electrical stimulation. Also, this point is of clinical relevance since electrical stimulation is used as an adjunctive method in therapy.

5 Summary

This work was integrated in the DFG funded research training group GRK 1505/2 welisa. Here, an *in vitro* system for electrical stimulation of cells and bacteria using alternating current was developed. Electrical stimulation of both cells and bacteria can be conducted under similar conditions using Ti6Al4V electrodes separated with an insulator in a non-conductive stimulation chamber. Prior to stimulation experiments, numerical simulations for the system were performed to predict potential and electric field distributions inside the stimulation chamber. Numerical simulations predicted more extensive potential gradients than could be observed in real measurements, resulting in higher field strength range anticipations. A basic methodical setup was established to evaluate effects of electrical stimulation on bacteria allowing determination of living bacteria in supernatants and on the electrode surfaces, quantification of produced biofilm mass, minimal inhibitory concentration (MIC) determination of selected antibiotics as well as pH measurements, biofilm composition analyses and FACS-based discrimination of living and dead bacteria.

Electrical stimulation of *S. epidermidis* and *S. aureus* with either 0.2, 1.4 or 2.8 V_{RMS} (either 3 x 45 min per day or continuously stimulated) showed significant but not consistent effects on bacterial growth and biofilm mass production. Regarding changes in antibiotic susceptibility of bacteria due to electrical stimulation, no effects could be observed when bacteria were subjected to electrical stimulation.

Following electrical stimulation of *S. epidermidis* with 1.4 V_{RMS} in DMEM, significantly decreased amounts of extracellular DNA were detected in the biofilm extracellular matrix. In contrast, extracellular DNA amounts were significantly increased after electrical stimulation of *S. aureus* with 1.4 V_{RMS} in DMEM.

When infecting hOB and MG63 cells with *S. epidermidis*, IL-6 and MCP-1 secretion were detected. hOB showed a faster response, while the maximum response was higher in MG63 cells. In a co-culture approach under electrical stimulation, increased CFU/ml *S. epidermidis* were found in supernatants, on and into MG63 cells on electrode surfaces and the chamber bottom.

No electrolytic and electrode reactions were observed during electrical stimulation experiments, excluding these factors for effects on bacteria in the developed system.

6 References

Abdel-Hady Gepreel M, and Niinomi M. (2013) *Biocompatibility of Ti-alloys for long-term implantation*. Journal of Mechanical Behavior of Biomedical Materials, Vol. 20: 407-415

Aires De Sousa M, and De Lencastre H. (2004) *Bridges from hospitals to the laboratory genetic portraits of methicillin-resistant Staphylococcus aureus clones.* FEMS Immunology and Medical Microbiology, Vol. 40(2): 101-111

Alla RK, Ginjupalli K, Upadhya N, Shammas M, Ravi, RK, and Sekhar R. (2011) *Surface roughness of implants: a review.* Trends in Biomaterials and Artificial Organs, Vol. 25(3): 112-118

Allesen-Holm M, Barken KB, Yang L, Klausen M, Webb JS, Kjelleberg S, Molin S, Givskov M, and Tolker-Nielsen T. (2006) *A characterization of DNA release in Pseudomonas aeruginosa cultures and biofilms.* Molecular Microbiology. Vol. 59(49: 1114-1128

Arrecubieta C, Asai T, von Bayern M, Loughman A, Fitzgerald JR, Shelton CE, Baron HM, Dang NC, Deng MC, Naka Y, Foster TJ, and Lowy FD. (2006). *The role of Staphylococcus aureus adhesins in the pathogenesis of ventricular assist device-related infections*. The Journal of Infectious Diseases. Vol. 193(8): 1109–1119

Arrecubieta C, Lee MH, Macey A, Foster TJ, and Lowy FD. (2007) *SdrF, a Staphylococcus epidermidis surface protein, binds type I collagen.* The Journal of Biological Chemistry. Vol. 282(26): 18767-18776

Arrecubieta C, Toba FA, von Bayern M, Akashi H, Deng MC, Naka Y, and Lowy FD. (2009) *SdrF, a Staphylococcus epidermidis Surface Protein, Contributes to the Initiation of Ventricular Assist Devicec Driveline-Related Infections.* PLoS Pathogens. Vol. 5(5): e1000411

Asadi MR and Torkaman G. (2014) *Bacterial Inhibition by Electrical Stimulation (Review)* Advances in Wound Care, Vol.3(2), 91-97

Bien J, Sokolova O, and Bozko P. (2011) *Characterization of Virulence Factors of Staphylococcus aureus: Novel Function of Known Virulence Factors That Are Implicated in Activation of Airway Epithelial Proinflammatory Response.* Journal of Pathogens, Vol. 2011, doi: 10.4061/2011/601905

Biswas R, Voggu L, Simon UK, Hentschel P, Thumm G, and Gotz F. (2006) *Activity of the major staphylococcal autolysin Atl.* FEMS Microbiology Letters. Vol 259: 260-268

Bost KL, Ramp WK, Nicholson NC, Bento JL, Marriott I and Hudson MC (1999) *Staphylococcus aureus Infection of Mouse or Human Osteoblasts Induces High Levels of Interleukin-6 and Interleukin-12 Production*. The Journal of Infectious Diseases, Vol. 180(6):1912-20

Bradshaw PJ, Stobie P, Knuiman MW, Briffa TG, and Hobbs MS. (2014) *Trends in the incidence and prevalence of cardiac pacemaker insertions in an ageing population.* Open Heart, Vol. 1(1), e000177

Büttner, H, Mack D, and Rohde H. (2015) *Structural basis of Staphylococcus epidermidis biofilm formation: mechanisms and molecular interactions.* Frontiers in Cellular and Infection Microbiology. Vol. 5, Article 14

Caubet R, Fedarros-Caubet F, Chu M, Freye E, de Belém Rodrigues M, Moreau JM, and Ellison WJ. (2004) *A Radio Frequency Electric Current Enhances Antibiotic Efficacy against Bacterial Biofilms*. Antimicrobial Agents and Chemotherapy, Vol. 48(12): 4662-4664

Christner M, Heinze C, Busch M, Franke G, Hentschke M, Bayard Dühring S, Büttner H, Kotasinska M, Wischnewski V, Kroll G, Buck F, Molin S, Otto M, and Rohde H. (2012) *sarA Negatively Regulates Staphylococcus Epidermidis Biofilm Formation by Modulating Expression of 1 MDa Extracellular Matrix Binding Protein and Autolysis-Dependent Release of eDNA.* Molecular Microbilogy. Vol. 86(2): 394-410

Cochran DL, Nummikoski PV, Higginbottom FL, Hermann JS, Makins SR, and Buser D. (1996) *Evaluation of an endosseous titanium implant with a sandblasted and acid-etched surface in the canine mandible.* Clinical Oral Implants Research, Vol. 7(3): 240-252

Cornet A, Muster D, and Jaeger JH. (1979) *Fatigue: corrosion of endoprosthesis titanium alloys.* Biomaterials Medical Devices and Artificial Organs, Vol. 7(1): 155-167

Costerton JW, Ellis B, Lam K, Johnson F, Khoury AE. (1994) *Mechanism of electrical enhancement of efficacy of antibiotics in killing biofilm bacteria*. Antimicrobial Agents and Chemotherapy, Vol. 38:2803-9

Costerton JW, Stewart PS, and Greenberg EP. (1999) *Bacterial biofilms: a common cause of infections.* Science, Vol. 284(5418), 1318-1322

Dauben TJ, Ziebart J, Bender T, Zaatreh S, Kreikemeyer B, and Bader R. (2016) *A Novel In Vitro System for Comparative Analyses of Bone Cells and Bacteria under Electrical Stimulation.* BioMed Research International, Vol. 2016, Article ID 5178640, http://dx.doi.org/10.1155/2016/5178640

del Pozo J L, Rouse M S, Mandrekar J N, Sampedro M F, Steckelberg J M, Patel R (2009a) *Effect of Electrical Current on the Activities of Antimicrobial Agents against Pseudomonas aeruginosa, Staphylococcus aureus, and Staphylococcus epidermidis Biofilms*. Antimicrobial Agents and Chemotherapy, Vol. 53(1): 35-40 (1)

del Pozo J L, Rouse M S, Mandrekar J N, Steckelberg J M, Patel R (2009b) *The Electricidal Effect: Reduction of Staphylococcus and Pseudomonas Biofilms by Prolonged Exposure to Low-Intensity Electrical Current*. Antimicrobial Agents and Chemotherapy, Vol. 53(1): 41-45 (2)

Dolbow JD, Dolbow DR, Gorgey AS, Adler RA, and Gater DR. (2014) *The effects of aging and electrical stimulation exercise on bone after spinal cord injury.* Aging and Disease, Vol. 4(3), 141-153

Ehrensberger MT, Menachem ET, Nodzo SR, Hansen LA, Luke-Marshall NR, Cole RF, Wild LM, Campagnari AA (2015) *Cathodic voltage-controlled electrical stimulation of titanium implants as treatment for methicillin-resistant Staphylococcus aureus periprosthetic infections.* Biomaterials, Vol. 41: 97-105

Ercan B, Kummer K M, Tarquinio K M, Webster T J. (2011) *Decreased Staphylococcus aureus biofilm growth on anodized nanotubular titanium and the effect of electrical stimulation*. Acta Biomaterialia, Vol. 7: 3003-3012

Fleck C, and Eifler D. (2010) *Corrosion, fatigue and corrosion fatigue behavior of metal implant materials, especially titanium alloys.* International Journal of Fatigue, Vol. 32(6): 929-935

Foster TJ, and Höök M. (1998) *Surface protein adhesins of Staphylococcus aureus.* Trends in Microbiology, Vol. 6(12): 484-488

Foster TJ, Geoghegan JA, Ganesh VK, and Hook M. (2014) *Adhesion, invasion and evasion: the many functions of the surface eproteins of Staphylococcus aureus*. Nature Reviews Microbiology. Vol. 12: 49–62

Giladi M, Porat Y, Blatt A, Wasserman Y, Kirson E D, Dekel E, Palti Y. (2008) *Microbial Growth Inhibition by Alternating Electric Fields*. AAC Vol. 52(10): 3517-3522

Grice EA, Kong HH, Conian S, Deming CB, Davis J, Young AC, Program NCS, Bouffard GG, Blakesley RW, Murray PR, Green ED, Turner ML, Segre JA. (2009) *Topographical and temporal diversity of the human skin microbiome*. Science, Vol. 324: 1190-1192

Griffin M and Bayat A. (2011) *Electrical stimulation in bone healing: critical analysis by evaluation levels of evidence.* ePlasty: Open Access Journal of Plastic Surgery, Vol. 11, e34

Grunert PC, Jonitz-Heincke A, Su Y, Souffrant R, Hansmann D, Ewald H, Krüger A, Mittelmeier W, and Bader R. (2014) *Establishment of a novel in vitro test setup for electric and magnetic stimulation of human osteoblasts.* Cell Biochemistry and Biophysics, Vol. 70(2): 805-817

Harrasser N, Lenze U, and Pohlig F. (2012) *Periprosthetic joint infection: diagnosis and treatment.* Deutscher Ärzte Verlag, OUP, Vol. 1(7-8), 16-22

Heilmann C, Hussain M, Peters G, and Gotz F. (1997) *Evidence for autolysin-mediated primary attachment of Staphylococcus epidermidis to a polystyrene surface.* Molecular Microbiology, Vol. 24: 1013-1024

Heilmann,C. (2011) *Adhesion mechanisms of staphylococci.* Bacterial Adhesion: Advances in Experimental Medicine and Biology, Vol. 715, eds, D. Linke and A. Goldman (Dordrecht: Springer), 105–123

Jamal M, Tasneem U, Hussain T, and Andleeb S. (2015) *Bacterial Biofilm: Its Composition, Formation and Role in Human Infections.* Research & Reviews: Journal of Microbiology and Biotechnology, Vol. 4(3), e-ISSN:2320-3528

Joh D, Wann ER, Kreikemeyer B, Speziale P, and Höök M. (1999) *Role of fibronectin-binding MSCRAMMs in bacterial adherence and entry into mammalian cells*. Matrix Biology. Vol. 18(1999): 211-223

Josefsson E, McCrea KW, Ní Eidhin D, O'Connell D, Cox J, Höök M, and Foster TJ. (1998) *Three new members of the serine-aspartate repeat protein multigene family of Staphylococcus aureus*. Microbiology. Vol. 144 (Pt. 12): 3387-3395

Josse J, Velard F, and Gangloff SC. (2015) *Staphylococcus aureus vs. Osteoblast: Relationship and Consequences in Osteomyelitis.* Front. Cell. Infect. Microbiol., Vol. 5(85)

Kern H, Salmons S, Mayr W, Rossini K, and Carraro U. (2005) *Recovery of long-term denervated human muscles induced by electrical stimulation.* Muscle & Nerve, Vol. 31(1), 98-101

Khalil H, Williams RJ, Stenbeck G, Henderson B, Meghji S, and Nair SP. (2007) *Invasion of bone cells by Staphylococcus epidermidis*. Microbes and Infection, doi: 10.1016/j.micinf.2007.01.002

Kieswetter K, Schwartz Z, Hummert TW; Cochran DL, Simpson J, Dean DD, and Boyan BD. (1996) *Surface roughness modulates the local production of growth factors and cytokines by osteoblast-like MG-63 cells.* Journal of Biomedical Materials Research, Vol. 32(1): 55-63

Kincaid CB and Lavoie KH. (1989) *Inhibition of Bacterial Growth In Vitro Following Stimulation with High Voltage, Monophasic, Pulsed Current.* Physical Therapy, Vol. 69(8): 651-655

Kloth LC. (2005) *Electrical stimulation for wound healing: a review of evidence from in vitro studies, animal experiments, and clinical trials.* International Journal of Lower Extremity Wounds, Vol. 4(1), 23-44

Klouche S, Sariali E, and Mamoudy P. (2010) *Total hip arthroplasty revision due to infection: a cost analysis approach.* Orthopaedics and Traumatology: Syrgery and Research, Vol. 96(2), 124-132

Kraus W. (1992) *The treatment of pathological bone lesions with nonthermal, extremely low-frequency electromagnetic-fields*. Bioelectrochemistry and Bioenergetics, Vol. 27(3):321-339.20

Kurtz SM, Lau E, Watson H, Schmier JK, and Parvizi J. (2012) *Economic burden of periprostethic joint infection in the United States.* The Journal of Arthroplasty, Vol. 27(8), 61-65

Kuzyk P. RT, Schemitsch E. H. (2009). *The science of electrical stimulation therapy for fracture healing*. Indian Journal of Orthopaedics, Vol. 43(2):127-131.

Lamagni T. (2014) *Epidemiology and burden of prosthetic joint infections.* Journal of Antimicrobial Chemotherapy, Vol. 69, Suppl 1: i5-i10

Latham W and Lau JTC. (2011) *Bone stimulation: a review of its use as an adjunct.* Techniques in Orthopaedics, Vol. 26(1), 14-21

Lee J-H, Wang H, Kaplan JB, and Lee WY. (2010) *Effects of Staphylococcus epidermidis on osteoblast cell adhesion and viability on a Ti alloy surface in a microfluidic co-culture environment.* Acta Biomaterialia. Vol. 6(11): 4422-4429

Liu GY. (2009) *Molecular Pathogenesis of Staphylococcus aureus infection.* Pediatric Research, Vol. 65(5 Pt 2): 71R-77R

Liu WK, Brown MRW, and Elliott TSJ. (1997) *Mechanisms of the bactericidal activity of low amperage electric current (DC).* Journal of Antimicrobial Chemotherapy, Vol. 39: 687-695

Lowy FD (1998) *Staphylococcus aureus infections.* The New England Journal of Medicine, Vol. 339: 520-532

Maadi H, Haghi M, Delshad R, Knagarloo H, Mohammadnezhady MA, and Hemmatyar GR. (2010) *Effect of alternating and direct currents on Pseudomonas aeruginosa growth in vitro.* African Journal of Biotechnology, Vol 9(38): 6373-6379

Mack D, Davies AP, Harris LG, Knobloch JK, Rohde H. (2009) *Staphylococcus epidermidis Biofilms: Functional Molecules, Relation to Virulence, and Vaccine Potential.* Topics in Current Chemistry. Vol. 288: 157-182

Mah TFC, and O'Toole GA. (2001) *Mechanisms of biofilm resistance to antimicrobial agents*. Trends in Microbiology, Vol. 9(1), 34-39

Marinucci L, Balloni S, Becchetti E, Belcastro S, Guerra M, Calvitti M, Lilli C, Calvi EM, and Locci P. (2006) *Effect of titanium surface roughness on human osteoblast proliferation and gene expression in vitro.* International Journal of Oral & Maxillofacial Implants, Vol. 21(5): 719-725

Martin JY, Schwartz Z, Hummert TW, Schraub DM, Simpson J, Lankford J Jr, Dean DD, Cochran DL, Boyan BD. (1996) *Effect of titanium surface roughness on proliferation, differentiation, and protein synthesis of human osteoblast-like cells (MG63).* Journal of Biomedical Materials Research, Vol. 29(3): 389-401

Matl FD, Obermeier A, Zlotnyk J, Friess W, Sternberger A, Burgkart R. (2011) *Augmentation of Antibiotic Activity by Low-Frequency Electric and Electromagnetic Fields Examining Staphylococcus aureus in Broth Media*. Bioelectromagnetics, Vol. 32: 367-377

Mavrogenis AF, Dimitriou R, Parvizi J, and Babis GC. (2009) *Biology of implant osseointegration.* Journal of Musculoskeletal Neuronal Interactions, Vol. 9(2): 61-71

McCrea KW, Hartford O, Davis S, Eidhin DN, Lina G, Speziale P, Foster TJ, and Höök M. (2000) *The serine-aspartate repeat (Sdr) protein family in Staphylococcus epidermidis.* Microbiology. Vol. 146 (Pt. 7): 1535-1546

Merriman HL, Hegyi CA, Albright-Overton CR, Carlos J Jr, Putnam RW, Mulcare JA. 2004. *A comparison of four electrical stimulation types on Staphylococcus aureus growth in vitro*. Journal or Rehabilitation Research & Development, Vol. 41(2):139-146

Meng S, Rouabhia M, Zhang Z. (2013) *Electrical stimulation modulates osteoblast proliferation and bone protein production through heparin-bioactivated conductive scaffolds*. Bioelectromagnetics, Vol. 34(3):189-99

Mirzaii M, Alfi A, Kasaeian A, Norozi P, Nasiri M, Sarokhalil DD, Khoramrooz SS, Fazli M, and Davardoost F. (2015) *Antibacterial effect of alternating current against Staphylococcus aureus and Pseudomonas aeruginosa.* Russian Open Medical Journal. Vol 4(2): e0203

Moormeier DE, Bose JL, Horswill AR; and Bayles KW. (2014) *Temporal and stochastic control of Staphylococcus aureus biofilm development.* mBio. Vol. 14(5): e01341-14

Ning R, Zhang X, Guo X, Li Q (2011) *Staphylococcus aureus regulates secretion of interleukin-6 and monocyte chemoattractant protein-1 through activation of nuclear factor kappaB signaling pathway in human osteoblasts.* Brazilian Journal of Infectious Diseases, 15(3):189-94

Nodzo S, Tobias M, Hansen L, Luke-Marshall NR, Cole R, Wild L, Campagnari AA, and Ehrensberger MT. (2015) *Cathodic Electrical Stimulation With Vancomycin Enhances Treatment of Methicillin-resistant Staphylococcus aureus Implant-associated Infections.* Clinical Orthopaedics and Related Research, doi: 10.1007/s11999-015-4280-3

Obermeier A, Matl FD, Friess W, Stemberger A. 2009. *Growth Inhibition of Staphylococcus aureus Induced by Low-Frequency Electric and Electromagnetic Fields.* Bioelectromagnetics, Vol. 30:270-279

Onibere R and Khanna A. (2008) *The Role Of Electrical Stimulation In Fracture Healing*. The Internet Journal of Orthopedic Surgery, Vol. 11(2)

Otto M (2009) *Staphylococcus epidermidis – the 'accidental' pathogen (Review)* Nature Reviews Microbiology, Vol. 7 (555-567)

Patti JM, Allen BL, McGavin MJ, and Höök M. (1994) *MSCRAMM-Mediated adherence of microorganisms to host tissues*. Annual Review of Microbiology. Vol. 48: 585–617

Perlmutter JS and Mink JW. (2006) *Deep Brain Stimulation.* Annual Review of Neuroscience, Vol. 29, 229-257

Petrofsky J, Laymon M, Chung W, Collins K, and Yang TN. (2008) *Effect of electrical stimulation on bacterial growth.* The Journal of Neurological and Orthopaedic Medicine and Surgery, Vol. 31: 43

Poole K. (2002) *Mechanisms of bacterial biocide and antibiotic resistance.* Journal of Applied Microbiology Symposium Supplement, Vol. 92, 55S-64S

Qin Z, Ou Y, Yang L, Zhu Y, Tolker-Nielsen T, Molin S, Qu D. (2007) *Role of autolysin-mediated DNA release in biofilm formation of Staphylococcus epidermidis.* Microbiology. Vol. 153 (Pt 7): 2083-2092

Rasigade JP, Moulay A, Lhoste Y, Tristan A, Bes M, Vandenesch F, Etienne J, Lina G, Laurent F and Dumitrescu O (2011) *Impact of sub-inhibitory antibiotics on fibronectin-mediated host cell adhesion and invasion by Staphylococcus aureus.* BMC Microbiology 11:263

Rice KC, Mann EE, Endres JL, Weiss EC, Cassat JE, Smeltzer MS, Bayles KW. (2007) *The cidA murein hydrolase regulator contributes to DNA release and biofilm development in Staphylococcus aureus.* Proceedings of the National Academy of Sciences of the USA. Vol. 104(19): 8113-8118

Rowley BA. (1972) *Electrical current effects on E. coli growth rates.* Proceedings of the Society for Experimental Biology and Medicine. Vol. 139(3): 929-934

Rushton DN. (2002) *Electrical stimulation in the treatment of pain.* Disability and Rehabilitation, Vol. 24(8), 407-415

Saadatian-Elahi M, Teyssou R, Vanhems P. (2008). *Staphylococcus aureus*, *the major pathogen in orthopaedic and cardiac surgical site infections: A literature review*. International Journal of Surgery, Vol. 6(3):238-245.

Sanchez Jr CJ, Ward CK, Romano DR, Hurtgen BJ, Hardy SH, Woodbury RL, Trevino AV, Rathborne CR, and Wenke JC. (2013) *Staphylococcus aureus biofilms decrease osteoblast viability, inhibits osteogenic differentiation, and increases bone resorption in vitro*. BMC Musculoskeletal Disorders, 14, 187

Sandvik EL, McLeod BR, Parker AE, and Stewart PS. (2013) *Direct Electric Current Treatment under Physiologic Saline Condition Kills Staphylococcus epidermidis Biofilms via Electrolytic Generation of Hypochlorous Acid*. PlosOne, Vol. 8(2), e55118

Schatz A, Röck T, Naycheva L, Willmann G, Wilhelm B, Peters T, Bartz-Schmidt KU, Zrenner E, Messias A, and Gekeler F. (2011) *Transcorneal electrical stimulation for patients with retinitis pigmentosa: a prospective, randomized, sham-controlled exploratory study.* Investigative Opthalmology & Visual Science, Vol. 52(7), 4485-4496

Sekhar S, Kumar R, and Chakraborti A. (2009) *Role of biofilm formation in the persistent colonization of Haemophilus influenzae in children from northern India.* Journal of Medical Microbiology, Vol. 58, 1428-1432

Shi S and Zhang X. (2012) *Interaction of Staphylococcus aureus with osteoblasts (Review).* Experimental and Therapeutic Medicine, Vol. 3: 367-370

Spadaro JA, Berger TJ, Barranco SD, Chapin SE, and Becker RO. (1974) *Antibacterial Effects of Silver Electrodes with Weak Direct Current.* Antimicrobial Agents and Chemotherapy, Vol. 6(5): 637-642

Speziale P, Pietrocola G, RIndi S, Provenzano M, Provenza G, Di Poto A, Visai L, and Aricola CR. (2009) *Structural and functional role of Staphylococcus aureus surface components recognizing adhesive matrix molecules of the host.* Future Microbiology, Vol. 4(10): 1337-52

Steckelberg JM, Osmon DR. (2000) *Prosthetic joint infection*. In: Bisno AL, Waldvogel FA, editors. Infections associated with indwelling medical devices, 3rd ed. Washington, DC: American Society for Microbiology, 173–209.

Suzuki K, Aoki K, and Ohya K. (1997) *Effects of surface roughness of titanium implants on bone remodeling activity of femur in rabbits.* Bone, Vol. 21(6): 507-514

Tande AJ, and Patel R. (2014) *Prosthetic Joint Infection*. Clinical Microbiology Reviews. Vol 27(2): 302-345

Thakral G, LaFontaine J, Najafi B, Talal TK, Kim P and Lavery LA (2013) *Electrical stimulation to accelerate wound healing.* Diabetic Foot & Ankle, Vol. 4: 22081

Valour F, Trouillet-Assant S, Rasigade JP, Lustig S, Chanard E, Meugnier H, Tigaud S, Vandenesch F, Etienne J, Ferry T, Laurent F (2013) *Staphylococcus epidermidis in Orthopedic Device Infections: The Role of Bacterial Internalization in Human Osteoblasts and Biofilm Formation* PlosOne Vol. 8 (6): e67240

Vandenesch F, Lina G., and Henry T. (2012) *Staphylococcus aureus hemolysins, bi-component leukocidins, and cytolytic peptides: a redundant arsenal of membrane-damaging virulence factors?* Cellular and Infection Microbiology, Vol. 2, Article 12

Velasco-Ortega E, Jos A Cameán AM, Pato-Mourelo J, and Segura-Egea JJ. (2010) *In vitro evaluation of cytotoxicity and genotoxicity of a commercial titanium alloy for dental implantology.* Mutation Research/Genetic Toxicology and Environmental Mutagenesis, Vol. 702(1): 17-23

Wang K. (1996) *The use of titanium for medical applications in the USA.* Materials Science and Engineering A, Vol. 213(1-2): 134-137

Whitchurch CB, Tolker-Nielsen T, Ragas PC, and Mattick JS. (2002) *Extracellular DNA required for bacterial biofilm formation.* Science. Vol. 295(5559): 1487

Windisch C, Kolb W, Röhner E, Wagner M, Roth A, Matziolis G, and Wagner A. (2014) *Invasive Electromagnetic Field Treatment in Osteonecrosis of the Femoral Head: A Prospective Cohort Study.* The Open Orthopaedics Journal, Vol. 8(1): 125-129

Yao Y, Sturdevant DE and Otto M (2005). *Genomwide Analysis of Gene Expression in Staphylococcus epidermidis Biofilms: Insights into the Pathophysiology of S. epidermidis Biofilms and the Role of Phenol-Soluble Modulins in Formation of Biofilms.* The Journal of Infectious Diseases, Vol. 191(2): 289-298

Zanotti E, Felicetti G, Maini M, and Fracchia C. (2003) *Peripheral muscle strength training in bed-bound patients with COPD receiving mechanical ventilation: effect of electrical stimulation.* Chest, Vol. 124(1), 292-296

Zeng F-G and Fay RR. (2013) *Cochlear Implants: Auditory Prostheses and Electric Hearing*. Springer Science and Business Media, Vol. 20

Zimmerli W, Trampuz A, Ochsner PE. (2004). *Prosthetic-joint infections*. The New England Journal of Medicine, Vol. 351:1645–1654.

Zituni D, Schütt-Gerowitt H, Kopp M, Krönke M, Addicks K, Hoffmann C, Hellmich M, Faber F, Niedermeier W. (2014) *The growth of Staphylococcus aureus and Escherichia coli in low-direct current electric fields.* International Journal of Oral Science, Vol. 6: 7-14

7 Appendix

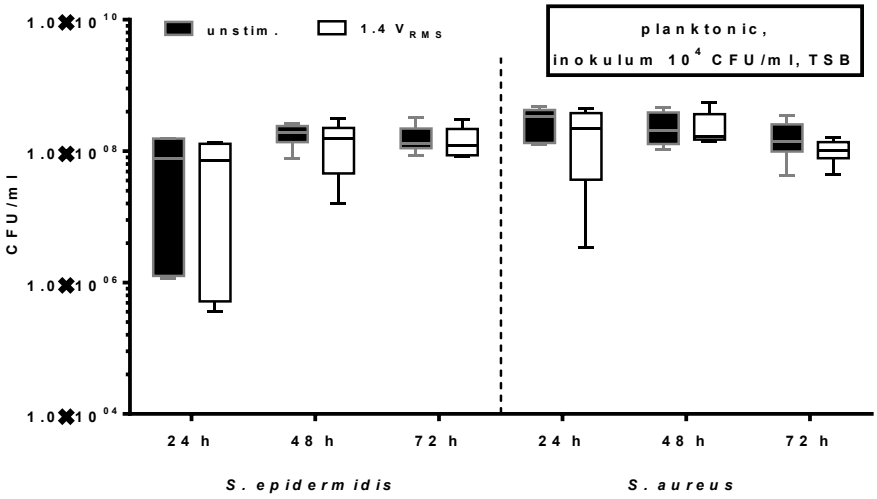

Figure 34: *Determination of planktonic S. epidermidis and S. aureus following electrical stimulation in TSB with 10^4 CFU/ml inoculum.* CFU/ml of planktonic *S. epidermidis* and *S. aureus* recovered from supernatants of stimulated and control samples. Unstimulated controls and bacteria stimulated with 1.4 V_{RMS}, stimulation period 3 x 45 min / day, inoculum of 10^4 CFU/ml in TSB. $n \geq 4$.

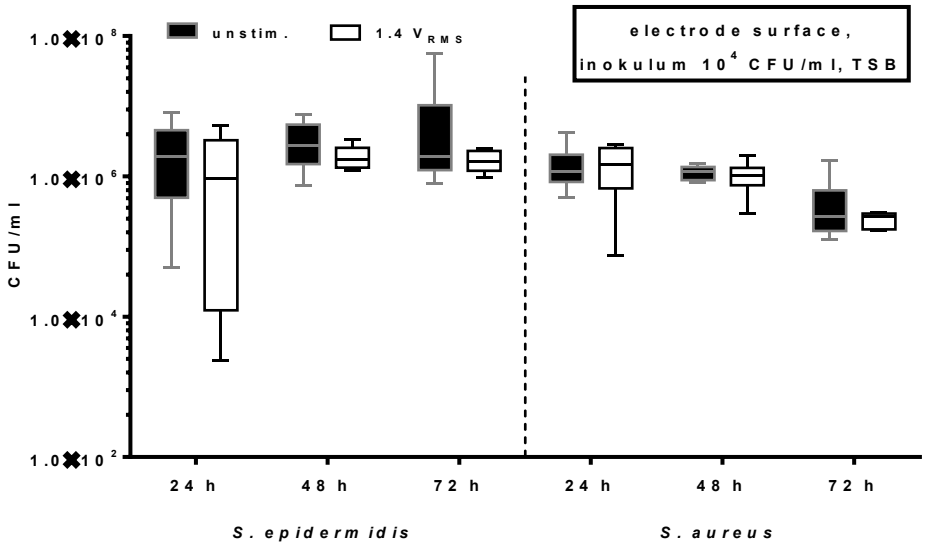

Figure 35: Determination of electrode-bound S. epidermidis and S. aureus following electrical stimulation in TSB with 10^4 CFU/ml inoculum. CFU/ml of adherent *S. epidermidis* and *S. aureus* recovered from electrode surfaces of stimulated and control samples. Unstimulated controls and bacteria stimulated with 1.4 V_{RMS}, stimulation period 3 x 45 min / day, inoculum of 10^4 CFU/ml in TSB. $n \geq 4$.

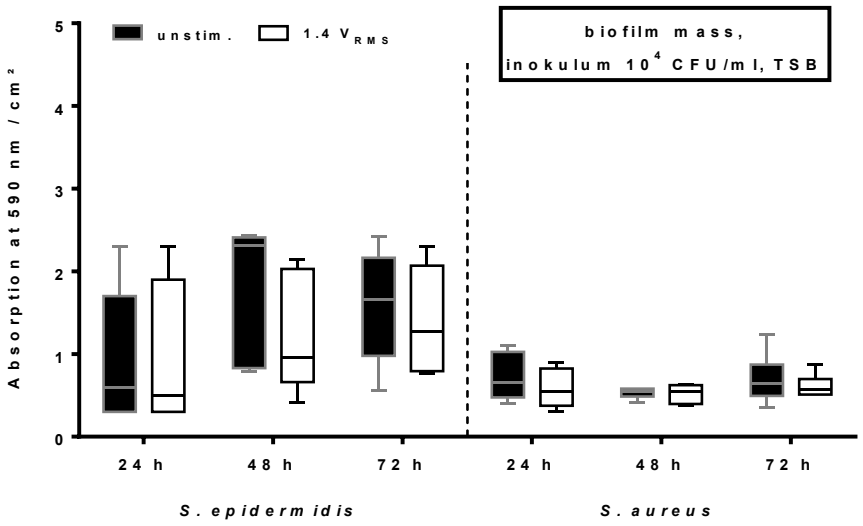

Figure 36: Quantification of biofilms formed by S. epidermidis and S. aureus following electrical stimulation in TSB with 10^4 CFU/ml inoculum. Biofilm mass quantification via crystal violet staining of *S. epidermidis* and *S. aureus* formed biofilm in relation to the surface area of the coverslip of stimulated and control samples. Unstimulated controls and bacteria stimulated with 1.4 V_{RMS}, stimulation period 3 x 45 min / day, inoculum of 10^6 CFU/ml in TSB. $n \geq 4$.

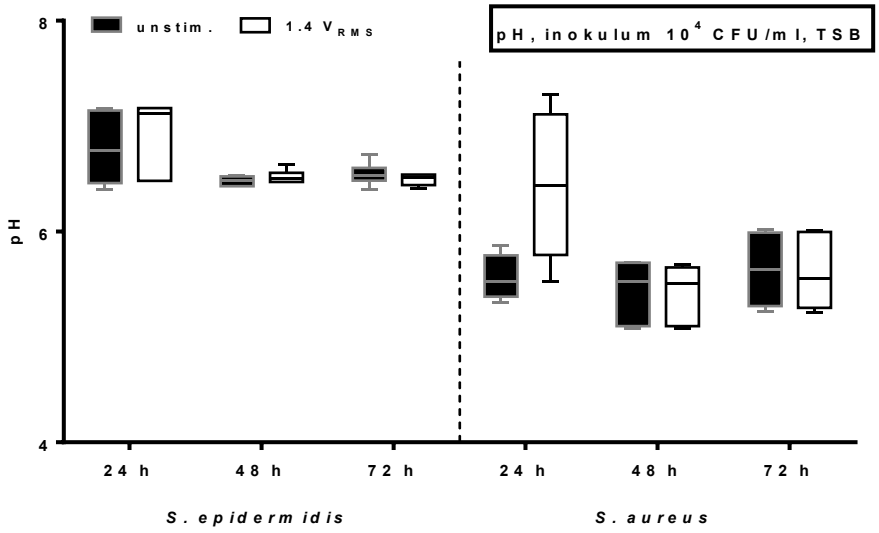

Figure 37: pH of supernatants of S. epidermidis and S. aureus samples following electrical stimulation in TSB with 10^4 CFU/ml inoculum. pH values of supernatants of *S. epidermidis* and *S. aureus* of stimulated and control samples. Unstimulated controls and bacteria stimulated with 1.4 V_{RMS}, stimulation period 3 x 45 min / day, inoculum of 10^4 CFU/ml in TSB. $n \geq 4$.

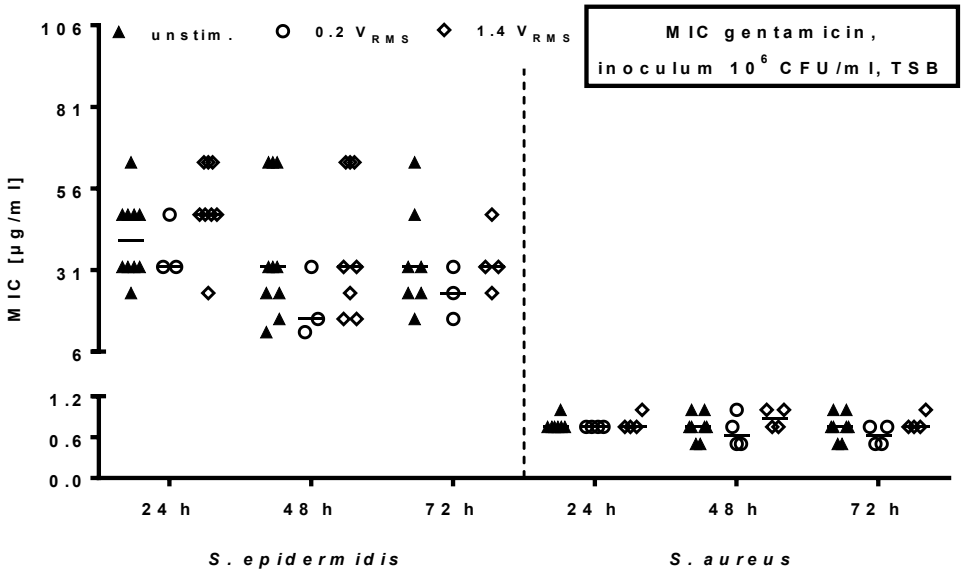

Figure 38: Minimal inhibitory concentrations of gentamicin following electrical stimulation of S. epidermidis and S. aureus in TSB with 10^6 CFU/ml inoculum. E-Test stripes were used to determine minimal inhibitory concentrations (MIC) of controls and with either 0.2 or 1.4 V_{RMS} treated samples over 72 h. Values are presented as median and single values. $n \geq 3$.

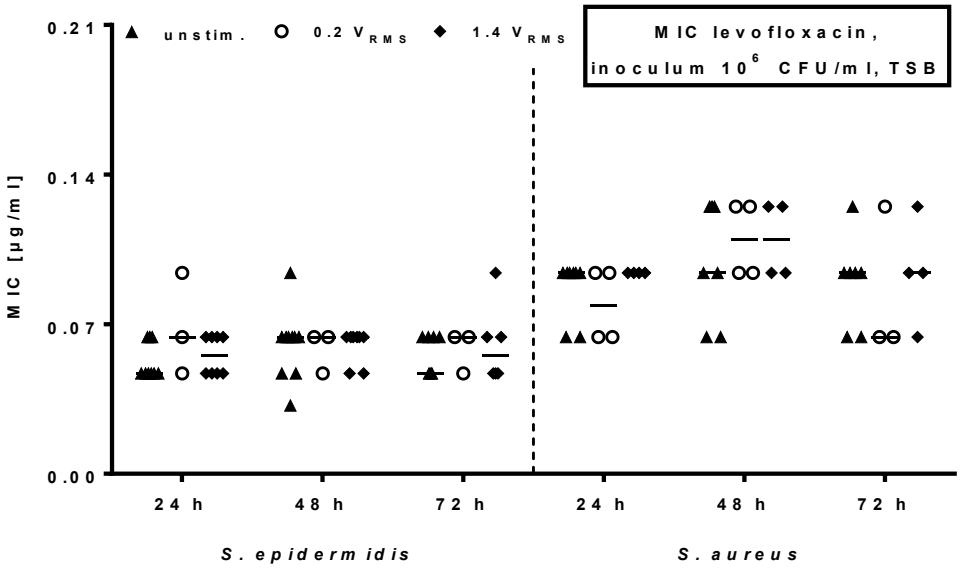

Figure 39: Minimal inhibitory concentrations of levofloxacin following electrical stimulation of S. epidermidis and S. aureus in TSB with 10^6 CFU/ml inoculum. E-Test stripes were used to determine minimal inhibitory concentrations (MIC) of controls and with either 0.2 or 1.4 V_{RMS} treated samples over 72 h. Values are presented as median and single values. $n \geq 3$.

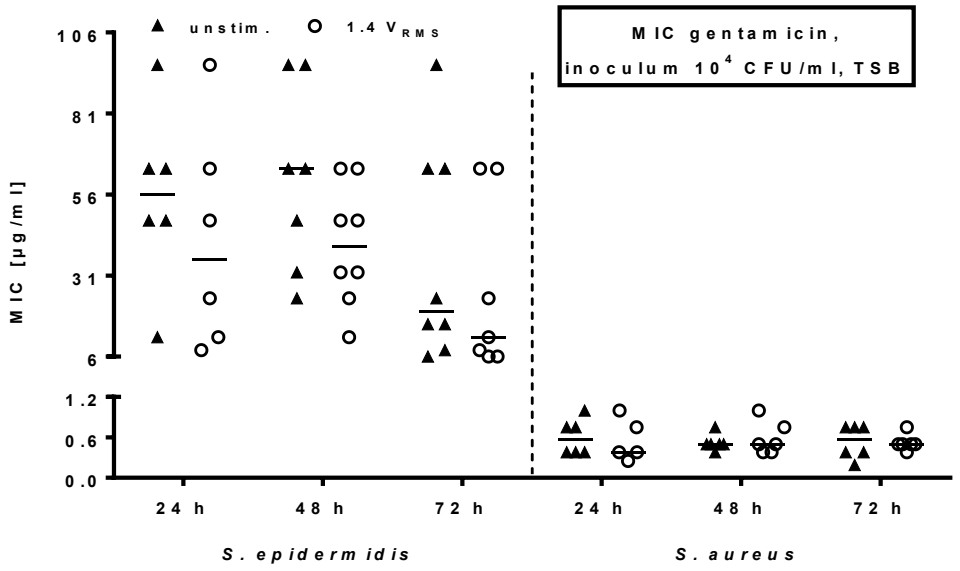

Figure 40: Minimal inhibitory concentrations of gentamicin following electrical stimulation of S. epidermidis and S. aureus in TSB with 10^4 CFU/ml inoculum. E-Test stripes were used to determine minimal inhibitory concentrations (MIC) of controls and with 1.4 V_{RMS} treated samples over 72 h. Values are presented as median and single values. n ≥ 5.

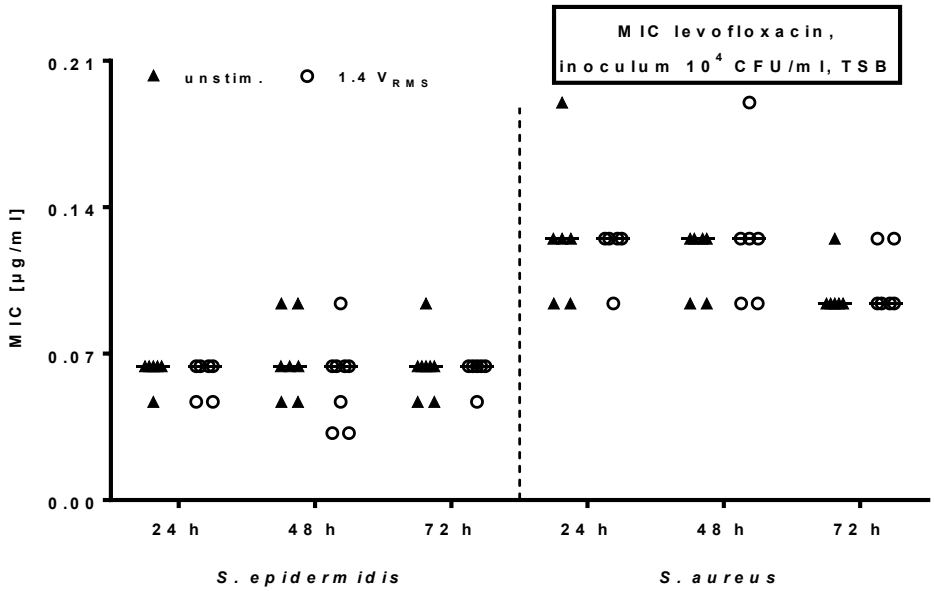

Figure 41: Minimal inhibitory concentrations of levofloxacin following electrical stimulation of S. epidermidis and S. aureus in TSB with 10^4 CFU/ml inoculum. E-Test stripes were used to determine minimal inhibitory concentrations (MIC) of controls and with 1.4 V_{RMS} treated samples over 72 h. Values are presented as median and single values. n ≥ 5.

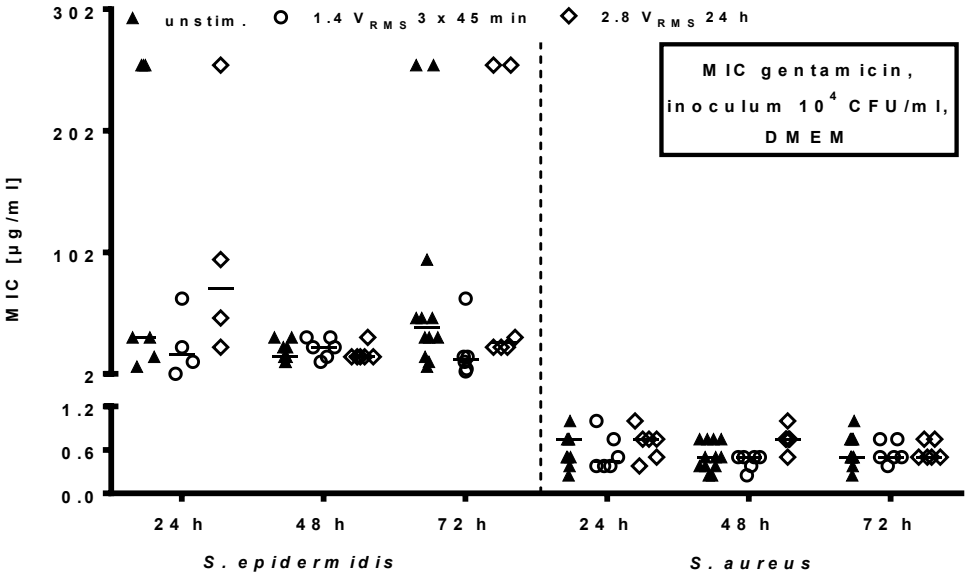

Figure 42: Minimal inhibitory concentrations of gentamicin following electrical stimulation of S. epidermidis and S. aureus in DMEM with 10^4 CFU/ml inoculum. E-Test stripes were used to determine minimal inhibitory concentrations (MIC) of controls and with either 1.4 or 2.8 V_{RMS} treated samples over 72 h. Values are presented as median and single values. $n \geq 4$.

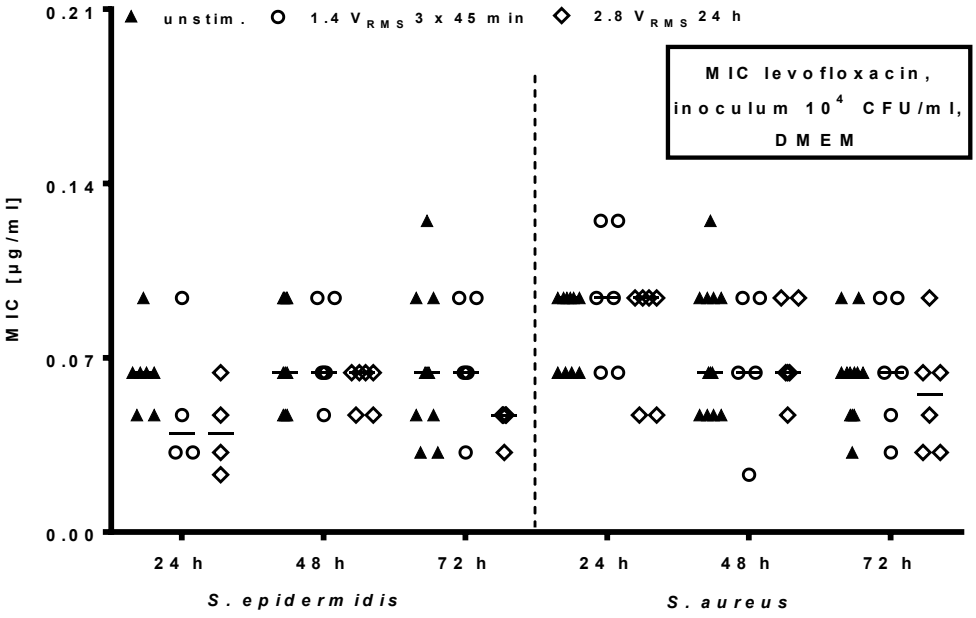

Figure 43: Minimal inhibitory concentrations of levofloxacin following electrical stimulation of S. epidermidis and S. aureus in DMEM with 10^4 CFU/ml inoculum. E-Test stripes were used to determine minimal inhibitory concentrations (MIC) of controls and with either 1.4 or 2.8 V_{RMS} treated samples over 72 h. Values are presented as median and single values. $n \geq 4$.

Acknowledgements

First, I would like to thank Prof. Dr. Bernd Kreikemeyer and Prof. Dr. Rainer Bader for entrusting this project to me and supervising as well as reviewing this work. Additionally, both contributed with constructive discussions to the progress and development of the stimulation system and experimental setups.

Next, I want to thank the Deutsche Forschungsgemeinschaft (DFG) for funding and support of interdisciplinary research within the research training group 1505 “Analysis and Simulation of Electrical Interactions of Implants with Biosystems – welisa”.

I also thank the whole research training group for a wonderful time and fruitful discussions and exchange of knowledge during our workshops and seminars.

Furthermore, I want to express my gratitude towards both teams of the Biomechanics and Implant Technology Research Lab (FORBIOMIT) and the Institute of Medical Microbiology, Virology and Hygiene Research working group for a wonderful time and friendly working climate with the right amount of fun and constructive and very enjoyable discussions about every imaginable subject. I really enjoyed the time I could spend within both research teams and I am very grateful to have been a part of both.

Especially, I want to thank Josefin Ziebart for a wonderful time regarding our cooperation and the development of our stimulation system, as well as for countless funny moments during our experiments and discussions. Furthermore, I would like to thank Thomas Bender and Yukun Su for doing numerical simulation for our system.

Also, I sincerely thank Katharina Wegner, Cathleen Hieke as well as Tomas Fiedler and Nadja Patenge for very fruitful discussions and enjoyable times.

I would also like to thank the Electron Microscopy Center (EMZ) of the University Medical Center Rostock for technical support in SEM imaging, as well as the Institute of Physics of the University of Rostock for processing electrodes and contact rods as well as assistance with impedance spectroscopy.

Eventually I want to thank my family and friends and especially Kieran Sanchéz for support, encouragement, motivation and lots of love and understanding of the struggles during my work.

Selbstständigkeitserklärung

Ich versichere hiermit an Eides statt, dass ich die vorliegende Arbeit selbstständig angefertigt und ohne fremde Hilfe verfasst habe. Dazu habe ich keine außer den von mir angegebenen Hilfsmitteln und Quellen verwendet und die den benutzten Werken inhaltlich und wörtlich entnommenen Stellen habe ich als solche kenntlich gemacht.

Rostock, 27.06.2017

Thomas J. Dauben